Integration of Biotechnological Intervention and Machine Learning Approaches for Enhancing Phosphorous Acquisition Efficiency in Plants

By

Zumrah Rehman

(Registration No: 00000399904)

Department of Chemical Engineering

School of Chemical and Materials Engineering

National University of Sciences & Technology (NUST)

Islamabad, Pakistan

(2024)

Integration of Biotechnological Intervention and Machine Learning Approaches for Enhancing Phosphorous Acquisition Efficiency in Plants

By

Zumrah Rehman

(Registration No: 0000039904)

A thesis submitted to the National University of Sciences and Technology, Islamabad,

in partial fulfillment of the requirements for the degree of

Master of Science in

Chemical Engineering

Supervisor: Dr. M. Bilal Khan Niazi

Co-Supervisor: Dr. M. Nouman Aslam Khan

School of Chemical and Materials Engineering

National University of Sciences & Technology (NUST)

Islamabad, Pakistan

(2024)

THESIS ACCEPTANCE CERTIFICATE

Certified that final copy of MS Thesis entitled **"Integration of Biotechnological Intervention and Machine Learning Approcaches for Enhancing Phosphorous Acquisition Efficiency in Plants"** written by Ms **Zumrah Rehman**(Registration No 00000399904), of School of Chemical & Materials Engineering (SCME) has been vetted by undersigned, found complete in all respects as per NUST Statues/Regulations, is free of plagiarism, errors, and mistakes and is accepted as partial fulfillment for award of MS degree. It is further certified that necessary amendments as pointed out by GEC members of the scholar have also been incorporated in the said thesis.

Signature: _____

Name of Supervisor: **Dr M. Bilal Khan Niazi**

Date: 20/11/2024

Signature (HOD): _____

Date: 20/11/24

For Signature (Dean/Principal): _____

Date: 21/11/24

Form TH-1

National University of Sciences & Technology (NUST)

MASTER'S THESIS WORK

Formulation of Guidance and Examination Committee (GEC)

Name: Zumrah Rehman NUST Reg No: 00000399904

Department: Department of Chemical Engineering Specialization: Master of Science in Chemical Engineering

Credit Hour Completed: 24.0 CGPA: 3.94

Course Work Completed

S/No:	Code:	Title:	Core/Elective:	CH:	Grade:
1.	CHE-843	Separation Processes In Che	Compulsory	3.0	A
2.	CHE-847	Chemical Kinetics& Reactor Design	Compulsory	3.0	A
3.	RM-898	Research Methodology	Additional	2.0	Q
4.	ESE-911	Carbon Capture And Utilization	Elective	3.0	A
5.	CHE-873	Membrane Technology	Elective	3.0	A
6.	CHE-814	Product Technology	Elective	3.0	A
7.	EME-921	Momentum Heat & Mass Transfer In CHE	Compulsory	3.0	A
8.	PSE-802	Optimization and Decision Analysis	Elective	3.0	A
9.	CSE-801	Computational Fluid Dynamics	Elective	3.0	B+

Date 11 - Dec - 2023 Student's Signature [redacted]

Thesis Committee

1. Name: Muhammad Bilal Khan Niazi (Supervisor) Signature
   Department: Department of Chemical Engineering
2. Name: Muhammad Nouman Aslam Khan (Cosupervisor) Signature
   Department: Department of Chemical Engineering
3. Name: Zaib Jahan (Internal) Signature [redacted]
   Department: Department of Chemical Engineering
4. Name: Ghulam Haider (Internal) Signature
   Department: Department of Plant Biotechnology

Date: 11 - Dec - 2023 Signature of Head of Department:

APPROVAL

Date: 11 - Dec - 2023 Signature of Dean/Principal:

National University of Sciences &Technology (NUST)

FORM TH-4

MASTER'S THESIS WORK

We hereby recommend that the dissertation prepared under our supervision by

Regn No & Name: **00000399904 Zumrah Rehman**

Title: **Integration of Biotechnological Intervention and Machine Learning Approaches for Enhancing Phosphorous Acquisition Efficiency in Plants.**

Presented on: **24 Oct 2024** at: **1430 hrs in SCME Seminar Hall**

Be accepted in partial fulfillment of the requirements for the award of Master of Science degree in **Chemical Engineering.**

Examination Committee Members

Name: **Dr Ghulam Haider** Signature:

Name: **Dr Zaib Jahan** Signature:

Name: **Dr M. Nouman Aslam Khan** (Co-Supervisor) Signature:

Supervisor's Name: **Dr M. Bilal Khan Niazi** Signature:

Dated: 07/11/2024

Head of Department 08/11/24 Date

COUNTERSIGNED

Date 8/11/24

Dean/Principal

School of Chemical &Materials Engineering (SCME)

AUTHOR'S DECLARATION

I Zumrah Rehman hereby state that my MS thesis titled "Integration of Biotechnological Intervention and Machine Learning Approaches for Enhancing Phosphorous Acquisition Efficiency in Plants" is my own work and has not been submitted previously by me for taking any degree from National University of Sciences and Technology, Islamabad or anywhere else in the country/ world.

At any time if my statement is found to be incorrect even after I graduate, the university has the right to withdraw my MS degree.

Name of Student: Zumrah Rehman

Date: October 24, 2024

PLAGIARISM UNDERTAKING

I solemnly declare that the research work presented in the thesis titled "**Integration of Biotechnological Intervention and Machine Learning Approaches for Enhancing Phosphorous Acquisition Efficiency in Plants**" is solely my research work with no significant contribution from any other person. Small contribution/ help wherever taken has been duly acknowledged and that complete thesis has been written by me.

I understand the zero-tolerance policy of the HEC and National University of Sciences and Technology (NUST), Islamabad towards plagiarism. Therefore, I as an author of the above-titled thesis declare that no portion of my thesis has been plagiarized and any material used as reference is properly referred/cited.

I undertake that if I am found guilty of any formal plagiarism in the above-titled thesis even after award of MS degree, the University reserves the rights to withdraw/revoke my MS degree and that HEC and NUST, Islamabad has the right to publish my name on the HEC/University website on which names of students are placed who submitted plagiarized thesis.

Student Signature: 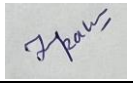

Name: Zumrah Rehman

DEDICATION

This thesis is dedicated to my parents and siblings who supported me in my every career decision. This would not have been possible without their unconditional support.

ACKNOWLEDGEMENTS

Starting with the utmost gratitude and praise to Allah Almighty, who has granted me the opportunity to conduct this research study and bring it to a satisfactory conclusion with significant findings. Peace and blessings be upon the Holy Prophet Muhammad, his family, and all illustrious companions, after the praise and thanks to Allah.
I am immensely grateful to my research supervisor, **Prof. Dr. Muhammad Bilal Khan Niazi,** for his unwavering support during this research. It was an honor to work under his supervision. I will always be grateful for his advice, support, and encouragement during my challenging times.

In addition to my research supervisor, I'd like to thank the other members of my guiding committee: **Dr. Muhammad Nouman Aslam Khan, Dr. Zaib Jahan, and Dr. Ghulam Haider** for their assistance. I would like to acknowledge **Dr. Ghulam Abbas Shah** (Associate Professor, PMAS Arid Agriculture University) for his support in providing the research facility for pot experiments and **Dr. Hazrat Ali** (National Institute for Biotechnology and Genetic Engineering) for his guidance.

I am grateful to my SCME seniors, Bilal Beig, Misbah Iqbal, and Mairaj Yousaf, for sharing their knowledge, which assisted my research. I am grateful to my friends, especially Nida Naeem and Shanza Nasir for their emotional support and encouragement throughout this journey. Furthermore, I'd like to thank Mahzeb, Shehzad, and my lab fellows for their help.

Finally, I'd like to thank my parents for always supporting me in my decisions. I am grateful to my siblings, who encouraged me to pursue higher education and supported me throughout this journey.

TABLE OF CONTENTS

ACKNOWLEDGEMENTS **IX**
TABLE OF CONTENTS **X**
LIST OF TABLES **XIII**
LIST OF FIGURES **XIV**
LIST OF SYMBOLS, ABBREVIATIONS AND ACRONYMS **XV**
ABSTRACT **XVI**
CHAPTER 1 INTRODUCTION **1**
1.1 Background **1**
1.2 P role in Plants **4**
1.3 Machine Learning **6**
CHAPTER 2 LITERATURE REVIEW **9**
2.1 Phosphorous cycle in soil **9**
2.1.1 Precipitation and adsorption reaction 10
2.1.2 Dissolution, Desorption, and Mineralization Reactions 11
2.2 Factors affecting phosphorous availability in soils **12**
2.2.1 Clay content and mineralogy 12
2.2.2 Organic matter 13
2.2.3 Soil pH 13
2.2.4 Sesquioxides 14
2.2.5 Calcium carbonate 15
2.2.6 Effect of Cations 15
2.2.7 Effect of Anions 15
2.2.8 Temperature 15
2.2.9 Liming 15
2.3 Phosphorous Solubilizing Bacteria (PSB) **16**
2.4 Mechanism of Phosphorous Solubilization through PSB **17**
2.4.1 Physiological Mechanism 18
2.4.2 Molecular Mechanism 21
2.4.3 Mechanisms of Microbial Community Effects 22
2.5 Overview of Machine Learning Models **23**
2.5.1 Genetic Algorithm 23
2.5.2 Particle Swarm Optimization (PSO) 24
2.5.3 Ensemble Learning Tree 25
2.5.4 Gaussian Process Regression 25
CHAPTER 3 OBJECTIVES **27**
CHAPTER 4 MATERIALS AND METHODS **28**
4.1 Materials **28**
4.2 Determination of Optimum Polymer concentration **28**
4.3 Microbial Survival Evaluation **29**
4.4 Preparation of coated DAP fertilizer **30**
4.5 Microbial Survival Evaluation of coated granules **30**
4.6 Physical and Chemical analysis of PSB and polymer-coated DAP **30**

4.6.1 Scanning Electron Microscopy (SEM) 30
4.6.2 X-ray diffraction (XRD) 31
4.6.3 Fourier Transform Infrared (FTIR) 31
4.6.4 Crushing Strength 31
4.6.5 Phosphorous Release Rate Analysis of DAP granules 32
4.6.6 Nitrogen Release Rate Analysis of DAP granules 32
4.7 Pot Test Experimentation 33
4.7.1 Experiment Location 33
4.7.2 Design of Experimental Work 33
4.7.3 Treatments 33
4.8 Plant Analysis 34
4.8.1 Plant height 34
4.8.2 Plant diameter 34
4.8.3 Number of leaves 34
4.8.4 Area per leaf 34
4.8.5 Plant fresh yield 34
4.8.6 Plant dry yield 35
4.8.7 Plant Total Phosphorous 35
4.8.8 Plant Total Nitrogen 35
4.9 Soil analysis 35
4.9.1 Soil pH 36
4.9.2 Soil Electrical Conductivity 36
4.9.3 Soil Organic Matter 36
4.9.4 Soil Mineral Nitrogen 37
4.9.5 Soil available Phosphorous 37
4.9.6 Soil Microbial Phosphorous 38
4.10 Machine Learning Model development 38
4.11 Statistical Analysis 39
CHAPTER 5 RESULTS AND DISCUSSION 40
5.1 Microbial Survival Evaluation 40
5.2 Physical and Chemical analysis of PSB and polymer-coated DAP 40
5.2.1 Scanning Electron Microscopy (SEM) 40
5.2.2 X-ray diffraction (XRD) 42
5.2.3 Fourier Transform Infrared Diffraction (FTIR) 43
5.2.4 Crushing Strength 44
5.2.5 Phosphorous Release Rate Analysis of DAP granules 46
5.2.6 Nitrogen Release Rate Analysis of DAP granules 48
5.3 Plant Analysis 49
5.3.1 Plant height 49
5.3.2 Plant Diameter 50
5.3.3 Number of leaves 51
5.3.4 Area per leaf 52
5.3.5 Plant Fresh Yield 53
5.3.6 Plant Dry yield 54
5.3.7 Plant total Phosphorous 55
5.3.8 Total Plant Nitrogen 56

5.4 Soil Analysis **57**
5.4.1 Soil pH 57
5.4.2 Soil EC 58
5.4.3 Soil Organic matter 59
5.4.4 Soil Mineral Nitrogen 60
5.4.5 Soil available Phosphorous 61
5.4.6 Soil Microbial Phosphorous 62
5.5 Machine Learning **64**
5.5.1 Box and Violin Plot Presentation 64
5.5.2 Correlation Heat Map 64
5.5.3 Performance Evaluation Criteria 65
5.5.4 Hyperparameter Tuning 66
5.5.5 Prediction Performance 67
5.5.6 Shapley Plot 68
5.5.7 Partial Dependence Plots 69
5.5.8 Graphical User Interface 70
CHAPTER 6 CONCLUSION AND RECOMMENDATIONS **71**
REFERENCES **72**

LIST OF TABLES

Table 1.1: Essential Plant Nutrients and Their Plant-Available Forms 3
Table 2.1: Organic acids secreted by different PSBs 18
Table 2.2: Different enzymes secreted by PSBs 20
Table 4.1: Composition of solutions 29
Table 4.2: Different treatments of DAP used in Pot Trials 33
Table 4.3: Initial Soil Properties 36
Table 5.1: Comparison of different ML models 66
Table 5.2: Optimized values of selected parameters 66

LIST OF FIGURES

Figure 1.1: Primary, Secondary and Micro-nutrients 2
Figure 1.2: Role of Phosphorous in plants and the effect of its deficiency 5
Figure 2.1: Phosphorous Cycle in Plants 10
Figure 2.2: Precipitation (a) and adsorption (b) reaction in phosphorous fixation process 11
Figure 2.3: Factors affecting Phosphorous availability in soil 12
Figure 2.4: Effect of pH on Phosphorous availability in soil 14
Figure 2.5: Mechanism of Phosphorous Solubilization 17
Figure 4.1: Experimental Design Methodology 28
Figure 4.2: Machine Learning Strategy Workflow 39
Figure 5.1: Microbial Survival Evaluation (a) Coating Solution (b) DAP Granules 40
Figure 5.2: SEM Micrographs of coated DAP fertilizer 41
Figure 5.3: XRD Pattern of coated DAP fertilizer. 43
Figure 5.4: FTIR Spectrum of Coated DAP fertilizer. 44
Figure 5.5: Crushing Strength of different fertilizer treatments. 46
Figure 5.6: Release rate kinetic for Phosphorous release rate of DAP fertilizer. 47
Figure 5.7: Release rate kinetic for Nitrogen release of DAP fertilizer. 49
Figure 5.8: Effect of different DAP treatments on Plant height. 50
Figure 5.9: Effect of different treatments on Plant diameter. 51
Figure 5.10: Effect of different treatments on Number of leaves. 52
Figure 5.11: Effect of different DAP treatments on Area of leaves. 53
Figure 5.12: Effect of different treatments on Plant fresh yield. 54
Figure 5.13: Effect of different treatments on Plant dry yield. 55
Figure 5.14: Effect of different treatments on Plant Total Phosphorous. 56
Figure 5.15: Effect of different treatments on Plant Total Nitrogen. 57
Figure 5.16: Effect of different treatments on Soil pH. 58
Figure 5.17: Effect of different treatments on Soil EC. 59
Figure 5.18: Effect of different treatments on Soil Organic matter. 60
Figure 5.19: Effect of different treatments on Soil Mineral Nitrogen. 61
Figure 5.20: Effect of different treatments on Soil Available Phosphorous. 62
Figure 5.21: Effect of different treatments on Soil Microbial Phosphorous. 63
Figure 5.22: Box and Violin Plot presentation of data 64
Figure 5.23: Heat map presentation of data 65
Figure 5.24: Validation of GA-ELT model 68
Figure 5.25: Shapley Plot 69
Figure 5.26: Partial Dependence Plots 69
Figure 5.27: Graphical User Interface 70

LIST OF SYMBOLS, ABBREVIATIONS AND ACRONYMS

PSB	Phosphorous Solubilizing Bacteria
PVA	Polyvinyl Alcohol
DAP	Di-Ammonium Phosphate
P	Phosphorous
N	Nitrogen
T1	Uncoated DAP fertilizer
T2	PSB coated DAP
T3	PVA coated DAP
T4	PSB and PVA coated DAP
SEM	Scanning Electron Microscopy
UV-VIS	Ultraviolet Visible (UV) Spectroscopy
FTIR	Fourier Transform Infra-Red
XRD	X-Ray Diffraction
EC	Electric Conductivity
CRD	Completely Randomize Design
ANOVA	Analysis of Variance
PSO	Particle Swarm Optimization
GA	Genetic Algorithm
DT	Decision Tree
ELT	Ensembled Learning Tree
GPR	Guassian Process Regression

ABSTRACT

Pakistan's economy is significantly dependent on agriculture, as it is an agricultural country. The agriculture industry requires continuous improvement to satisfy the increasing demand for food, which is a result of the increasing population. It is important to optimize the efficiency of synthetic fertilizers in order to increase crop yield. The most frequently applied synthetic phosphorous fertilizer to soils is Di-Ammonium Phosphate (DAP). This fertilizer is used to increase the phosphorus content of the soil, a significant portion of which is lost in the soil and is not accessible for plant uptake. This research study concentrates on the integration of biotechnological interventions and machine-learning strategies to improve the uptake of phosphorus by plants.

The Microbial Strain *Bacillus velezensis* FB2 and Polyvinyl alcohol solution were coated to the DAP fertilizer. *Bacillus velezensis* FB2 can solubilize unavailable phosphorous in soil and convert it to available phosphorous, while PVA serves as a barrier for the effective slow release of nutrients in soil. The coating was applied using a fluidized bed coater with a solution of 0.5% PVA and 4% PSB in water. The surface morphology of the developed product was evaluated using scanning electron microscopy (SEM). The presence of functional groups and crystallinity of coated granules were analyzed using X-ray diffraction techniques and Fourier Transform Infrared spectroscopy (FTIR). UV-Vis Spectroscopy was employed to analyze the release rate of phosphorous and nitrogen in water, and the ability of the coated product to resist applied force was assessed using crushing strength.

The product that was developed was subjected to pot trials to evaluate the impact of various treatments on plant yield. The impact of various treatments on the height, diameter, number of leaves, area of leaves, soil EC, soil pH, fresh matter yield, dry matter yield, quantity of available phosphorus, and change in phosphorus and nitrogen uptake of the plants were assessed after they were at full growth. Based on soil and plant analysis, it was determined that DAP coated with both PSB and PVA was the most effective fertilizer in terms of plant growth and the quantity of nutrients in the soil and plants. This is due to the ability of microbial strains to solubilize phosphorus and the effective release of nutrients as a result of PVA coating. A machine learning model was developed to

predict changes in the amount of soluble phosphorus caused by the use of a microbial strain. Data was obtained from the literature and utilized to train and test a number of models, such as Ensembled Learning Tree (ELT), Guassian Process Regression (GPR), Decision Tree (DT) based on Genetic Algorithm (GA), and Particle Swarm Optimization (PSO). The GA-based ELT model demonstrated the highest performance among all developed models with an R^2 value of 0.7938.

CHAPTER 1 INTRODUCTION

1.1 Background

Fertilizers are the primary and most significant materials in agricultural fields. The need for food is rising due to the alarming rate at which the world's population is growing. Over the next 40 years, meeting this demand will be difficult due to changes in the climate, a decline in arable land, an increase in water shortages, and rising costs for agricultural inputs [1].

Fertilizers will play a major role in satisfying the demand for food by increasing the output per unit area. Soluble fertilizers are used in considerable amounts on low-fertility soils in order to achieve the necessary nutritional requirements[2]. Crop yield and nutrient uptake efficiency are therefore essential for both fertilizer producers and users to maximize the efficiency of any fertilizer. Because it can have an adverse influence on the environment if used incorrectly or if its capacity to absorb nutrients is insufficient [3].

The growth and metabolism of plants depend on the study of chemical elements and molecules. Plants cannot complete the vegetative growth or reproductive stages of their life cycle when there is an elemental shortage. By utilizing the energy from sunlight to mix chemical elements that they have absorbed in the form of inorganic compounds, all green plants can produce their sustenance. It is believed that seventeen elements are necessary for plant growth. Plants are unable to complete their vegetative or reproductive life cycles if any one of these 17 components is missing which are shown in Figure 1.1 [4].

Plants take up inorganic minerals from the soil or water to use as nourishment. These minerals are found at the soil's surface. The weathering of rock minerals, and the decomposition of organic materials, plants, animals, and bacteria combine to generate these mineral nutrients [5]. Plants receive their carbon, hydrogen, and oxygen from the atmosphere through the air and water. It is estimated that approximately 95 percent of the total dry matter of the plants is composed of these three components. Depending on the amount that plants need, the 17 mineral nutrients needed for plant growth are categorized as primary, secondary, or micronutrients. Sometimes referred to as macro or major nutrients, primary and secondary nutrients work together. Although they are

macronutrients, secondary nutrients are less commonly lacking in soils [6]. Mineral nutrients have crucial and distinct roles in the metabolism of plants. For example, they can be charge carriers, osmo-regulators, enzyme reaction activators, or components of basic structures [7]. Plant growth and yield levels are negatively impacted by nutritional deficiencies. Plants create chemicals that minimize diseases, but plant nutrients are necessary for both their manufacture and transportation [8].

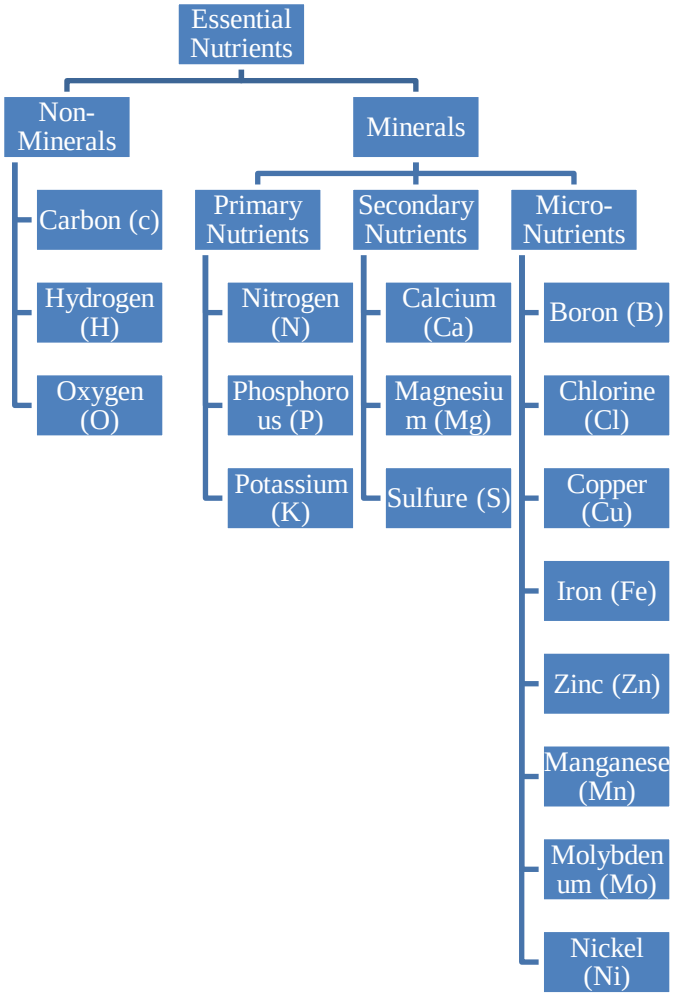

Figure 1.1: Primary, Secondary and Micro-nutrients [9]

Plants absorb the elements through their roots and leaves in a variety of ways. Although the soil has high concentrations of these elements, only a small portion of them are typically available [10]. The chemical characteristics and forms of the nutrient determine its availability to plants. Additional variables include the pH, colloid interaction, and physical characteristics of the soil, such as moisture, air temperature, and moisture. Soil

contains essential elements in all three physical phases (solid, liquid, and gas) [11]. Table 1.1 lists the essential components along with their various forms.

Table 1.1: Essential Plant Nutrients and Their Plant-Available Forms [12]

Plant Nutrient	**Plant Usable form**	**Average concentration in plant tissue**
Basic Elements		
Carbon (C)	CO_2	45 per cent
Hydrogen (H)	H_2O	6 per cent
Oxygen (O)	H_2O, O_2	45 per cent
Primary Elements		
Nitrogen (N)	NO_3^-, NH_4^+	1.5 per cent
Phosphorous (P)	$H_2PO_4^-$, HPO_4^{2-} , PO_3^{3-}	02 per cent
Potassium (K)	K^+	
Secondary elements		
Sulfur (S)	SO_4^{2-}	0.1 per cent
Calcium (Ca)	Ca^{2+}	0.5 per cent
Magnesium (Mg)	Mg^{2+}	0.2 per cent
Micronutrients		
Iron (Fe)	Fe^{2+}, Fe^{3+}	100 mg/kg
Zinc (Zn)	Zn^{2+}	20 mg/kg
Maganese (Mn)	Mn^{2+}	20 mg/kg

Boron (B)	H_3BO_3, $H_2BO_3^-$, BO_3^{3-}	20 mg/kg
Copper (Cu)	Cu^{2+}	6 mg/kg
Chloride (Cl)	Cl^-	100 mg/kg
Molybdenum (Mo)	MoO_4^{2-}	0.1 mg/kg
Nickel (Ni)	Ni^{2+}	

1.2 P role in Plants

Phosphorous (P) is a main nutrient essential for plant growth because of its important role in metabolic and various other activities. P has a significant role in soil having both acidic and basic properties as it controls the yield of crops. ADP and ATP have a major role in energy conversion and storage processes in plants which are made up of P. Other than these, P is important for many major processes essential for plant development including photosynthesis, respiration, membrane development, and glycolysis [13], which is illustrated in Figure 1.2.

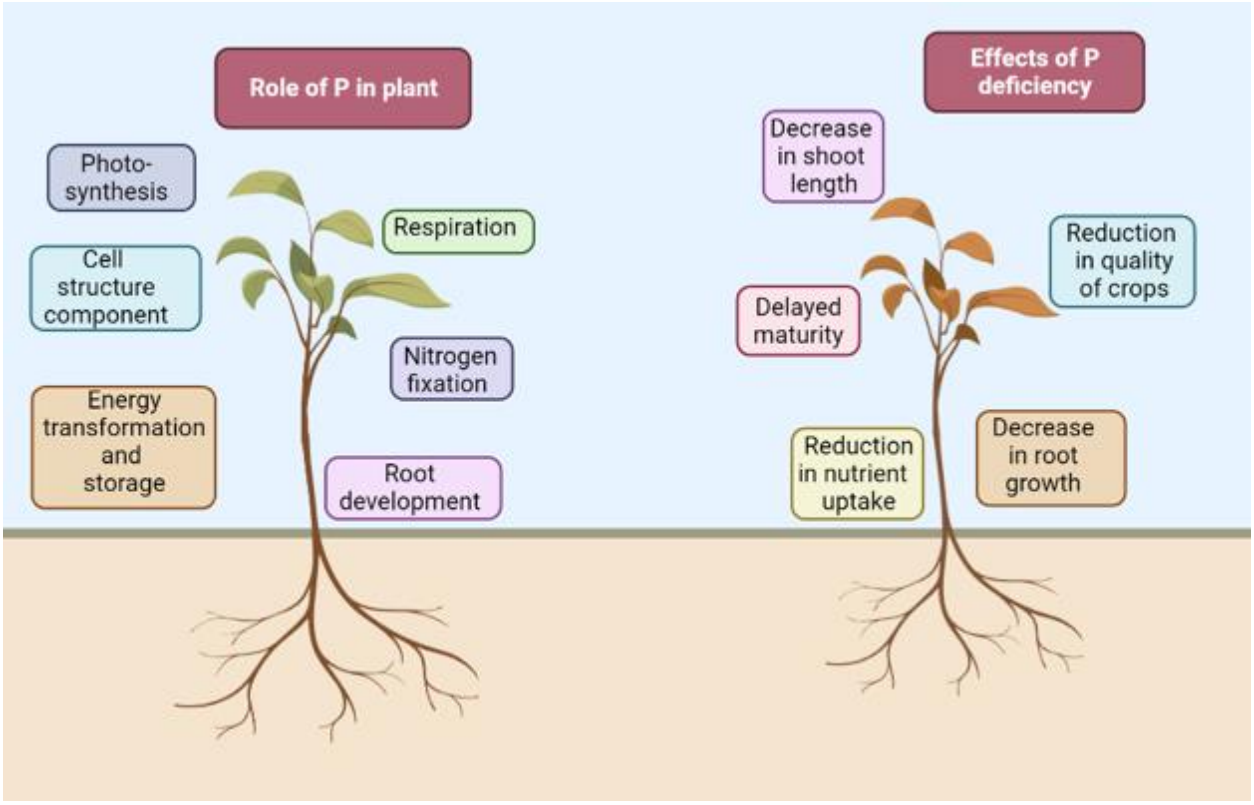

Figure 1.2: Role of Phosphorous in plants and the effect of its deficiency

It helps in root growth, development of stem, seed production, maximum crop production, and nitrogen fixation processes, all of these make P an important part of plants and crops and its availability affects the yield. Figure 1.2 shows the role of P in plant growth and the effect of P deficiency in soil. Although soil contains 170 minerals that supply phosphorous, only a very small amount (<1%) is dissolved in soil [14]. P reacts with ions present in both acidic and basic soil; in acidic soil, it gets bonded with Fe and Al while in basic soil it forms bonds with Ca, Mg, K, and Na ions. P is present in soil in two forms including organic P (Orthophosphate, nucleic acid, and phospholipids) and inorganic P (Soil Solution, Sorbed P, and mineral P) [15]. The only forms of P that are utilized by plants include primary and secondary orthophosphate ions $(H_2PO_4)^{-1}$ and $(HPO_4)^{-2}$ [16]. P deficiency in plants is caused by the fixation of added P from chemical fertilizers with ions present in the soil as a result of adsorption and precipitation reactions [17].

Due to the ability of P to rapidly react with cations like Ca^{2+} and Mg^{2+} in calcareous soils or Al^{3+} and Fe^{3+} in acidic soils, P is quickly immobilized in the soil when applied as

fertilizer. Additionally, due to a large number of soil microorganisms P cycle is impacted in numerous ways: although some rhizobacteria and arbuscular mycorrhizal (AM) fungi may help plants acquire phosphorus (P), some microorganisms have the reverse effect since they compete with roots to uptake P and since their actions converts P in organic form which is challenging for plants to absorb [18].

Even with a carefully designed P fertilization plan, only 30% of P applied can be used by plant roots; the remaining part is lost due to microbial activity and soil fixation. Due to these conditions, excessive fertilizer use has taken place, resulting in the accumulation of water reserves with undesired nutrients which produce eutrophication and hazardous algal blooms [19].

Due to these factors, effective uptake and utilization of P in soil is of very importance and must be enhanced. There are different ways to increase P uptake in plants by solubilizing precipitated P using microorganisms, zeolites, and organic matter [20]. The primary objective of this study is to find out and optimize the ways to enhance P acquisition efficiency in plants.

1.3 Machine Learning

Agricultural activities have been the primary and most conspicuous activity of all societal structures since the beginning of human history. Not only does it constitute a substantial part of the growing economy, but it is also essential for human survival. In addition to this, it holds an important part of the employment market. With time, there has been a significant increase in the need for manufacturing. The incorporation of technology in order to get the intended results is the challenge that the agriculture industry in Pakistan is looking to overcome [21]. To be successful, the new agricultural system needs to be effective, resilient, diverse, and long-term in character. Additionally, it needs to expand rapidly. Artificial Intelligence (AI) and Machine Learning (ML) can address the challenges posed by this new paradigm if they are able to make use of the data that they have obtained [22]. Agricultural markets can make better judgments based on data with the assistance of these methods. People are generating, delivering, and consuming food in different ways because of the impact of artificial intelligence. To provide support and insight into sustainable farming, crop protection, infection control, optimal harvesting,

food preferences, logistics, food security, and other agricultural-based duties, scientists apply methodologies driven by artificial intelligence (AI) throughout the entire food supply chain [23]. A number of factors, including its adaptability, superiority, and cost-effectiveness, are the primary reasons for the application of artificial intelligence in farming. The usage of these technologies results in a reduction in the quantity of water, pesticides, and herbicides that are employed. Additionally, they contribute to the efficient utilization of labor and enhance the quality of the product.

The primary objective of this study is to examine the utilization of technologies such as Machine Learning (ML) to estimate the quantity of phosphorous present in soil and, consequently, its impact on crop production. A relatively new technology known as machine learning is providing farmers with comprehensive crop suggestions and insights, which is helping them to reduce the amount of money they lose from farming [24]. The technique is a quickly expanding strategy that is supporting every industry in making feasible judgments to create the most renowned of its applications. They are doing this by assisting the technique. To increase the overall productivity of the agriculture industry, the basic idea is to make use of Machine Learning models. The purpose of the research is to devise a method that will not only automate agricultural processes but also provide farmers with the ability to make educated decisions regarding the most efficient way to apply fertilizer [25].

Supervised learning is one of the two primary branches of machine learning that enables models to predict future outcomes after they have been trained based on data from the past with the help of supervised learning. To train the model, we make use of input/output pairs or labeled data [26]. Our objective is to generate a function that is sufficiently approximated to be able to predict outputs for new inputs when they are presented to them. Regression and classification problems are the two available categories of supervised learning opportunities. In situations where the outputs are continuous, a regression problem arises; in situations where the outputs are categorical, a classification problem arises.

The prediction of the amount of available phosphorous in the soil after a phosphorous-solubilizing bacteria has been used falls in the category of regression analysis [27] . This research study aims to determine the links that exist between the amount of phosphorous,

which is the dependent variable, and other independent factors such as the pH of the soil and the amount of phosphorous that is present in the soil. The significance of regression analysis lies in the fact that it enables one to determine the factors that are of the utmost importance, those that are susceptible to being neglected, and the connections that exist between those variables [28].

CHAPTER 2 LITERATURE REVIEW

2.1 Phosphorous cycle in soil

The soil contains three P pools: labile P which is regarded as active P, non-labile P also known as fixed P, and soil solution. In the soil solution, phosphorus exists as the orthophosphate ions. Highly acidic soils (pH 4 to 5.5) are dominated by monovalent anions $(H_2PO_4)^{-1}$, while higher pH levels are dominated by divalent anions $(HPO_4)^{-2}$ [29]. Normally, this P pool is easily accessible to plants or can be converted into secondary minerals. The portion of phosphorus (P) that is uptaken by plants and chemically free, ready to exchange ions, and can react in the soil is termed labile P (Al-P, Fe-P, and Ca-P) [30]. Sesquioxides or carbonates, crystalline substances, are abundant with labile and bioavailable phosphate bonded onto their surfaces. By forming relatively weak bonds, P is attached to the components of soil and organic material. When quantity of P in the soil solution falls, P in labile pool refills the dissolved P. The amount of phosphorus (P) that is not easily accessible to plants due to formation of complexes with oxides and hydroxides of Fe, Ca and Al is contained in mineral complexes like apatite also referred as non-labile part. The transformation of non-labile P to labile P and soil solution is slower because the non-labile P is difficult to solubilize. Only primary and secondary minerals can dissolve to release non-labile P. The P in these three pools is continuously transferred from one form to another; in order to maintain equilibrium as illustrated in Figure 2.1. For instance, when plants absorb P from the solution, the labile fraction replaces it, whereas the non-labile fraction restores it more gradually [31].

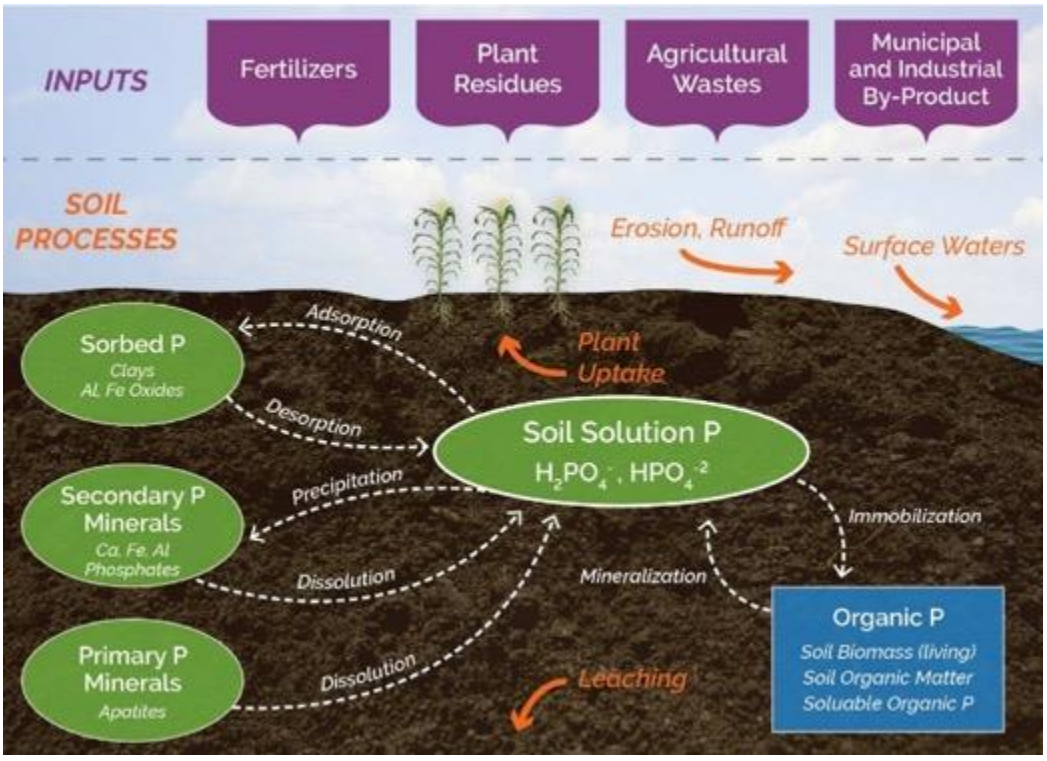

Figure 2.1: Phosphorous Cycle in Plants [32]

2.1.1 Precipitation and adsorption reaction

The retention mechanism of phosphates involves both precipitation and adsorption processes. Phosphate ion adsorption over crystalline clay compounds, sesquioxides, or carbonate surfaces is the predominant mechanism when the concentration of orthophosphate is less. On the other hand, soluble P gets precipitated with cations at high orthophosphate concentrations to form Fe and Al phosphates at low pH and Ca and Mg phosphates at high pH in acidic and basic soil respectively. The adsorption procedure is thought to be crucial for controlling the dissolution of P for a short period of time.

A rapid increase in soil solution P content is viewed by the addition of soluble P in the soil as fertilizers or additives. These P parts then go through processes like precipitation or adsorption to lose some of their solubility. The soil pH is the governing parameter in certain chemical processes. Al^{3+} and Fe^{3+} ions typically precipitate with H_2PO_4 ions in acidic soils resulting in insoluble hydroxyl phosphates (Figure 2.2) which can hardly be accessed by plants [33].

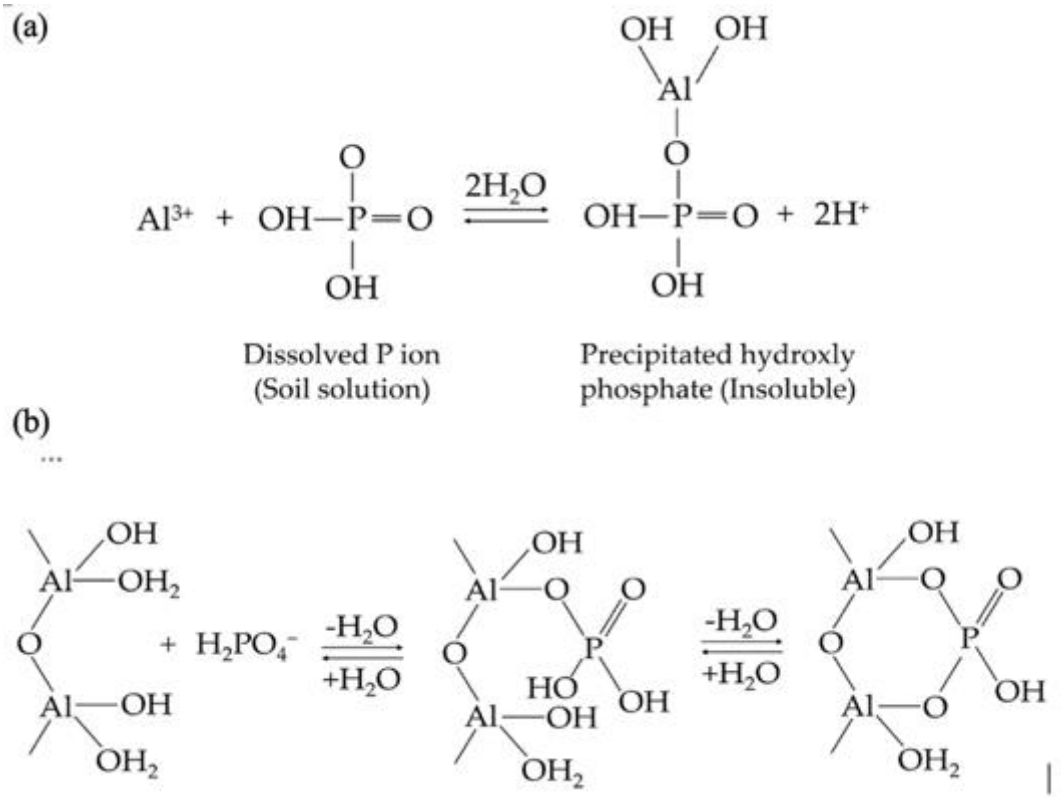

Figure 2.2: Precipitation (a) and adsorption (b) reaction in phosphorous fixation process [34]

Ligand exchange reaction takes place when orthophosphate ions replace metal hydroxide or oxides on clay surface (Figure 4b). Because P becomes an essential part of the oxide mineral during the reaction, its ability to desorb in soil solution is less.

2.1.2 Dissolution, Desorption, and Mineralization Reactions

Dissolution is the process of dissolving phosphate minerals releasing P back in soluble form. The dissolution of soil minerals depends on hydrogen ions, which often come from the soil or through the discharge of roots or microorganisms which act as a sink for calcium and phosphorus [35].

Desorption, which is the opposite of sorption, is the process by which sorbed P is dissolved from clays, oxides, and minerals and diffuses into the soil solution, having a concentration gradient as a driving force. This happens when plant uptake of P reduces the quantity of soluble P in the soil solution to a minimal level and creates a

concentration gradient that makes it easier for the gradual release of P adsorbed from the soil components to maintain equilibrium in P pools [36].

Mineralization and solubilization can enhance accessible P in addition to dissolution and desorption processes. A large number of microorganisms present in soil and its rhizosphere, in the natural environment, are effective in releasing P from the total soil P by mineralization and solubilization. Phosphate-solubilizing microorganisms are microbes that convert insoluble P into soluble P and monitor P cycle in soil [37].

2.2 Factors affecting phosphorous availability in soils

Phosphorus is returned to the soil solution by dissolution, desorption, and mineralization of organic materials. The soil properties that control P sorption and desorption affect P availability to plants. It includes the amount of clay and its mineralogy, organic matter, soil pH and concentration of Al^{3+}, Fe^{3+}, and Ca^{2+} ions in the soil solution as shown in Figure 2.3.

Figure 2.3: Factors affecting Phosphorous availability in soil

2.2.1 Clay content and mineralogy

Fe and Al concentration as well as the amount of clay in acidic soils regulate phosphorus release. Al and Fe oxides present in clay cause adsorption of P due to which clays with high concentrations of Fe and Al oxides such as 1:1 Clays (Kaolinite) have a higher tendency for P adsorption as compared to 2:1 clays (monmorillonite). In other words, a given type of clay has a stronger potential to adsorb P; the more surface area it exposes. By exchanging out the hydroxide ion (OH) from clays, phosphate is strongly adsorbed on clay surfaces. Additionally, the degree of P retention is significantly influenced by the amount of clay in a soil profile, with higher P retention in soils having high clay content [38] [39].

2.2.2 Organic matter

The addition of organic matter can increase P availability since it can solubilize fixed P in soil and chelate Al^{3+} and Fe^{3+} ions. Humic compounds, such as carboxyl, hydroxyl, and carbonyl, which have several negative charges and functional groups, make up organic matter [40]. These functional groups prevent their interactions with P by forming stable complexes with Al and Fe. Sesquioxides can be coated with organic material to minimize adsorption of P, releasing more P for plant uptake [41]. Low molecular weight organic acids like citric, oxalic, tartaric, and malic acids are created when organic matter is mineralized. By strongly competing for the adsorption sites, this process decreases P adsorption in soil. Organic acids produced due to the breakdown of organic matter or that are introduced to the soil system via wastewater also help to maintain a larger amount of soluble phosphorus by lowering P adsorption [42].

2.2.3 Soil pH

In terms of orthophosphate bioavailability, soil pH is significant. Soil pH can alter the content of Fe and Al oxides present in soil which cause precipitation of P in soil. The best pH range for soil P availability is between 6.5 and 7.0. The relationship between soil pH and P fixation is shown in Figure 2.4.

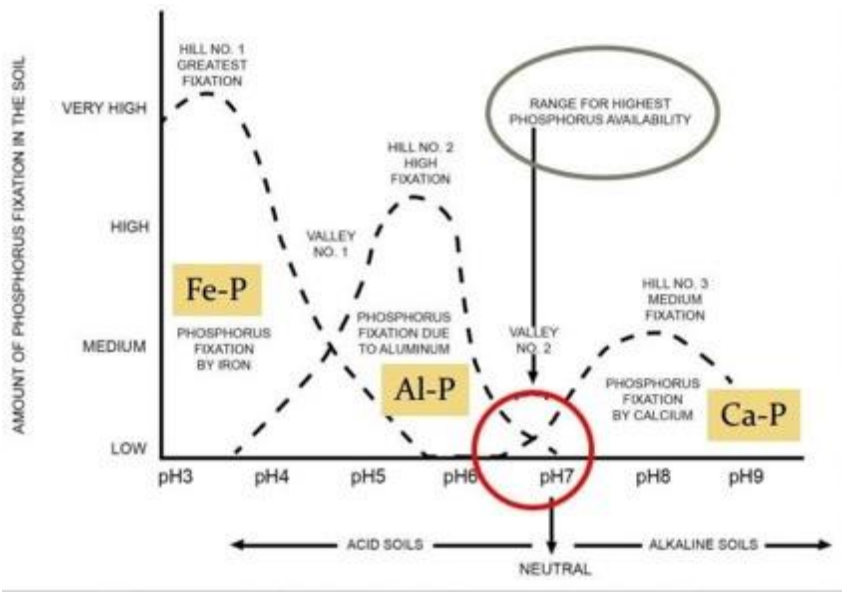

Figure 2.4: Effect of pH on Phosphorous availability in soil [43]

Due to the possibility of orthophosphate being locked out of the soil solution, Al^{3+} and Fe^{3+} ions can be problematic in acidic soils. Orthophosphate reacts with Fe and Al ions present in soil forming insoluble compounds of Fe-P and Al-P In acidic soil, P becomes unavailable due to two different reactions: Precipitation of P with Al^{3+} and Fe^{3+} ions and sorption reaction of P with oxides and hydroxides. Following chemical reactions take place as a result [44].

Precipitation reaction;

$$Fe^{3+} + H_2PO_4^- \rightarrow Fe(H_2PO_4)^{2+}$$

Sorption reaction;

$$Al(OH)_3 + H_2PO_4^- \rightarrow Al(OH)_2H_2PO_4 + OH^-$$

$$Fe(OH)_3 + H_2PO_4^- \rightarrow Fe(OH)_2H_2PO_4 + OH^-$$

Reaction with Ca;

$$3Ca(OH)_2 + 2H_3PO_4^- \rightarrow Ca_3(PO_4)_2 + 6H_2O$$

$$3CaCO_3 + 2H_3PO_4^- \rightarrow Ca_3(PO_4)_2 + 3CO_2 + 3H_2O$$

2.2.4 Sesquioxides

The oxides of iron and Al present in soil adsorb a large amount of P. Iron and Al oxides in soil adsorb a high content of P which can be related to their high P fixation ability. It has also been found that the amount of sesquioxides in the soil affects the adsorption

capacity of soils. Al-oxides have a higher ability to adsorb P as compared to Fe-oxides [45].

2.2.5 Calcium carbonate

P in soil gets adsorbed on $CaCO_3$ particles present in soil which have a high surface area. The coating of Fe oxides increases the adsorption ability of $CaCO_3$ [46].

2.2.6 Effect of Cations

The presence of divalent cations like Ca^{2+} in soil increases P retention considerably more than the presence of monovalent ions like Na. The occurrence of Ca^{2+} ions in the soil increases the potential of P adsorption by increasing the availability of positively charged sites to phosphate ions. This happens when the pH drops below 6.5 [47].

2.2.7 Effect of Anions

Anions including NO^{3-} and Cl^{-} have a low impact on P adsorption, whereas OH^{-}, $(SO_4)^{2-}$, and $HSiO_3^{-}$ have the tendency to compete with P anions to get adsorb on available sites. Their bonding strength determines the resultant effect [48].

2.2.8 Temperature

The inability of plant roots to expand in low temperatures limits the amount of phosphorus (P) available to plants. When soil temperatures are raised to the optimal range (25-30°C), microbial activity is increased, leading to a high mineralization rate [49].

2.2.9 Liming

When acid soils are limed, polynuclear complexes of Al are formed, and they significantly adsorb P, reducing the available P concentration present in the soil. In addition, $H_2PO_4^{-}$ is dissociated into HPO_4^{-}, which is more conveniently adsorbed by soil, when the pH of the soil is raised through liming. To increase plant availability of phosphorus, soil pH can be raised at low rates using lime, leading to a significant decrease in soil exchangeable Al [50].

2.3 Phosphorous Solubilizing Bacteria (PSB)

For a long time, scientists have recognized that the bacterial population displays significant differences in its capacity to solubilize P in soil. Pseudomonas, Azotobacter, Burkholderia, Bacillus, and Rhizobium are all prominent soil bacteria that have been shown to increase P availability [51]. PSB produces organic acids and converts fixed soil phosphorus, to transform inorganic insoluble P to soluble form. The use of PSB would therefore not only reduce the need for fertilizers but would also aid in converting insoluble phosphates already in the soil to more usable form. Since the beginning of the eighteenth century, PSB-related research has been documented [52].

Bacilli and Pseudomonas stains are found to be the most efficient in Ecto-rhizospheric isolates, a bacterial community in soil. Most PSB may be found in the rhizosphere, and P solubilizers from the rhizosphere act more metabolically than those from other sources. There are several distinct types and populations of PSB, which vary from soil to soil. The bacterial population in 1g of fertile soil ranges between 100 to 1,000 bacteria, which are present in many shapes and sizes, like bacilli (rod, 0.3–0.5 µm), spiral (1–100 µm), and cocci (sphere, 0.5 µm) [53].

Therefore, it may be possible to develop more effective biofertilizer agents by identifying the underlying genetic pathways and working to improve their rhizosphere competency. Phosphorus solubilization with bacteria depends on the creation of metabolites such organic acids, which can chelate cations linked with phosphates with their carboxyl and hydroxyl groups [54].

Hormones for plant growth including auxin, gibberellins (GA1, GA3, GA5, GA18, and GA19), and abscisic acid have been reported to be secreted by the novel strain Bacillus tequilensis, and inoculation with this strain has been proven to develop plant biomass, leaves structure, and photosynthetic pigment in soybean in heat stress. An increase in jasmonic acid concentration and salicylic acid amount was also detected in the rhizosphere, but the amount of stress abscisic acid decreased [55]. *Pseudomonas plecoglossicida* isolated from soybean rhizosphere, is an example of a recently identified elite strain that can be used as a biofertilizer to solubilize large amounts of phosphate and create hormones required for the development of plants which include indole acetic acid at levels as high as 38.89 ppm. The strain of *Gordonia terrae* is known for its ability to

solubilize phosphorus to an extent of 299.3 mgL^{-1} under extreme brine conditions, i.e., 1.5 M NaCl concentration. Through interaction with the host immune system, the bacterial hormone indole acetic acid inhibits fungal pathogen growth [56] [57].

2.4 Mechanism of Phosphorous Solubilization through PSB

The primary focus of phosphorus solubilization mechanisms is the regulation of critical parameters of the phosphorous cycle in soil, including dissolution-precipitation, mineralization-fixation, and adsorption-desorption [58]. These components are not only associated with microbial strains but also governed by phospholipids-related genes. Acids and enzymes are secreted by most phosphate-solubilizing bacteria, which can also form chelates or complex metal ions (Ca^{+2}, Fe^{2+}, Al^{3+}) in the soil to liberate phosphate ions. This process mineralizes or hydrolyzes the insoluble phosphate ions in the soil. There are a few of PSBs that can alter the pH of the environment by the release of gases like CO_2 to solubilize unavailable phosphorous. PSB has a tendency to maximize phosphorus accumulation in soils by modifying the microbial community within the soil. The diversity of the microbial community and the associated enzymes are increased by PSB in the soil, which in turn alters the phosphorus composition of the soil and improves crop yield [59] (Figure 2.5).

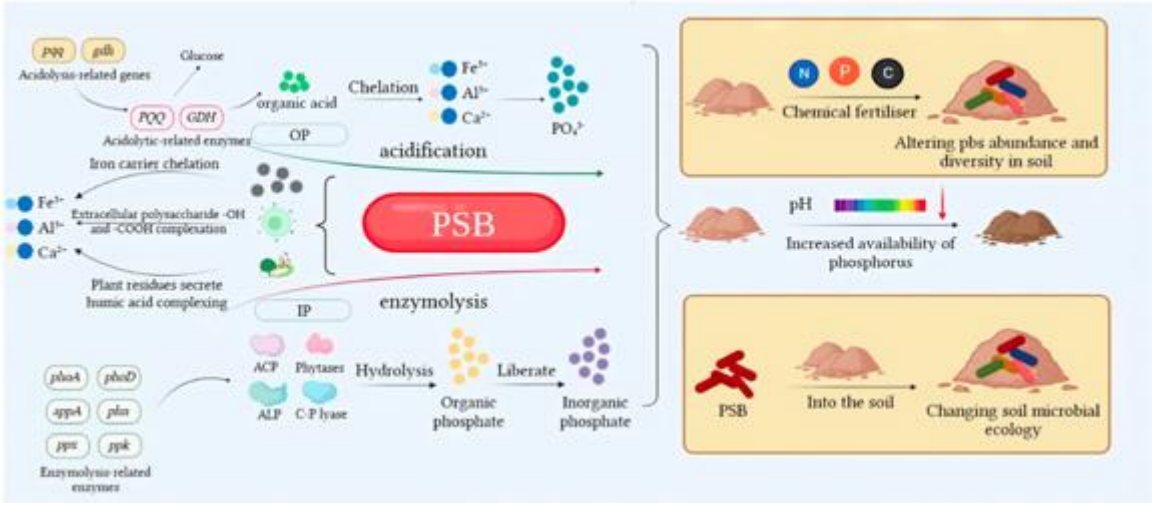

Figure 2.5: Mechanism of Phosphorous Solubilization [51]

The solubilization mechanism of PSB is changed by altering structure and occurrence of bacterial communities in the soil, which are discussed below:

2.4.1 Physiological Mechanism

2.4.1.1. Solubilizing Mechanism of Acids

The mechanism of both organic and inorganic acids is involved in acidolysis; the majority of PSB secrete organic acids, while only a small number secrete inorganic acids. During the growth process, PSB bacteria have the capacity to secrete a variety of lower molecular weight organic acids, like malic acid, acetic acid, succinic acid, tartaric acid, fumaric acid, propionic acid, glutamic acid, 2-ketogluconic acid, saccharinic acid, lactic acid, and oxalic acid [60]. Under low pH conditions, these low-molecular-weight organic acids can chelate with metal ions in the soil (Ca^{2+}, Fe^{2+}, Al^{3+}) through hydroxyl and carboxyl groups [61]. They can compete with phosphate ions for adsorption sites in the soil due to their Ca^{2+} chelation ability, which is their most important trait. Both the solubilizing capacity of inorganic phosphorus and the uptake of phosphate by the soil is increased because of this disparity, which ultimately leads to an increase in the solubility and availability of mineral phosphates [62]. Nevertheless, the adsorption capacities of various organic acids for phosphate are significantly different, and distinct PSBs produce different types of organic acids (Table 2.1). A small number of PSBs also secrete inorganic acids, such as hydrochloric, sulfuric, nitric, and carbonic acids. These acids are capable of dissolving inorganic phosphorus and lowering the soil pH. When compared to organic acids, however, they do not perform as efficient at same pH level [63].

Table 2.1: Organic acids secreted by different PSBs

Phylum	**PSB Species**	**PSB Source**	**Secreted Organic Acids**	**Reference**
Proteobacteria	Enterobacter aerogenes	Mangrove rhizosphere soil	Lactic acid, succinic acid, isobutyric and acetic acid	[64]
Firmicutes	Bacillus	Rice paddy soil	Citric acid, Gluco-oxalic	[65]

			acid, Succinic acid	
Actinobacteria	Tsukamure-llatrosinosolvens	Tea tree rhizosphere soil	Lactic acid and maleic acid	[66]

It is PSB that secretes organic molecules that influence the roots of plants. This rhizosphere effect, which involves an increase in the bacterial communities and relative abundance of controlling bacteria in the rhizosphere zone, has an indirect impact on the amount of phosphorus that is accessible in the soil [67]. Although the acidic environment that is produced by organic acids compatible for the enrichment of PSBs, it is also rather specific. Take, for example, the bacteria Pseudomonas fluorescens WCS365, which is capable of colonizing tomato roots and may be responsive to both citric and malic acids [68]. Watermelon roots produce citric and malic acids, which enhance the colonization of roots by the rhizosphere microbial strain Bacillus polymyxa SQR-21 [69].

It is possible to significantly improve the mechanism of phosphate solubilization through research into the synthesis of organic acids in the interaction between the plant root system, the PSB network, and the plant root system.

There have been several studies that have found that the release of organic acids is one of the primary ways that PSB operates; nevertheless, there are still some people who have alternative opinions. During their research, Zhao and colleagues came to the realization that the phosphorus-solubilizing capacity of PSB did not have any connection with the amount of organic acid present in the medium [70]. A strong association between the ability of bacteria to solubilize phosphate and the secretion of organic acids was not always shown to exist, according to the findings of this study. In addition, the crucial mechanism that exists between organic acids and bacteria that are capable of phosphate-solubilizing was not completely investigated, and it is necessary to conduct additional research on this topic.

2.4.1.2 Mineralization Action of Enzymes

PSB is responsible for the secretion of enzymes that are responsible for the mineralization of organophosphorus, which is one of the key processes of

dephosphorylation (Table 2.2). There are a few enzymes that have been found to have a dephosphorylating action, the most prominent of which are phytases, phosphatases, and C-P enzymes. It has also been established in many trials that PSB boosts enzyme activity in the soil, which ultimately increases the amount of phosphorus that is available in the soil [71]. However, the mineralization of organic phosphorus is influenced by various hydrolytic enzymes in distinct ways. Phosphatase, which is also referred to as phosphomonolipase, is primarily encoded by olpA and is organized into three types: acidic, alkaline, and neutral phosphatases [72]. ACP is more effective in mineralizing organic phosphorus in acidic soils with pH values below 7. Alkaline phosphatases, also known as ALPs, are enzymes that are largely responsible for the hydrolysis of phospholipids (such as phosphoglucose-6 and ATP) and the release of inorganic phosphorus in soils that have a pH of more than 7. In contrast, neutral phosphatases do not have a significant impact on phosphorus mineralization and hydrolysis, as opposed to acid and alkaline phosphatases. Phytase is an additional type of phosphatase that is primarily responsible for the mineralization of organic phosphorus in phytate [73].

Table 2.2: Different enzymes secreted by PSBs

PSB Species	**PSB Source**	**Secreted Enzymes**	**Source**
Pantoea sp.	Forest soil	Phytase	[74]
Enterobacter sp.	Rhizosphere soil of bamboos	ACP	[75]
Pseudomonas asiatica	Ant hill soil	ALP	[76]
Burkholderia sp.	Zea mays soil	ACP	[77]

2.4.1.3 Chelation and Complexation

Chelation and complexation are two fundamental processes that play a role in phosphorus solubilization. These mechanisms are based on the idea that the functional group binds to

metal cations in the soil, which then releases phosphate and makes it easier for phosphorus to be dissolved [78]. The degradation of plant and animal wastes, the formation of siderophores by phosphorus-solubilizing bacteria, and the utilization of extracellular polysaccharides are the keyways that are now utilized for the processes of chelation and complexation. Siderophores are molecules that are quite small and have a low relative molecular weight. Phosphate-dissolving bacteria create siderophores that chelate Ca^{+2}, $Fe^{3+,}$ and Al^{3+} in the soil, thereby releasing phosphate ions for phosphate dissolution. This occurs when the amount of iron stress in the soil is low [79]. As a result of the formation of metal-iron carrier complexes, these complexes have the capability of binding to iron carrier receptor proteins that are located on cell membranes, which enables them to enter cells. The uptake of iron by plants is facilitated by this mechanism, which also accelerates the growth of the plants. PSB is responsible for the secretion of extracellular polysaccharides, which are sugar polymers with a high molecular weight that are linked to the surfaces of bacteria [80]. Anions, such as phosphate, carboxyl, and succinate groups, as well as numerous -OH and -COOH acid groups on the surface of these polymers, can form complexes with the metal cations that are present in the soil. PSB is responsible for the production of compounds that are like humic acid during the process of degrading plant and animal wastes. In addition, these chemicals can chelate Ca^{+2}, Fe^{3+}, Al^{3+} in the soil, which results in an increase in the amount of phosphorus that is available and the release of phosphate [81].

2.4.2 Molecular Mechanism

The molecular mechanism of PSB is also crucial, in addition to the physiological mechanism that it possesses. It is important to note that the research community does not yet have a thorough understanding of the molecular mechanism that underlies the PSB pathway [82]. Because of this, the mechanism of PSB metabolism is gradually developed by the integration of several functional genes and the metabolites that they regulate [83].

2.4.2.1 Functional Genes Related to the Regulation of Acidolysis

The synthesis and secretion of organic acids are the key processes by which PSB solubilizes phosphorus. This is even though the mechanism of acidolysis has not been thoroughly studied [84]. Among the genes that have been discovered as potential regulators of phosphate solubilization, only a limited number of genes have been

identified. These genes include pyruvate dehydrogenase (poxB), glyoxylate reductase (gyaR), l-lactate dehydrogenase (ldh), and 6-ketoglucuronate reductase (ghrB) [85]. The research that has been done on the TCA cycle and the acidolysis mechanism of PSB is limited, and additional research is required to acquire a complete understanding of these topics [86].

2.4.2.2 Functional Genes for Enzymolysis

There are several enzymes that are encoded by several carrier genes in PSB. These enzymes include alpha-phosphatases, phytase, acid phosphatases , extracellular polyphosphatase, C-P cleavage enzyme , and polyphosphate kinase. Alkaline phosphatases, specifically phoD and phoA, have been the subject of a significant amount of research among these enzymes [84]. There are three gene families (phoA, phoD, and phoX) that are identical to one another, and each of these gene families is responsible for determining the generation of alkaline phosphatase in PSB. Pho regulator is comprised of these genes in its entirety [87].

2.4.3 Mechanisms of Microbial Community Effects

Research that is currently being conducted on PSB mechanisms focuses primarily on microorganisms. Furthermore, in addition to the actions that are carried out by bacteria, changes in the nutrients that are present in the soil also have a specific influence on the phosphorus-solubilizing activity that bacteria have. In addition, the interaction between PSB and native microorganisms in the soil can have a direct impact on the composition and activity of soil microorganisms, which in turn means that the process of phosphorus conversion in the soil can be altered.

2.4.3.1 Influence of Soil Nutrients on the Occurrence of PSBs

A direct correlation exists between the population abundance of PSB and the phosphorus-solubilizing capacity of PSB. This population abundance is closely related to the nutrient cycling that occurs in the soil. Externally applied fertilizers can improve soil nutrients and influence the number of bacterial populations that are capable of dissolving phosphates. This is accomplished through the use of pH and C:N:P stoichiometry [88]. The ratios of carbon, nitrogen, and phosphorus content in the soil are the main factors that influence changes in the composition and activity of PSB [89]. Multiple experiments have successfully verified that the continuous and external introduction of inorganic

phosphorus, biochar, and organic carbon leads to an increase in pH. Additionally, the presence of PSB communities is found to be positively associated with pH, biomass, phosphorus content, and phosphorus uptake [90] [91]. However, the impact of applying nitrogen fertilizer on the number of PSB communities is not very evident.

2.4.3.2 Influence of PSB on Soil Microbial Systems

The biodiversity and microbiological makeup of soil are adversely affected by current agricultural techniques, which are also unsustainable [92]. PSB, on the other hand, has a more favorable impact on soil microbes. The incorporation of PSB into soils can impact the diversity and population of the native microbial community. While the presence of PSB may increase the amount and variety of microorganisms, certain studies have proved that the application of PSB leads to a notable reduction in the amount of the indigenous microbial community, an increase in the population of the inoculated PSB, and an elevation in the soil phosphorus content [93]. There exists a favorable correlation between the number of bacterial communities and the growth of certain compounds connected to the phospholysis mechanism, such as phosphatase and phytase [94]. Hence, the involvement of the bacterial community in the process of phosphorus solubilization can be indirectly enhanced through the interaction between PSB and native microorganisms [95] [96].

2.5 Overview of Machine Learning Models

As part of this research work, supervised machine learning models have been utilized. These models employ regression techniques to produce predictions regarding the quantity of phosphorous that has been solubilized. For the purpose of developing a model that can accurately anticipate output, approaches such as Genetic Algorithm (GA) and Particle Swarm Optimization (PSO) are utilized.

2.5.1 Genetic Algorithm

An evolutionary algorithm that models the process of biological evolution is referred to as a genetic algorithm (GA). In 1975, Holland put up an idea that may be applied to genetic algorithms. The theory of evolution proposed by Charles Darwin, which mimicked the preservation of superior species and the genes of those species, affected

genetic analysis. A great number of scholars have made use of generalized estimating equations to evaluate the resolution of difficult problems whose performance parameters do not possess the characteristics of continuity and differentiability.

An algorithm that works with a collection of solutions rather than selecting a single answer is called a genetic algorithm. This type of algorithm is a population-based feature selection type of algorithm. From the beginning, the population is selected, and each solution is encoded as a chromosome of genes or bits. A population is a collection of solutions, and each and every chromosome has its own fitness value. When all of these chromosomes are joined, they are referred to as a population.

The concepts of genetic inheritance and natural selection serve as the foundation for this method, which is known as an inhabitant's algorithm. Each set of solutions represents a chromosome, and each parameter represents a gene in the organism. Fitness is an objective function that is used by GA to measure the fitness of each individual member of the population. In order to improve solutions that are not satisfactory, a selection strategy is utilized to select the best possibilities in an arbitrary manner. Furthermore, throughout the process of selecting wrong replies, there is a greater possibility of avoiding local optimal solutions. It is necessary to repeat this process until either an optimal solution is found, an extreme integer of repetitions or population is understood, or a 15-point variance between solutions is smaller than a limit that has been defined. Because it retains the finest solutions in each iteration and makes use of them to improve succeeding possibilities, this method is dependable and can calculate the global optimal solution for a particular problem.

2.5.2 Particle Swarm Optimization (PSO)

PSO is a swarm-based stochastic algorithm that was initially introduced by Kennedy and Eberhart. It takes advantage of the principles of the social behavior of animals, such as fish schooling and bird flocking, to solve problems [97]. In PSO, every possible answer to a certain problem is viewed as a particle with a specific velocity that is moving through the space of the problem in the same manner as a flock of birds are moving through the space. Each particle then combines, with some random disturbances, some aspect of the record of its own historical best location and present location with those of one or more

agents of the swarm to calculate its next movement through the search space. This process is repeated until the desired movement was determined. When all of the particles have been relocated, the subsequent iteration will take place. It is likely that the swarm (for example, a flock of birds that are all looking for food together) will eventually get closer and closer to the optimal value of the objective function. PSO has finally been quite popular among researchers and has emerged as a method that offers great performance in a variety of application areas. It also can hybridize and specialize, as well as exhibit some emergent features that are interesting. One of the primary benefits of PSO is that it requires fewer parameters to be tuned. Particle swarm optimization (PSO) can get the optimal solution because to the interaction of particles; nevertheless, due to the high-dimensional search space, it converges at a relatively slow speed towards the global optimal solution. In addition, it produces findings of poor quality when applied to datasets that are both complex and extensive. There is a high probability that PSO will not be successful in locating the global optimal solution when the problem at hand contains a significant number of dimensions. It is not only the presence of a local optima trap that is responsible for this phenomenon; it is also the potential fluctuation of the velocities of particles that causes the consecutive range of trials to be bounded inside a sub-plain of the overall search hyper-plain [98].

2.5.3 Ensemble Learning Tree

Tree-based models that anticipate output by applying logical principles are the foundation of the decision tree, which is the machine learning technique that is utilized the most to this day. Instead of relying on a previous correlation between the input and output properties, it generates a regression model that is based on the tree structure of the conditional statement. Decisions are made by DT based on the attributes included within the dataset in order to divide the data into more manageable categories [99].

2.5.4 Gaussian Process Regression

GPR is a Bayesian tool that is implemented as an efficient learning model for the purpose of solving nonlinear regression issues. In addition to making predictions, this method is also capable of delivering the coefficient of determination for each prediction point. This coefficient is a measurement of the uncertainty associated with the forecast [100]. It is possible that probability distributions could be categorized as Gaussian processes. In

order to determine the probability of an input vector, the mean and variance of a Gaussian distribution are utilized in the calculation. The GPR model generates a mean and correlation vector rather than a scalar mean and variance. This makes the model more accurate. GPR provides a method for directly and quantitatively adjusting the locality of the interpolation, which is embedded in the assumption that the interpolation is smooth [101].

CHAPTER 3 OBJECTIVES

1. Optimization of polymer concentration for PSB coating
2. Synthesis of coated DAP fertilizer using fluidized bed coater
3. Microbial Survival Evaluation of coating solution and coated product
4. Physical and Chemical analysis of PSB and polymer-coated fertilizer
5. Pot test experiment and analysis
6. Development of a machine learning model for prediction of P uptake in plants using phosphorus-solubilizing bacteria

CHAPTER 4 MATERIALS AND METHODS

Coating materials and coating techniques are discussed in this chapter. Characterization techniques and pot trials are also described.

4.1 Materials

Phosphate Solubilizing Bacteria (*Bacillus Velezensis* FB2 strain) , Polyvinyl Alcohol, Tryptone, Agar, Yeast, NaCl, DAP fertilizer, urea and water were used in the experiments.

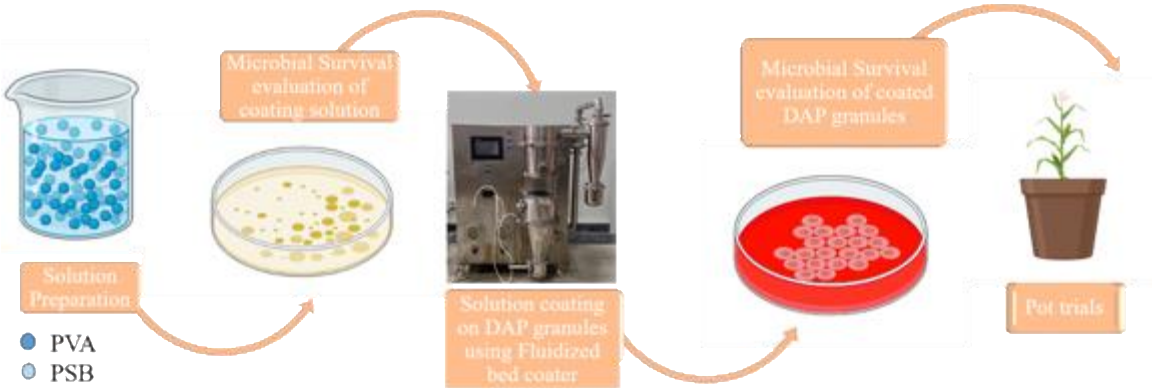

Figure 4.1: Experimental Design Methodology

4.2 Determination of Optimum Polymer concentration

Different solutions of Phosphate Solubilizing Bacteria (PSB) and Polyvinyl Alcohol (PVA) were specifically formulated. The PVA composition was experimentally altered in these solutions to determine the optimal composition for maximizing microbial viability. Table 4.1 provided lists several concentrations of the evaluated solution. The total volume of solution was maintained at 25ml.

Table 4.1: Composition of solutions

Solution No.	Quantity of PSB	PVA Concentration
1	1ml	0.5%
2	1ml	1%
3	1ml	1.5%

4.3 Microbial Survival Evaluation

500ml of LB agar was prepared using 5g tryptone, 10g agar, 2.5g yeast, 5g NaCl, and 500ml of distilled water. The solution was prepared in a 1L media bottle to keep it half empty and prevent it from boiling in an autoclave. The solution was thoroughly mixed by whirling. The bottle was capped properly and covered with aluminum foil. The solution was placed in an autoclave for 30-60 minutes at around 15 psi.

The solution was detached from the autoclave and after letting it slightly cool down it was poured into plates. The plates had been autoclaved before this step. Pouring must be done aseptically before the solution gets solidified.

The aperture of the bottle was thoroughly heated, and a sterile pipette was used. To prevent air bubbles, gradual pouring was started. This was done in Laminar Flow Hood to avoid any contamination. Petri dishes were covered and were allowed to cool down and harden. Plates were inverted to prevent moisture from dripping into the agar.

The plates were left in LFH for 24 hours. After that, the previously prepared solution was poured over the solidified plates drop and the plates were sealed again using a parafilm. The sealed plates were kept in a shaking incubator for 72 hours at 25 ± 3^0C.

4.4 Preparation of coated DAP fertilizer

At the Product Technology Laboratory of SCME, National University of Science & Technology, Islamabad, di-ammonium phosphate (commercial DAP) fertilizer [$(NH_4)_2$ HPO_4] with 46% P_2O_5 and 18% N was coated with an optimized polymer and bacteria solution. The DAP granules were coated using the YC-1000 Mini Spray Granulator (Shanghai Pilotech Instrument & Equipment Co., Ltd, China). The apparatus was made from Bosiloricate Glass and stainless-steel SUS 304. A 0.3 kg quantity of DAP granules was processed at a time, with a spray nozzle situated just below the fluidized bed that contained the feed. In the spray granulator, DAP granules with a spherical shape and a diameter of 2-4mm were employed. The coating solution was prepared by stirring 1.5% Polyvinyl alcohol and 4% PSB in 100 ml of de-ionized water at a constant temperature of 60°C for 30 minutes using a magnetic stirrer and a hot plate. The coating sample was atomized by pressurized air from an air compressor, and the granules were fluidized using hot air in a mini spray granulator. The peristaltic pump was employed to transfer the coating sample via a nozzle. After the coating was completed, the granules were removed from the bed and allowed to dry for 15 minutes [102].

4.5 Microbial Survival Evaluation of coated granules

Agar plates were prepared following the same procedure stated above. Coated granules were placed over solidified plates and placed in a shaking incubator for 72 hours at 25 ± 3^0C.

4.6 Physical and Chemical analysis of PSB and polymer-coated DAP

4.6.1 Scanning Electron Microscopy (SEM)

The morphology of the sample was investigated by analyzing the granular surface using a Scanning Electron Microscope (SEM). The coated samples were also cross-examined with DAP granules that were not coated for reference beforehand. Coated granules were

generated in an ion-sputtering machine before examination. The Ion Sputtering Machine JFC- 1500 of JEOL Ltd. was used to perform gold sputtering on DAP granules. The particles were gold-coated to a depth of 250 angstroms. The surface of the sample granules was analyzed using a secondary electron detector at an accelerating voltage of 10 kV [102].

4.6.2 X-ray diffraction (XRD)

The STOE Germany apparatus was used to conduct X-ray diffraction (XRD) of both uncompacted and compacted DAP granules. XRD was conducted to verify the crystallinity of all products that were developed. The scan angle ranged from 10º to 90º. The step measure and step time were set at 0.4 degrees and 1 second, respectively. The radiation employed for the illustration was Cu K α-1 [103].

4.6.3 Fourier Transform Infrared (FTIR)

Fourier Transform Infrared(FTIR) Spectroscopy of coated granules was done using an FTIR Perkin Elmer Spectrum 100 spectrometer. The presence of functional groups is indicated by the FTIR results. The bond formation in the biodegradable anionic polymer was investigated by analyzing the polymer within the 400 to 4000cm^{-1} range [103].

4.6.4 Crushing Strength

The objective of crushing strength analysis is to ensure that the DAP granules can withstand the transition from the production stage to the marketing and selling phase. Crushing experiments were conducted on compacted DAP granules using Universal testing equipment (AGX Plus). Compacted DAP granules were randomly selected from the sample set. During the experiment, DAP granules were subjected to a predetermined level of tension using a metal plunger. The observed force at the point of fracture of DAP granules served as an indicator of its strength. In general, this test was conducted on the primary particle size of DAP granules. The experiment involved the interaction of the DAP granules with a metal pusher and a predetermined stress intensity. The force at which the DAP granules ruptured was used to assess their rigidity. Typically, this experiment was conducted on the larger granules [103].

4.6.5 Phosphorous Release Rate Analysis of DAP granules

4.6.5.1 UV-Visible Spectrophotometry

Using the Ammonium Molybdenum Blue Method, the rate and efficiency of phosphorus release from PSB and polymeric-coated DAP was evaluated. The calibration curve was initially established using Analytical grade Potassium Dihydrogen Phosphate (99.9% Pure) with a GENESYST™ 20 UV-Visible spectrophotometer. Standardized solutions of Potassium Dihydrogen Phosphate of analytical grade (10ppm, 20ppm, 30ppm, 40ppm, 50ppm, 60ppm, 70ppm, and 80ppm) were prepared in advance to determine the slope of the established calibration curve. An ultraviolet-visible spectrophotometer was used to measure the absorbance of the standard solution. Thereafter, a calibration graph is generated by plotting the absorbance against the known phosphorous content. The dissolution rate of coated DAP was evaluated using the following test procedure [106].

4.6.5.2 Test Protocol

Sample DAP grains weighing 10 grams were placed in a 1-liter glass beaker containing deionized water. Following that, 1 ml of the sample was extracted from the middle of the beaker at time intervals of 1 hour, 2 hours, 3 hours, 4 hours, and 1 hour. The sample was then transferred into a 25 ml volumetric flask for absorbance measurement using a UV-Visible Spectrophotometer technique. The beaker was agitated for 15 seconds prior to sample collection. After transferring a 1 ml sample into a 25 ml volumetric flask, proceed to add 2 ml of solutions of Ammonium Molybdate (2.5 %) and 0.5 mL of Sulfuric Acid (10 N). Thoroughly agitate the reaction mixture. Next, introduce 1 mL of a 0.5 M hydrazine hydrate solution into it, together with de-ionized water, to get a correct volume. Incubate the solution for 45 minutes to get optimal color development. A wavelength of 840 mm was employed to measure absorbance to determine the unknown concentration of phosphorous in coated DAP, as well as the release rate and efficiency [106].

4.6.6 Nitrogen Release Rate Analysis of DAP granules

To determine the Nitrogen release rate of DAP granules, the extracted sample of 1mL and 0.5 mL of para-dimethyl amino benzaldehyde and 0.1 mL of HCL were added into a 25mL beaker. The prepared solution was analyzed in a spectrophotometer using a wavelength of 418nm to determine absorbance, which was then used to calculate

unknown Nitrogen concentration in coated DAP and release rate efficiency using Eq. 1 and Eq. 2 respectively [107].

$$N\ or\ P\ Concentration\ (ppm) = absorbance - \frac{Y-intercept}{Slope\ of\ calibration\ curve} \quad \text{Eq.1}$$

$$Efficiency\ (\%) = \frac{C_u - C_c}{C_u} \quad \text{Eq.2}$$

4.7 Pot Test Experimentation

4.7.1 Experiment Location

The department of agronomy, PMAS-Arid Agriculture University, Rawalpindi, Pakistan, was selected as a research site for experimental work. It is located at an altitude of 508 m, with latitude and longitude of 33.6492 °N and 33.6492 °E, respectively, from sea level. The temperature of the region may fluctuate between -4 and 25 °C in the winter and up to 40 °C in the summer. Rainfall is inconsistent and primarily contingent upon the season, with storms occurring frequently between July and August.

4.7.2 Design of Experimental Work

A completely randomized design (CRD) was used to place the pots in the study area. The study region included five treatments and six replications. This research location was also the source of the soil that was collected. There are 27 centimeters in the diameter of the pot and 0.057 square meters in its area. At the time of planting, each pot was filled with 18 kg of soil, and 101:72:47 $kghc^{-1}$ NPK ratio was used. The maize used in the experiment was grown from seed with 7 seeds per pot. Trimming was done after seed germination to keep three plants per pot. Every pot was watered daily to keep it at 60% moisture.

4.7.3 Treatments

Table 4.2: Different treatments of DAP used in Pot Trials

Nomenclature	Treatment	DAP (g/pot)	Urea (g/pot)
C	Control		
T_1	Uncoated DAP	0.845	0.906
T_2	PSB Coated DAP	0.905	0.906
T_3	PVA Coated DAP	0.897	0.906
T_4	PSB+PVA coated DAP	0.906	0.906

4.8 Plant Analysis

The maize plants were gathered after the ultimate harvest of the crop. Root and shoot analysis requires their segregation. The plant stem is cut for additional examination. To fully remove the dirt from the roots, separating them from the soil is necessary. Place the bundle of roots in a water bath and let them soak for two hours. Soil around roots breaks down after a heavy watering, and roots are able to pull themselves out from the soil. The following section will cover the parameters that will be estimated following the crop harvest.

- Height of the Plant
- Steam diameter
- Area of leaf
- Number of leaves
- Plant fresh yield
- Plant dry yield
- Total Phosphorous uptake
- Total Nitrogen uptake

4.8.1 Plant height

The height of the maize crop was estimated following the harvesting. Three plants were selected from every pot for this purpose, and their height was measured in centimeters using a measuring tape.

4.8.2 Plant diameter

After the maize crop was harvested, the diameter of the plant was estimated. Three plants were selected from every pot for this purpose, and the diameter of each plant was measured using a Vernier caliper.

4.8.3 Number of leaves

Number of leaves for each plant were counted and recorded.

4.8.4 Area per leaf

To measure leaf area, three leaves were selected, and their length and width were measured from random points using measuring tape. It was converted to area.

4.8.5 Plant fresh yield

The fresh weight of the crop is promptly measured following its harvest. Plants are chopped into tiny pieces to determine their fresh weight. The fresh weight of plants can be measured in grams using a weight balance. Roots were separated from soil and were soaked in water for 2hrs. After washing them fully, their fresh weight was taken.

4.8.6 Plant dry yield

Plant samples including shoots and roots were dried at 70^0C for 72hrs or till constant weight. Dry weight was measured using a weight balance.

4.8.7 Plant Total Phosphorous

Ammonium molybdenum solution was used as color developing solution and was mixed with digested samples. Phosphorous content was measure by measuring absorbance of sample at 840nm.

4.8.8 Plant Total Nitrogen

The nitrogen content of the plant is determined using the Kjeldahl apparatus. Add 5 g of ground dry plant powder to the digestion tube. Following that, add 10 ml of concentrated sulfuric acid (H_2SO_4) and 3.5 g of digestion catalyst mixture. Carefully shake the mixture. Heat for a minimum of three hours at 420^0C. The subsequent procedure involves the distillation of ammonia using a 40% sodium hydroxide (NaOH) solution. Boric acid (HBO_3) is employed to capture and form the solvated ammonium ions. The titration is currently conducted with the assistance of 0.01N H_2SO_4.

$$\text{Nitrogen apparent recovery (\%)} = [(N_s \times DM_s) - (N_0 \times DM_0)]/TN_\alpha$$

N_s= Nitrogen content in maize plant samples

DM_s= Maize DM yield (Kg ha^{-1})

N_0= Maize nitrogen content in control treatment

TN_α= Total amount of applied Nitrogen

4.9 Soil analysis

Three samples of the initial soil and the sample collected after the final harvest of the crop are used to assess the impact of DAP fertilizer on the chemical characteristics of the

soil. Soil analysis includes the measurement of pH, Electrical Conductivity (EC), pH, Soil Organic Matter, Soil Mineral nitrogen, Soil Available Phosphorous, Soil Microbial Phosphorous. Table 4.3 shows the properties of the soil sample collected before experimentation.

Table 4.3: Initial Soil Properties

Parameter	**Value**
Soil pH	7.89
Soil EC	3.198 dS m^{-1}
Soil Organic Matter	4.01 g Kg^{-1}
Soil Mineral Nitrogen	9.08 mg Kg^{-1}
Soil Available Phosphorous	15.02 mg Kg^{-1}
Soil Microbial Phosphorous	6.02 mg Kg^{-1}

4.9.1 Soil pH

The pH of the soil was determined by utilizing a 2:1 ratio of water to soil suspension. To achieve this ratio, a soil-water suspension will be formed by mixing 20 g of soil and 40 ml of distilled water in a glass. The pH was determined using a pH meter after the solution was agitated for 30 minutes at 25 °C [106].

4.9.2 Soil Electrical Conductivity

The electrical conductivity of samples is measured using an EC meter, which is normalized with a 0.01 N KCl solution, using the same solution that is used to measure pH. [108]

4.9.3 Soil Organic Matter

In a 250 ml beaker, place 0.5 g of soil. This was followed by the injection of 5 mL of 1 N potassium dichromate solution and 10 mL of concentrated H_2SO_4. The soil in the treatment container was subsequently agitated to ensure that it was thoroughly mixed, resulting in a release of fumes. Allow the beaker to reach ambient temperature to eliminate fumes. The beaker solution will now be replenished with 5 mL of concentrated orthophosphoric acid and 100 mL of distilled water. Afterward, utilize a magnetic stirrer to ensure that the solution is thoroughly mixed. Insert 10-15 droplets of diphenylamine indicator and stir the solution until it turns violet blue. A ferrous ammonium sulfate

solution (0.5 M) was employed to titrate the solution. The completion of the titration is indicated by the appearance of an intense green color. All reagents will be mixed and titrated ferrous ammonium sulfate solution (0.5 M) will be used for the blank sample, which is devoid of soil. The formula for calculating the total organic carbon (TOC) of soil is as follows: [108]

$$\%Oxidizable\ Organic\ Carbon = \frac{\left[V_{blank} - V_{sample}\right] \times 0.3 \times M}{Weight\ of\ air - dry\ soil}$$

$$\%Total\ Organic\ Carbon = 1.334 \times Oxidizable\ Organic\ Carbon$$

M= Molarity of ferrous ammonium sulfate solution

V_{blank}= Volume of ferrous ammonium sulfate solution

V_{sample}= Volume of solution required to titrate the sample (ml)

4.9.4 Soil Mineral Nitrogen

Kjeldahl digestion was used to evaluate the nitrogen content of samples in all treatments. The digestion procedure was conducted in a digestion apparatus using 1 g of dried wheat samples and concentrated sulfuric acid. By incorporating a tri-acid mixture, the reaction temperature was progressively elevated to 145 °C for 1 hour. The temperature of the system was further elevated to 240°C. Subsequently, the mixture was allowed to settle to room temperature. The mixture was subsequently filtered using Whatman filter paper No. 42. The process was followed by distillation and titration. [108]

4.9.5 Soil available Phosphorous

Weigh 5 g of air-dry soil (2-mm) into a 250-mL Erlenmeyer flask. Add 100 mL of a 0.5 M NaHCO3 solution. Cover the flask with a silicone stopper and shake it on a shaker at 200–300 rpm for 30 minutes. Only one flask (Blank) should be included, which should contain all chemicals but not soil. Utilize a Whatman No. 40 filter paper to filter the suspension.

Transfer 10 mL of the clear filtrate to a 50-mL vial using a pipette. To acidify each 10 mL $NaHCO_3$ extract to pH 5, add 1 mL of 5 N H_2SO_4 to all the unknown solutions. Dilute the solution to a 40-mL volume by adding DI water. Then, add 8 mL of Reagent-B, agitate thoroughly, and then bring it to volume. In order to generate a standard curve,

Pipette 2 mL of each standard (1–5 ppm) and proceed in the same manner as the samples. Use 10 mL of a 0.5 M $NaHCO_3$ solution to create a blank and proceed in the same manner as the samples. The absorbance of the blank, standards, and samples should be measured on the Spectrophotometer at a wavelength of 882 nm after 10 minutes. Develop a calibration curve for standards by plotting the absorbance against the corresponding P concentrations. Utilize the calibration curve to determine the concentration of P in the unknown samples [108].

$$Extractable\ P\ (ppm) = ppm\ P\ (from\ calibration\ curve) \times \frac{V}{W_t} \times \frac{V_2}{V_1}$$

4.9.6 Soil Microbial Phosphorous

The microbial biomass phosphorus in soil was regulated through the application of a fumigation extraction technique (Reddy, 2008). Soil from the specimen weighing 5 g was transferred to a test tube and deposited in a desiccator with chloroform (ethanol-free) for 36 hours. Subsequently, the test containers should be extracted from the desiccator and placed in the water bath at 80°C for 120 minutes. The sediment from the test is subsequently transferred to the beaker. Next, introduce 25 ml of 0.5 M NaHCO3 solution and maintain constant agitation of the solution in a swirling round inoculator for 2 hours. The solution was filtered using Whatman no. 42 filter paper. For non-fumigated samples, combine 5 g of soil with 25 ml of 0.5 M NaHCO3 solution. The solution was thoroughly agitated to obtain the clear filtrate, and Whatman no. 42 filter paper was employed. In order to quantify microbial phosphorous, add 1 mL of extract to a test tube and 2.5 mL of color developing solution. A spectrophotometer was employed to quantify the optical density of phosphorus [110].

4.10 Machine Learning Model development

Figure 4.2 shows the methodology that was adopted for the development of the machine learning model in this research study. In the present study, data is gathered from a complete literature review of experimental experiments that have been published related to phosphorous solubilization using phosphorous solubilizing bacteria. The primary factors that were retrieved from the literature include bacteria species, fertilizer used, crop, soil pH, soil available phosphorus, and amount of phosphorus solubilized. Following the completion of the process of collecting data from linked publications, the

process of extracting feature data and categorizing it was finished in order to construct and test machine learning models.

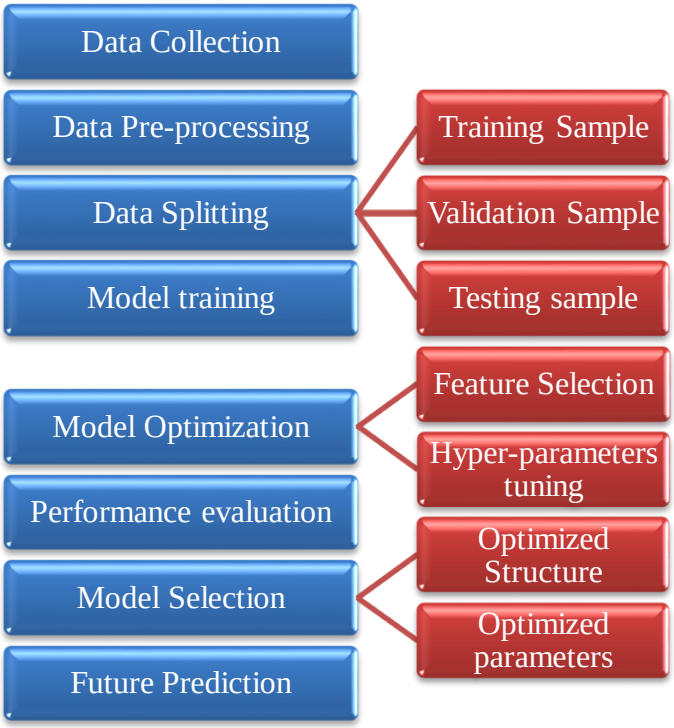

Figure 4.2: Machine Learning Strategy Workflow

MATLAB was used to import data from excel sheet. Data was preprocessed using MATLAB code to fill missing data, remove outliers and to smooth data.

Using MATLAB code different machine learning models were trained to analyze the developed model on the basis of R-square value, RMSE, MAE values. Data was further modified through feature selection to optimize results. Hyper tuning parameters were determined and the model was optimized using the optimal value of the hyper tuning parameter.

4.11 Statistical Analysis

Statistical Analysis was carried out using Python and MATLAB by Analysis of Variance (ANOVA). Tukey's Honest Significant Difference Test was performed to statistically analyze effect of treatment for each variable. All graphs were plotted using MATLAB and Origin Software.

CHAPTER 5 RESULTS AND DISCUSSION

5.1 Microbial Survival Evaluation

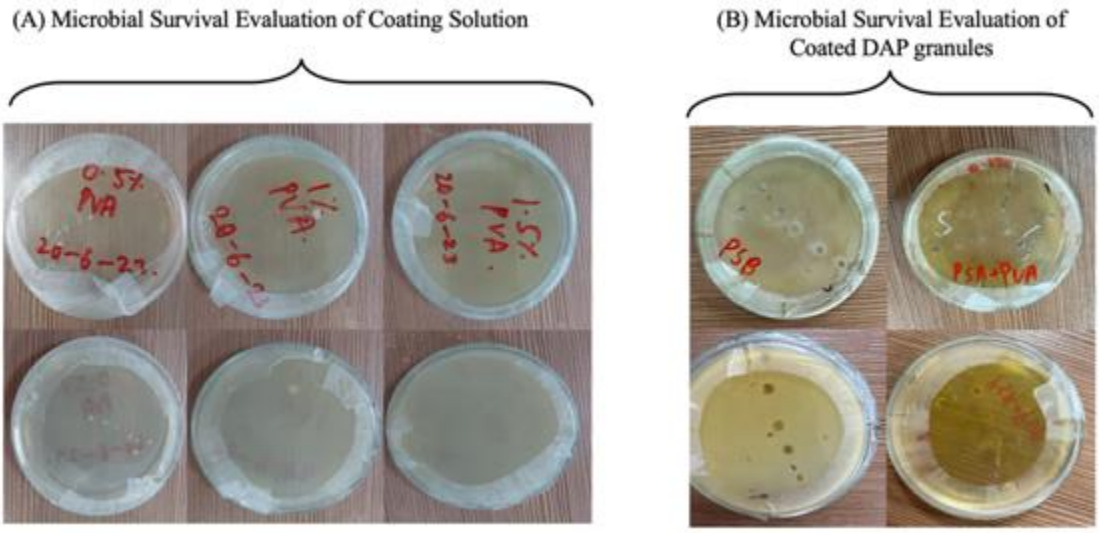

Figure 5.1: Microbial Survival Evaluation (a) Coating Solution (b) DAP Granules

Following the evaluation of the coating solution on agar plates, the microbial activity that was observed is shown in Figure 5.1. There were three different concentrations of polyvinyl alcohol (PVA) used in the preparation of microbial solutions: 0.5%, 1%, and 1.5%. When the concentration of PVA was 0.5%, the highest level of microbial activity was found. DAP granules were coated with this solution. In order to determine the microbial activity of the DAP granules, they were subjected to another round of testing after being coated with a microbial solution. Additionally, microbial activity can be seen around each of the coated DAP granules illustrated in Figure 5.1 (b). Additionally, it was discovered that bacteria were able to survive the coating procedure.

5.2 Physical and Chemical analysis of PSB and polymer-coated DAP

5.2.1 Scanning Electron Microscopy (SEM)

The technique of scanning electron microscopy was used in order to analyze the morphological structure of both coated and uncoated DAP granules. To determine the shape and formation of an outer coating layer on DAP granules, the coated surface and its

formation was investigated. The scanning electron micrograph (SEM) depicts uncoated DAP granules at three distinct magnification levels, which are respectively *33, *5000, and *2000. In Figure 5.2(a), a scanning electron micrograph (SEM) of DAP granules coated with PSB is displayed at several levels of magnification. On granules of DAP that have porous surfaces, the existence of the film can be observed. The presence of bacteria causes pores to be formed and causes the coating film to be broken. The SEM image of DAP granules that have been coated with PVA is shown in Figure 5.2 (b). A coating layer can be seen to have tiny pores on the surface. Due to the presence of PVA, the structure of the coating was similar to that of a chain network that was cross-linked. The SEM image of DAP granules that have been coated with both PSB and PVA is shown in Figure 5.2 (c). In certain areas, the coating thickness is greater than in others because of the irregular structure of the DAP granules. As can be observed, the coating has a more compact appearance.

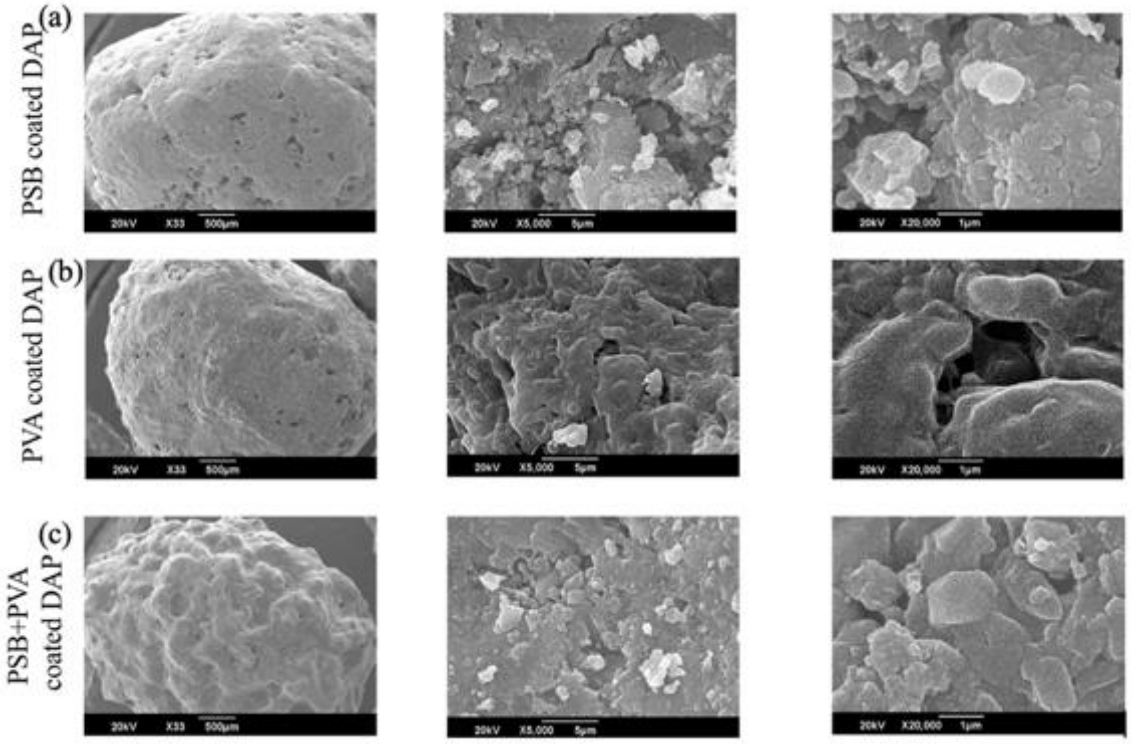

Figure 5.2: SEM Micrographs of coated DAP fertilizer

5.2.2 X-ray diffraction (XRD)

For the purpose of analyzing the crystalline properties of coated DAP granules, X-ray diffraction (XRD) is an extremely useful technique. It was noted that the typical diffraction peaks of DAP granules were located at 16-18.2 degrees, 26-29 degrees, and 32-35.5 degrees in the XRD pattern as illustrated in Figure 5.3. The peaks that were more prominent were observed within the 16° to 36° range. The XRD spectra of coated DAP granules, which are displayed in Figure 5.3, all had prominent peaks that were comparable to those of uncoated DAP. Peaks exhibited a high degree of crystallinity, which led to the formation of a transparent coating on DAP granules at the same time. There were no significant variations in the location or intensity of the peaks between the spectrum of coated DAP granules and the spectrum of uncoated DAP granules found in the spectrum. Due to the absence of new peaks in the coated DAP grains, it is possible that no new phases were formed or that the structure underwent deformation during the coating process. Slight variations in peak sharpness were observed in the case of PVA coating.

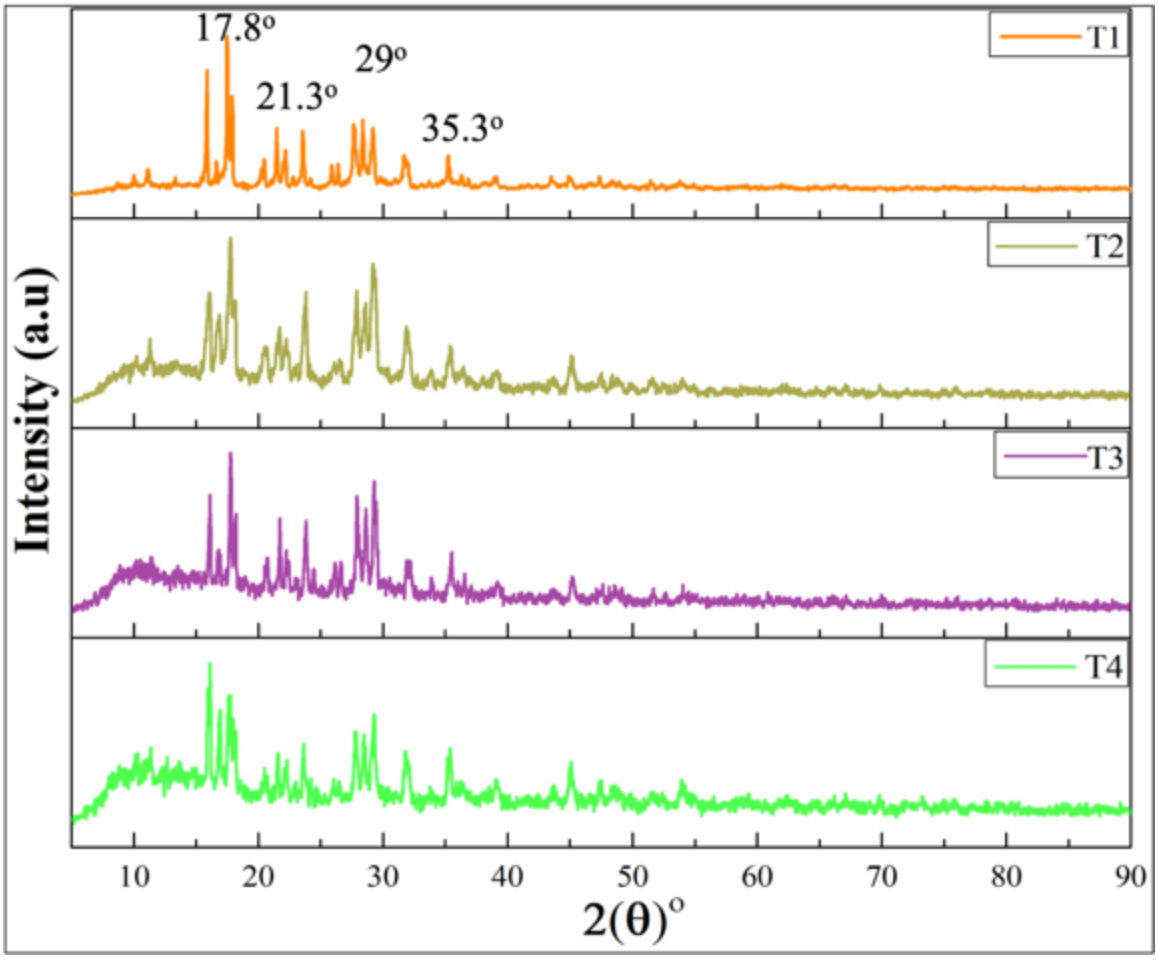

Figure 5.3: XRD Pattern of coated DAP fertilizer. T1_Uncoated DAP, T2_DAP coated with PSB, T3_DAP coated with PVA, and T4_DAP coated with PSB and PVA.

5.2.3 Fourier Transform Infrared Diffraction (FTIR)

A FTIR spectrum of DAP granules that have been coated with PSB is shown in Figure 5.4. Considering that the coating of bacteria is primarily associated with amide groups that are visible at 1550 cm-1, the C–H stretching vibrations of lipids and fatty acids that come from bacteria can be observed in a band that extends from 2850 to 2950 cm^{-1}. The stretching of the phosphate group may be observed at 1000-1100 cm-1, but this stretching has been shifted because of the microbial coating. In the case of DAP coated with PVA, as illustrated in Figure 5.4 the stretching vibrations of the O–H bond, which are obtained from the hydroxyl groups of polyvinyl alcohol, are observed in this FTIR spectrum at a range of 3200 to 3600 cm^{-1}. PVA coating has been identified to be present as a result of

this. There is a visible P–O stretching for the DAP phosphate group at around 1000–1100 cm^{-1}; however, the degree of this stretching has been broadened as a result of the PVA coating.

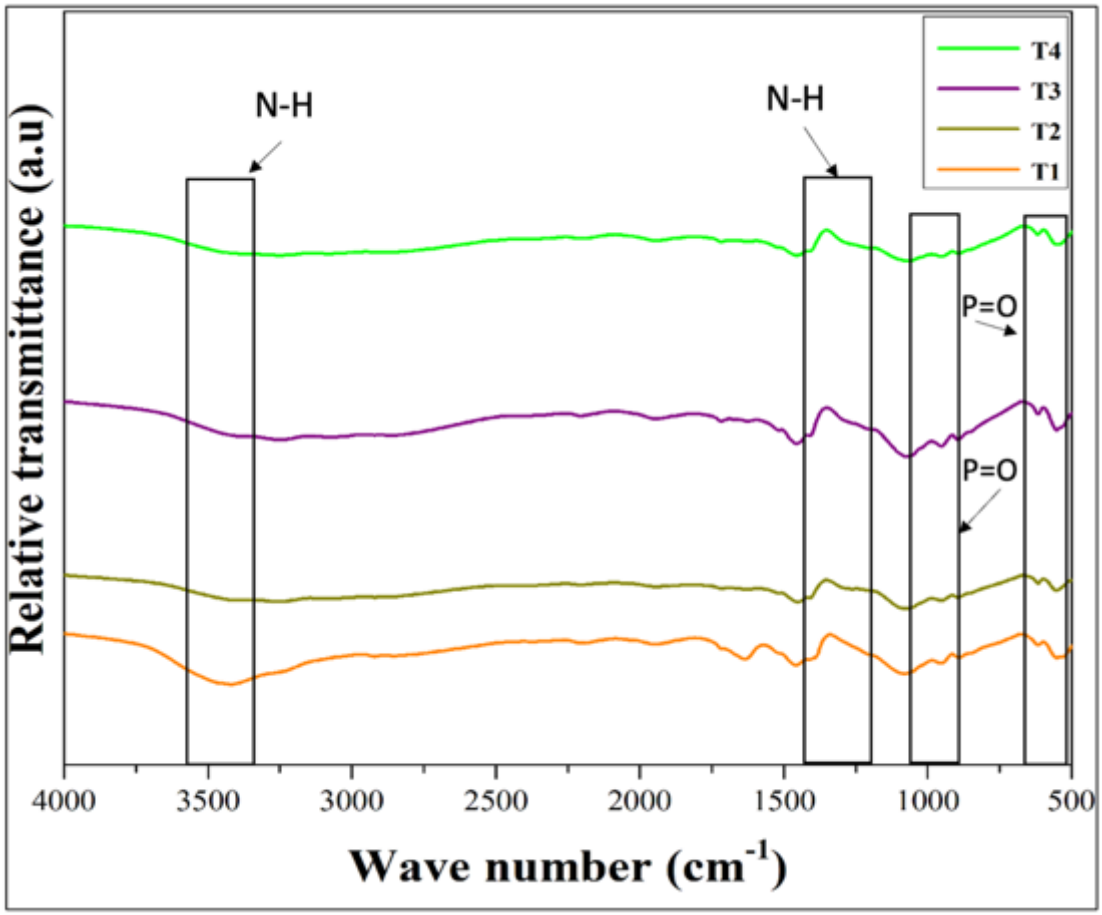

Figure 5.4: FTIR Spectrum of Coated DAP fertilizer.T1_uncoated DAP, T2_DAP coated with PSB, T3_DAP coated with PVA, and T4_DAP coated with PSB and PVA.

5.2.4 Crushing Strength

Following the application of the coating, if the granular DAP were to fracture, the availability of nutrients such as nitrogen and phosphorus would be comparable to that of granular DAP that did not contain any coating material applied. The samples that have higher impact resistance against all odd forces will be preferred from the point of view of storage, bagging, and shipping as they are more likely to be preserved. For this research

study, DAP was coated with different coating materials. These coatings were then put through a series of tests in which they were subjected to pressure using a tensile tester until they broke. Following its passage through the universal testing equipment, the crushing strength results are presented in Figure 5.5. The final reading was taken at the point in time when the DAP granules were totally crushed into a powder. The granules of uncoated DAP were crushed with a force of 28.573 N. It was found that the crushing strength of PVA-covered DAP was the highest. The cross-linked structure of PVA is the reason for this phenomenon. By increasing the crushing strength of the material through the use of effective coating materials, the efficiency of the storage and transportation processes will be improved. When compared to the industrial-grade product that is already on the market, the average force required to crush polymer-coated granules is significantly higher. Therefore, the utilization of coating substances resulted in an increase in the compressive resistance of granules because of this.

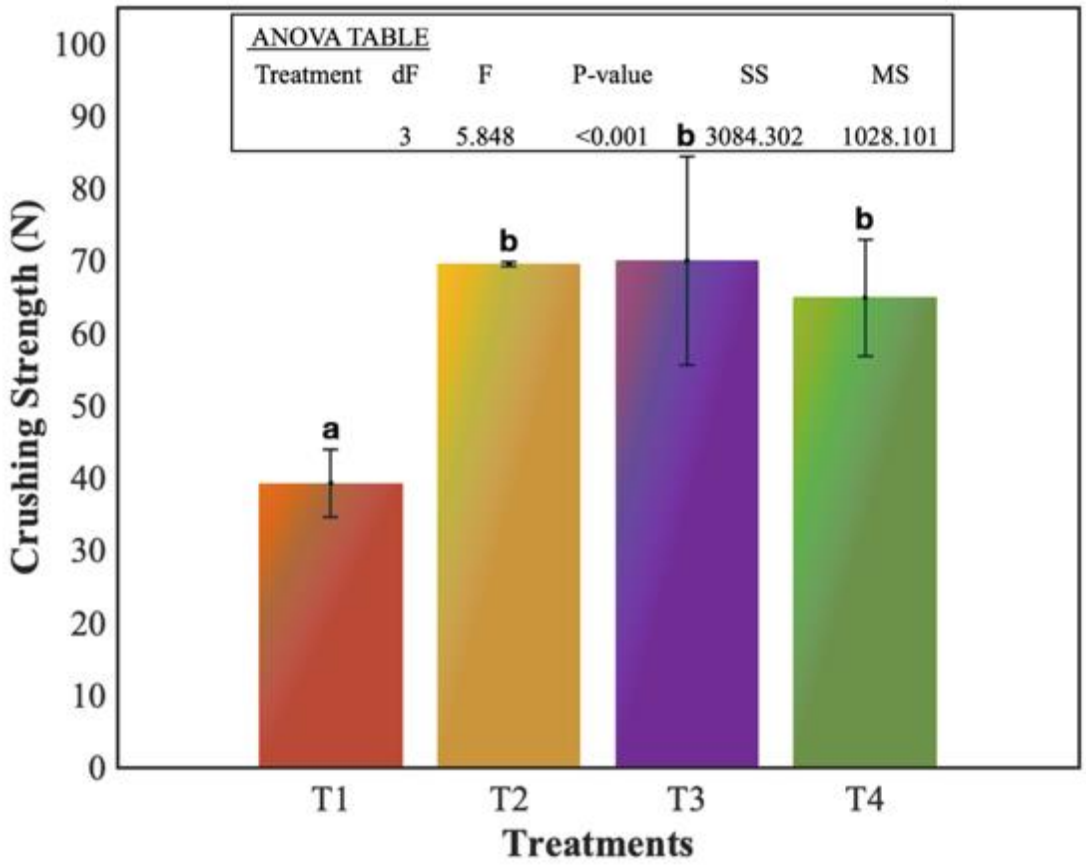

Figure 5.5: Crushing Strength of different fertilizer treatments. T1_uncoated DAP, T2 _ DAP coated with PSB, T3 _ DAP coated with PVA, and T4 _ DAP coated with PSB and PVA.

5.2.5 Phosphorous Release Rate Analysis of DAP granules

The mechanism by which phosphorous is released from DAP granules when they come into contact with water is shown in Figure 5.6. When it came to the release of phosphorous, a similar pattern was observed in nitrogen. It was noticed that there was a quick release of phosphorous when there was no coating present. This occurred because of the exposed bare surface, which allowed a greater penetration of water molecules from the surrounding environment. However, the degree of efficiency varied depending on the type of coating material. Although all coating materials were successful in slowing down the rate at which phosphorous was released, the degree of effectiveness varied accordingly. This observation happened to come about as a result of the presence of a

coating layer, that acts as a barrier to the release of nutrients from DAP granules. In comparison to DAP that had not been coated with PSB, DAP which had been coated with PSB was able to reduce the rate of phosphorus release to a greater level. The polyvinyl alcohol coating caused a further decrease in the rate of release because of its presence. The reason for this is that the cross-linked structure of PVA prevents it from releasing nutrients as quickly as it would otherwise. When both coatings were used together, there was an even greater reduction in the rate of release that was observed.

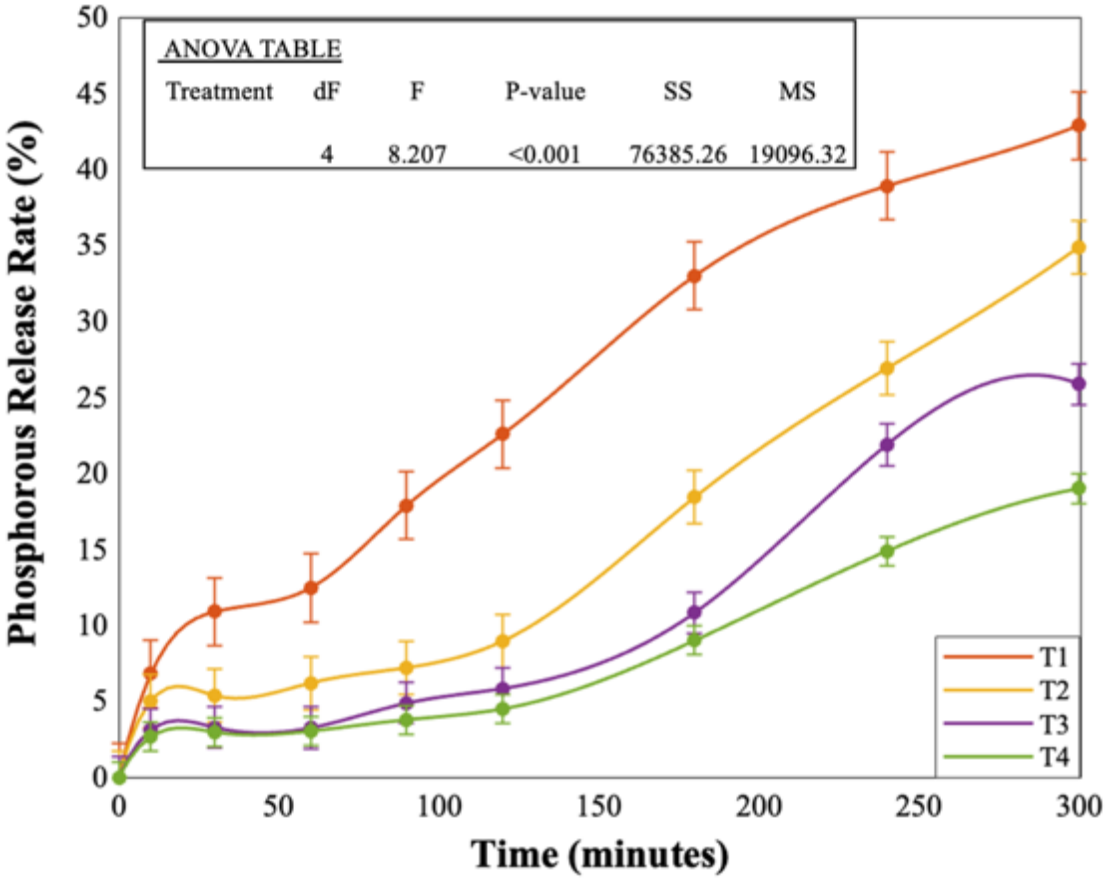

Figure 5.6: Release rate kinetic for Phosphorous release rate of DAP fertilizer. T1_ uncoated DAP, T2_DAP coated with PSB, T3_DAP coated with PVA, and T4_ DAP coated with PSB and PVA. One-way ANOVA was performed for statistical analysis of data. Error bars represent the standard error.

5.2.6 Nitrogen Release Rate Analysis of DAP granules

The objective of this analytical technique was to evaluate the rate of nitrogen release after the coating application on DAP granules. After adding the coated DAP granules to the deionized water, the test was carried out successfully. To make comparisons with coated granules, uncoated granules were investigated as well. The pattern of how coated DAP responds when in contact with water was demonstrated by the release rate of DAP granules. This test also evaluates the effectiveness of coating materials which inhibit the release of nitrogen and phosphorus.

Figure 5.7 illustrates the pattern of nitrogen release from uncoated and coated DAP granules. The concentration of nitrogen was measured at various time intervals, and the results were used to calculate the release rate. This was accomplished by comparing the differences in concentration that occurred at two separate time intervals. The absence of a coating on the uncoated DAP caused it to release its nitrogen in a short amount of time. This occurred as a result of the exposed bare surface, which allowed for a larger penetration of water molecules. All coating materials were successful in slowing down the rate at which nitrogen was released, however, the degree of effectiveness varied depending on the type of coating material. The presence of a coating layer, which acts as a barrier to the release of nutrients from DAP granules, was responsible for this observation.

To a greater extent than uncoated DAP, the release rate of nitrogen was slowed down by DAP that had been coated with PSB. An additional drop-in release rate occurred by the polyvinyl alcohol coating. This is because the cross-linked structure of PVA causes it to slow down the release of nutrients. Further reduction in release rate was observed when both coatings were utilized when combined.

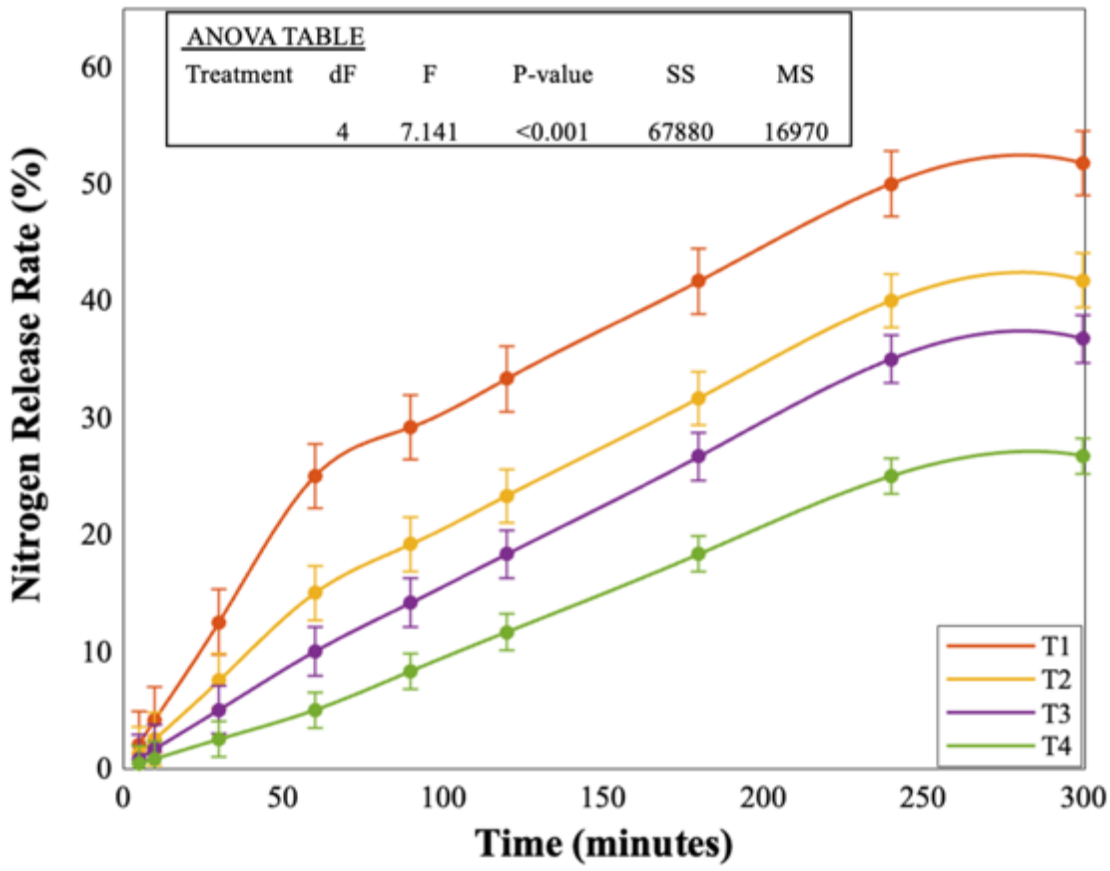

Figure 5.7: Release rate kinetic for Nitrogen release of DAP fertilizer. T1_uncoated DAP, T2_DAP coated with PSB, T3_DAP coated with PVA, and T4_DAP coated with PSB and PVA. One-way ANOVA was performed for statistical analysis of data. Error bars represent the standard error.

5.3 Plant Analysis

5.3.1 Plant height

Figure 5.8 illustrates the impact that various types of coated DAP have on the height of plants. It can be seen in the figure that the T4 treatment resulted in the highest plant height (158.17±14.17), followed by the T2 treatment (150.66±2.16). In the control group, the lowest plant height (60.83±18.68) was measured.

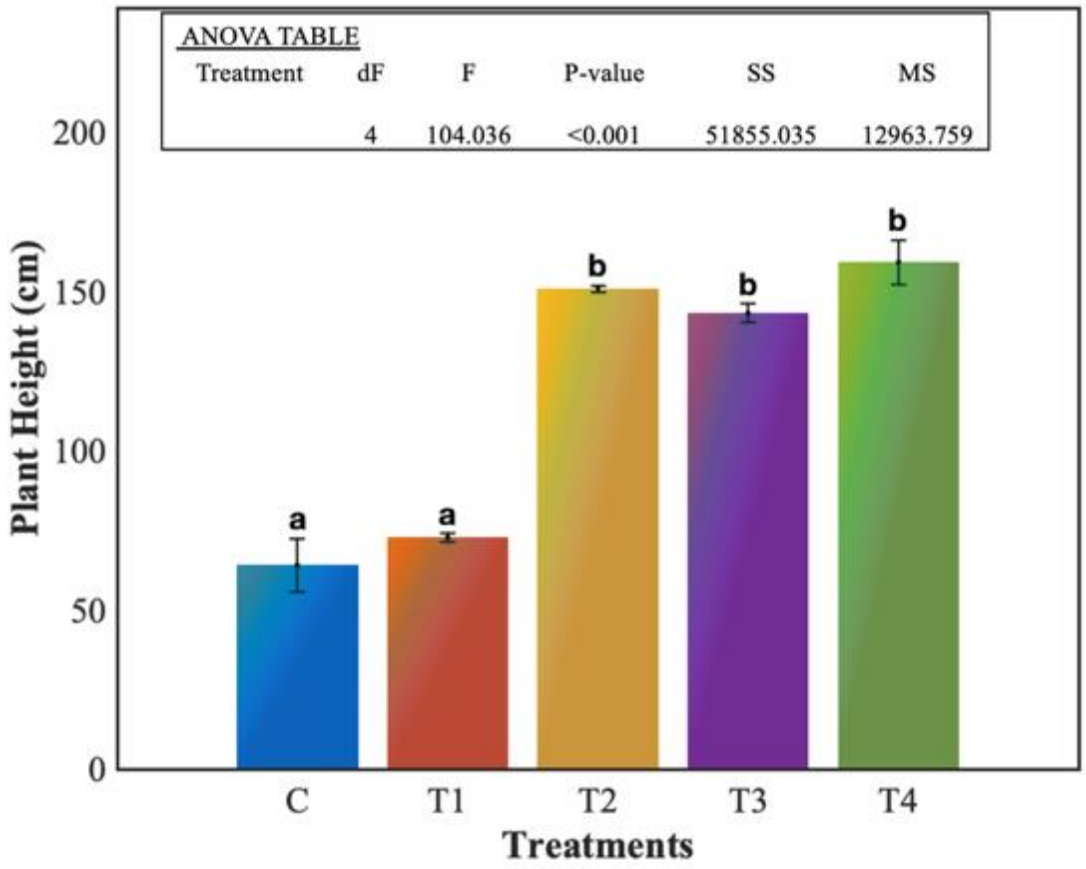

Figure 5.8: Effect of different DAP treatments on Plant height. C_Control, T1_uncoated DAP, T2_DAP coated with PSB, T3_DAP coated with PVA and T4_DAP coated with PSB and PVA. One-way ANOVA was performed for statistical analysis of data. Error bars represent the standard error of the mean (n=6).

5.3.2 Plant Diameter

Figure 5.9 illustrates the impact that various types of coated DAP have on the diameter of plants. It can be seen in the figure that the T4 treatment resulted in the highest plant diameter (1.13±0.09), followed by the T2 treatment (1.09±0.08). In the control group, the lowest plant diameter (0.62±0.21) was depicted.

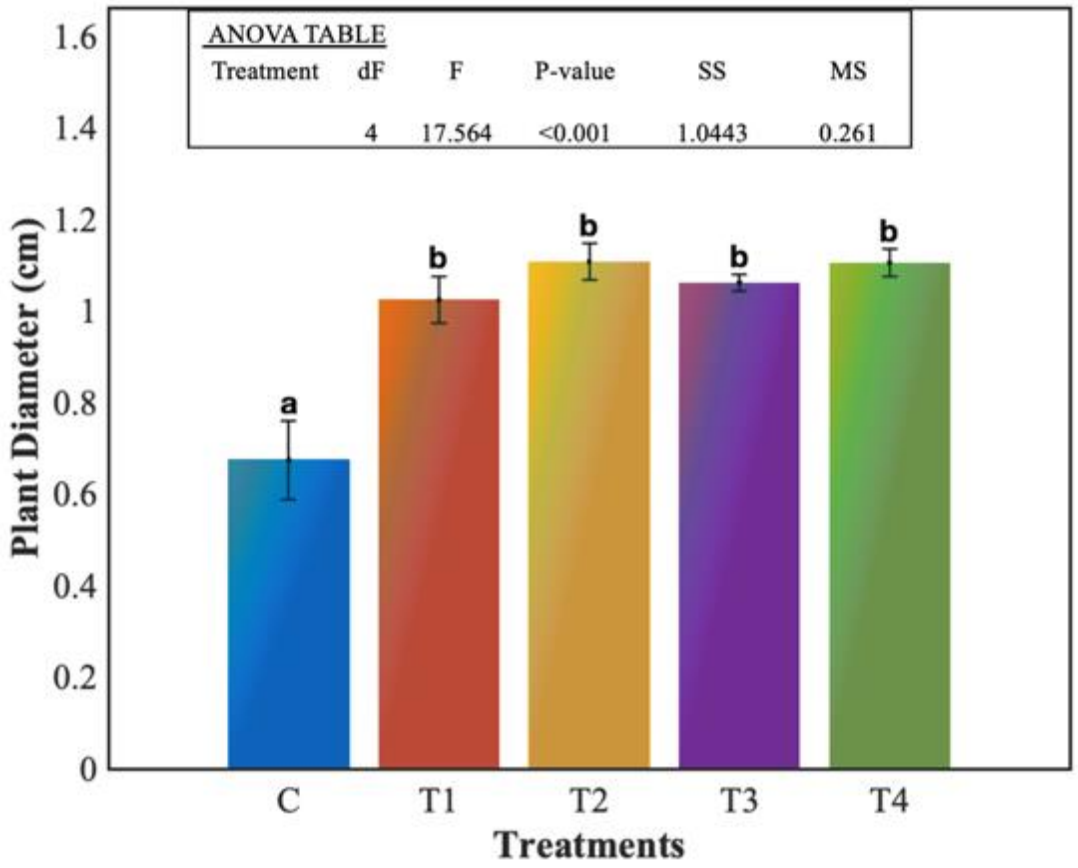

Figure 5.9: Effect of different treatments on Plant diameter. C_Control, T1_uncoated DAP, T2_DAP coated with PSB, T3_DAP coated with PVA, and T4_DAP coated with PSB and PVA. One-way ANOVA was performed for statistical analysis of data. Error bars represent the standard error of mean (n=6).

5.3.3 Number of leaves

Before plants were harvested, the number of leaves in each pot was counted. Highest number of leaves were counted to be in T3 (16±2.3) followed by T2 (15±3.9) as shown in Figure 5.10.

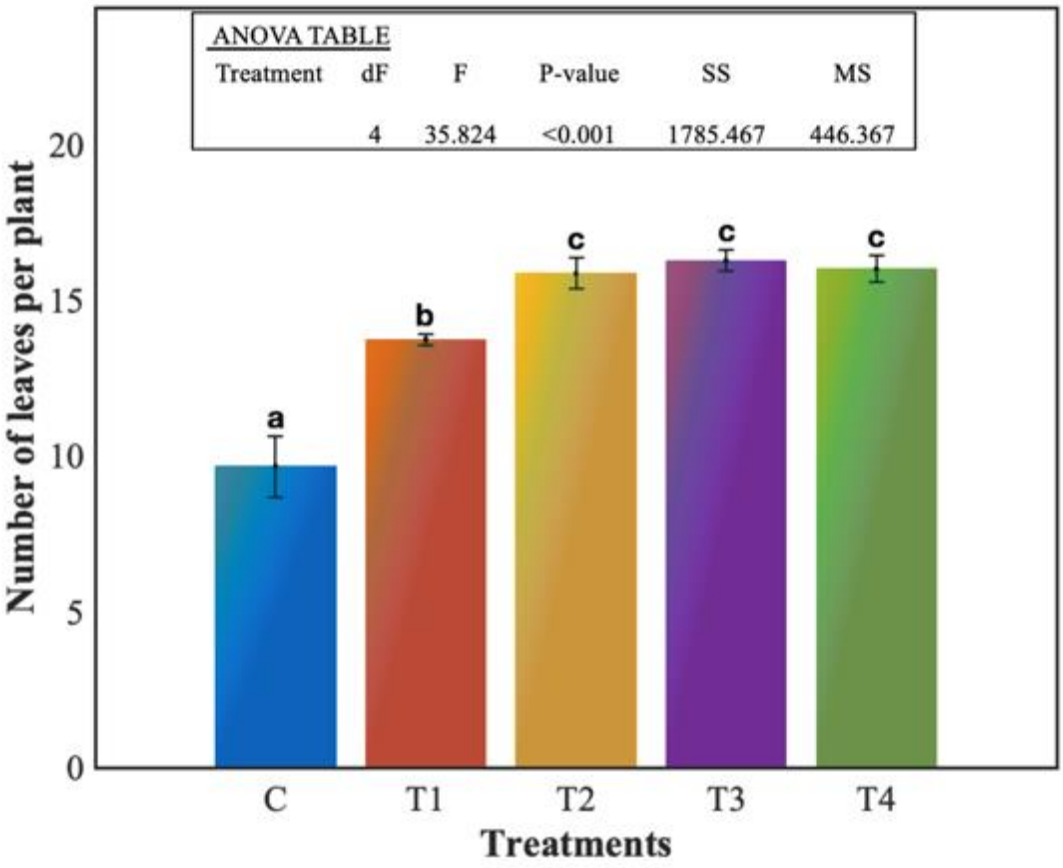

Figure 5.10: Effect of different treatments on Number of leaves. C_Control, T1_uncoated DAP, T2_DAP coated with PSB, T3_DAP coated with PVA, and T4_DAP coated with PSB and PVA. One-way ANOVA was performed for statistical analysis of data. Error bars represent the standard error of mean (n=6).

5.3.4 Area per leaf

Figure 5.11 illustrates the impact that various types of coated DAP have on the area of leaves. It can be seen in the figure that the T4 treatment resulted in the highest area of leaves (263.88±30.18), followed by the T2 treatment (245.61±36.62). In the control group, the lowest plant diameter (99.24±34.58) was depicted.

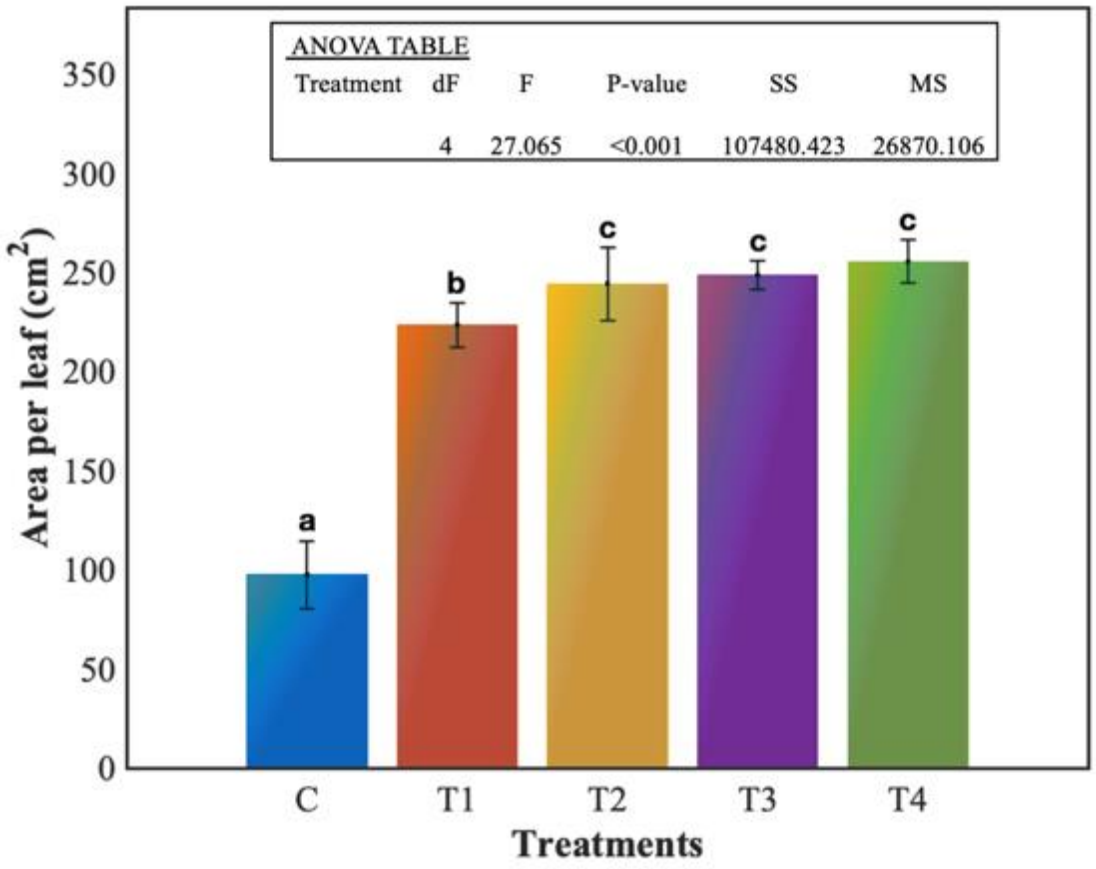

Figure 5.11: Effect of different DAP treatments on Area of leaves. C_Control, T1_uncoated DAP, T2_DAP coated with PSB, T3_DAP coated with PVA, and T4_DAP coated with PSB and PVA. One-way ANOVA was performed for statistical analysis of data. Error bars represent the standard error of the mean (n=6).

5.3.5 Plant Fresh Yield

The impact that various types of coated DAP have on the amount of fresh matter that is produced is illustrated in Figure 5.12. As can be shown in the figure, the T4 treatment yielded the highest amount of shoot fresh matter (327.67±28.10) followed by the T2 treatment (319.33±66.83). The lowest shoot fresh matter yield (153.17±98.34) was observed in the control group. The highest root fresh matter yield was recorded in T4 (429.00±96.46), followed by T2 as the second highest (292.00± 148.56). The root fresh matter yield in the control was found to be the lowest (95.17± 64.75).

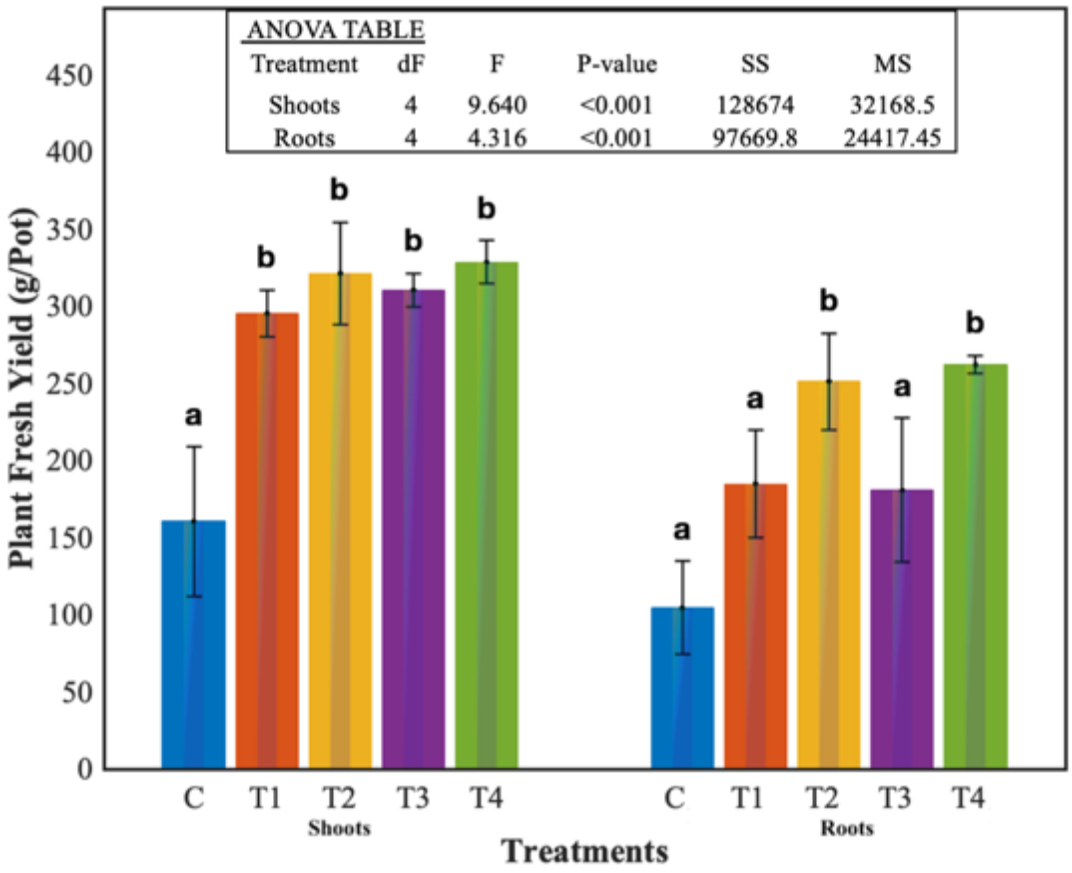

Figure 5.12: Effect of different treatments on Plant fresh yield. C_Control, T1_uncoated DAP, T2_DAP coated with PSB, T3_DAP coated with PVA, and T4_DAP coated with PSB and PVA. One-way ANOVA was performed for statistical analysis of data. Error bars represent the standard error of mean (n=6).

5.3.6 Plant Dry yield

The impact that various types of coated DAP have on the amount of dry matter that is produced is illustrated in Figure 5.13. As can be shown in the figure, the T4 treatment yielded the highest amount of shoot dry matter (60.17± 9.62) followed by the T2 treatment (46.5 ± 7.55). The lowest shoot dry matter yield (31.5± 17.34) was observed in the control group. The highest root dry matter yield was recorded in T4 (78.33 ± 25.97), followed by T2 as the second highest (71.33 ± 29.65). The root dry matter yield in the control was found to be the lowest (20.33 ± 13.35).

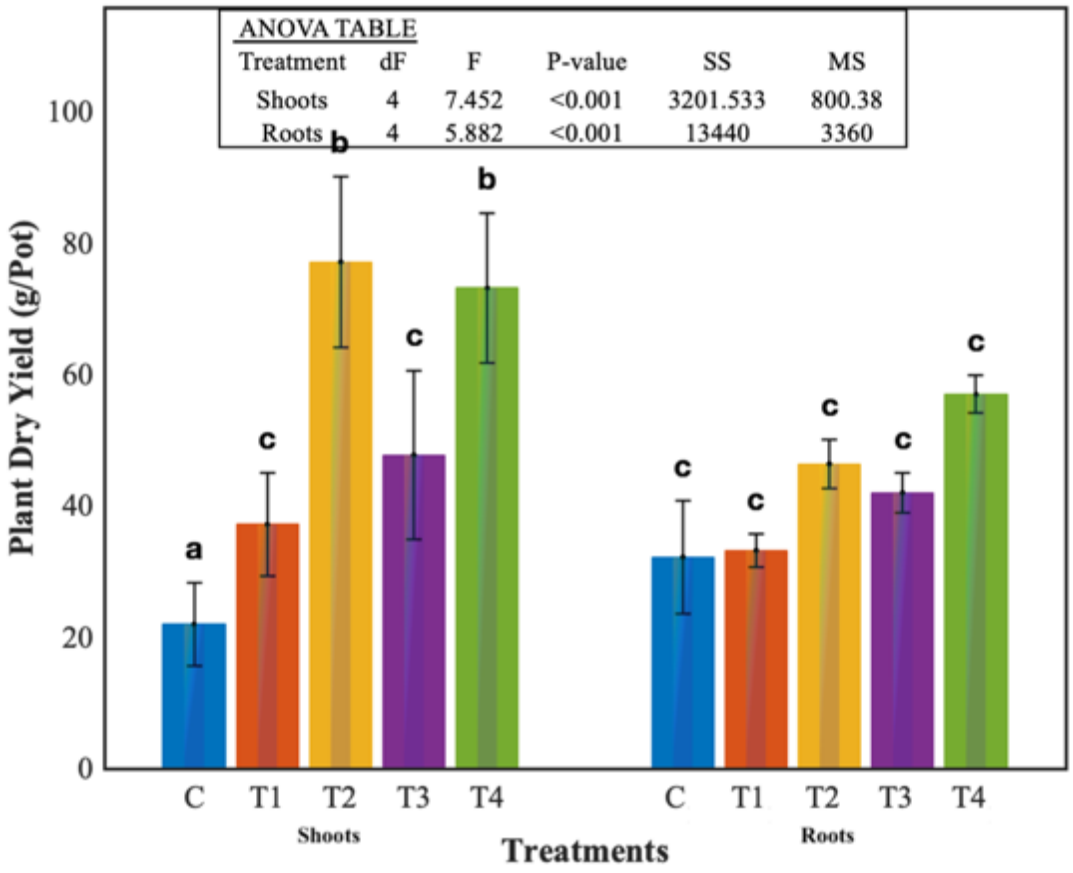

Figure 5.13: Effect of different treatments on Plant dry yield. C_Control, T1_uncoated DAP, T2_DAP coated with PSB, T3_DAP coated with PVA and T4_DAP coated with PSB and PVA. One-way ANOVA was performed for statistical analysis of data. Error bars represent the standard error of mean (n=6).

5.3.7 Plant total Phosphorous

The effect that various types of coated DAP have on total phosphorous content in plants is shown in Figure 5.14. As can be shown in the figure, T2 yielded the highest Phosphorous content (0.98 ± 0.031) in shoots, followed by T4 (0.85 ± 0.019).

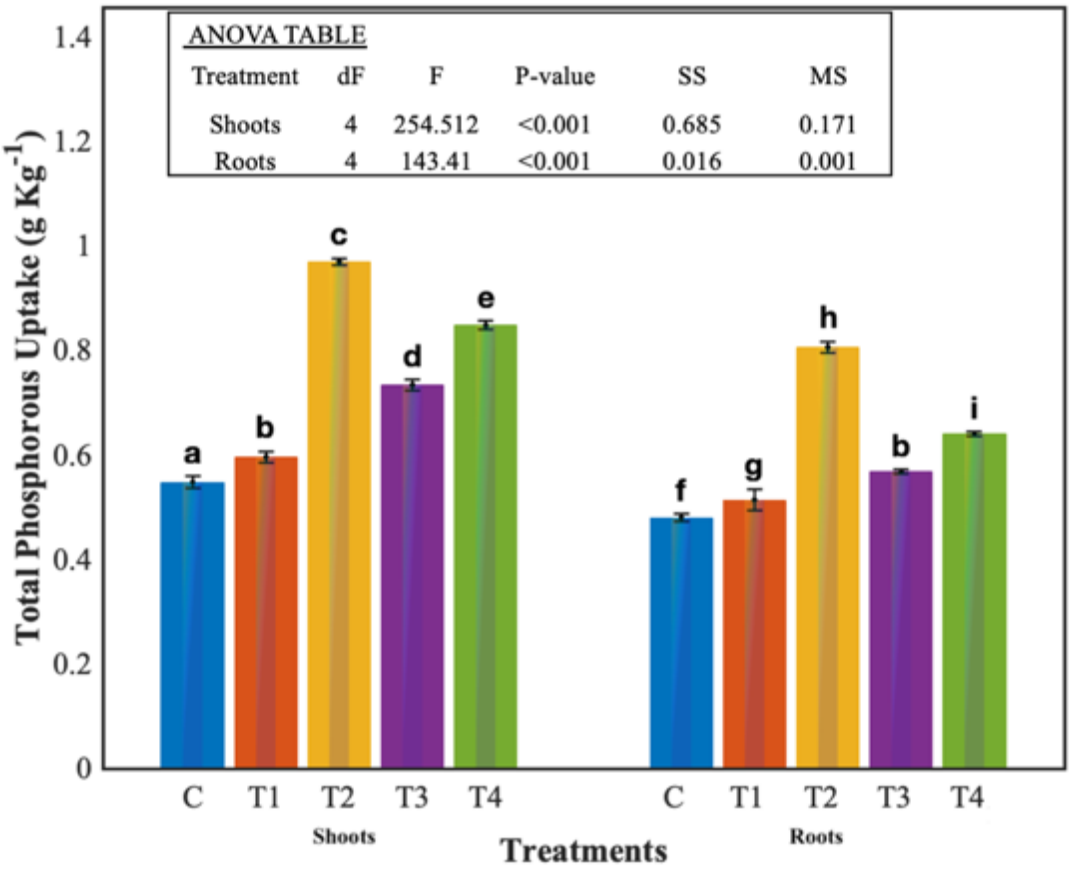

Figure 5.14: Effect of different treatments on Plant Total Phosphorous. C_Control, T1_uncoated DAP, T2_DAP coated with PSB, T3_DAP coated with PVA and T4_DAP coated with PSB and PVA. One-way ANOVA was performed for statistical analysis of data. Error bars represent the standard error of mean (n=6).

5.3.8 Total Plant Nitrogen

The impact that various types of coated DAP have on total nitrogen content in plants is shown in Figure 5.15. As can be shown in the figure, T4 yielded the highest nitrogen content (0.62 ± 0.031) in shoots, followed by T2 (0.47 ± 0.019). The lowest nitrogen content (0.31 ± 0.001) was found in control. The highest nitrogen content in roots was found to be in T4 (0.88 ± 0.02), followed by T2 (0.76 ± 0.02). The lowest nitrogen content (0.57 ± 0.02) was found to be in control.

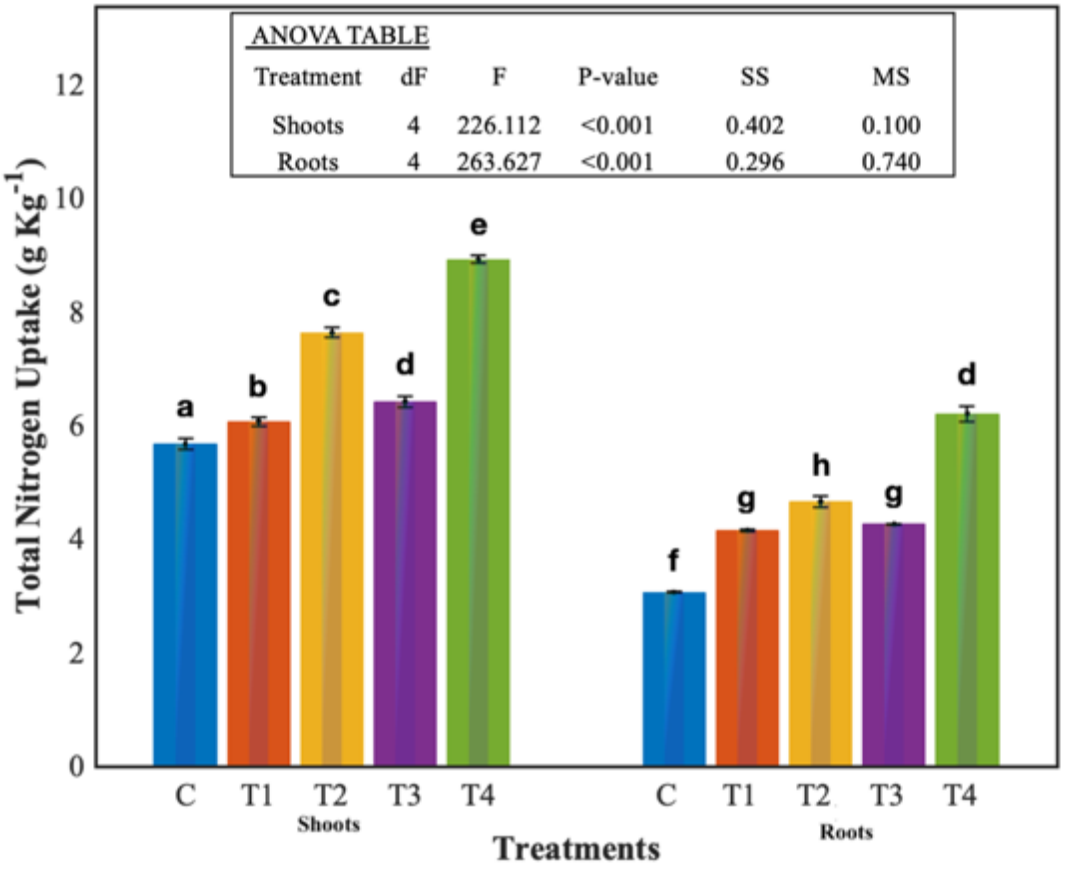

Figure 5.15: Effect of different treatments on Plant Total Nitrogen. C_Control, T1_uncoated DAP, T2_DAP coated with PSB, T3_DAP coated with PVA and T4_DAP coated with PSB and PVA. One-way ANOVA was performed for statistical analysis of data. Error bars represent the standard error of the mean (n=6).

5.4 Soil Analysis

5.4.1 Soil pH

A slight decrease in pH was recorded in the soil after harvesting compared to the initial pH of the soil as shown in Figure 5.16. The highest decrease of 0.39 was recorded in T2 followed by a decrease of 0.14 in T4. This can be attributed to the presence of PSB in soil. PSB has the characteristics to decrease soil pH releasing acids.

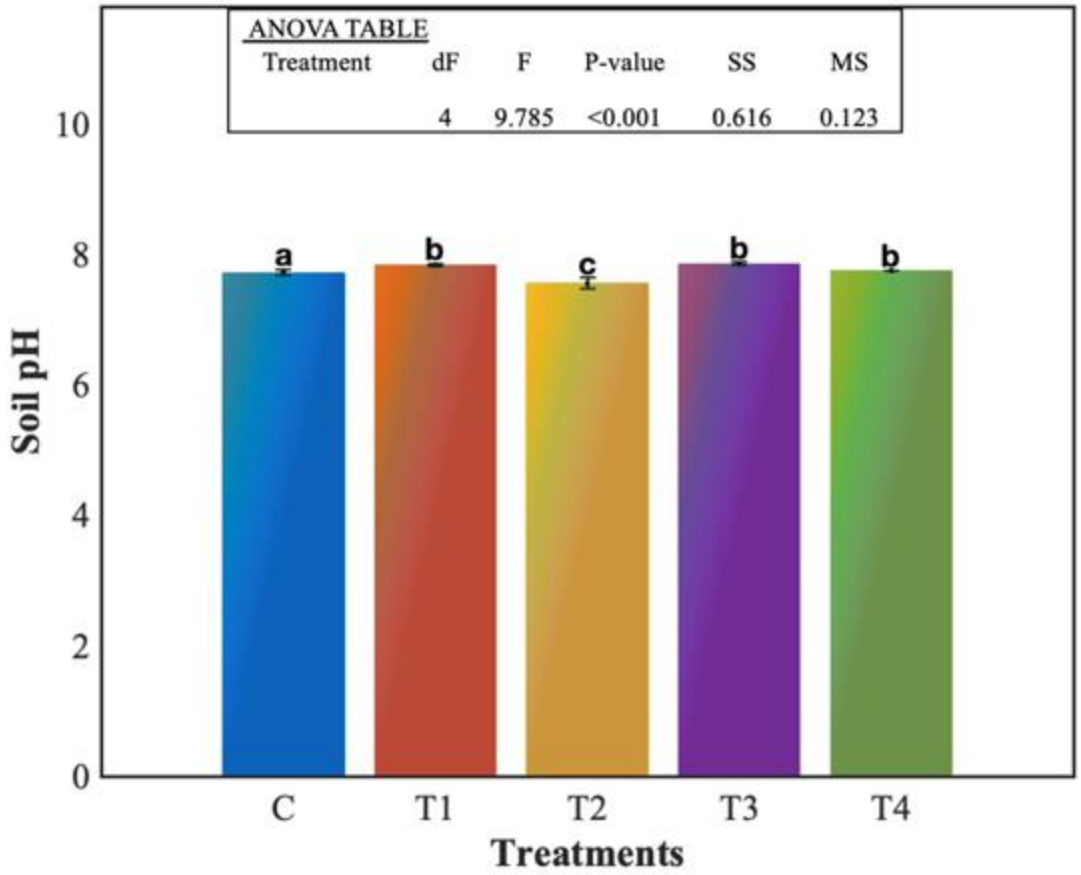

Figure 5.16: Effect of different treatments on Soil pH. C_Control, T1_uncoated DAP, T2_DAP coated with PSB, T3_DAP coated with PVA and T4_DAP coated with PSB and PVA. One-way ANOVA was performed for statistical analysis of data. Error bars represent the standard error of mean (n=6).

5.4.2 Soil EC

A slight increase in the value of EC was recorded for all treatments compared to the initial EC value, as shown in Figure 5.17. The highest value of EC was recorded for T3 (3.4 ± 0.02) and the lowest was recorded for T1 and T4 (3.2± 0.05).

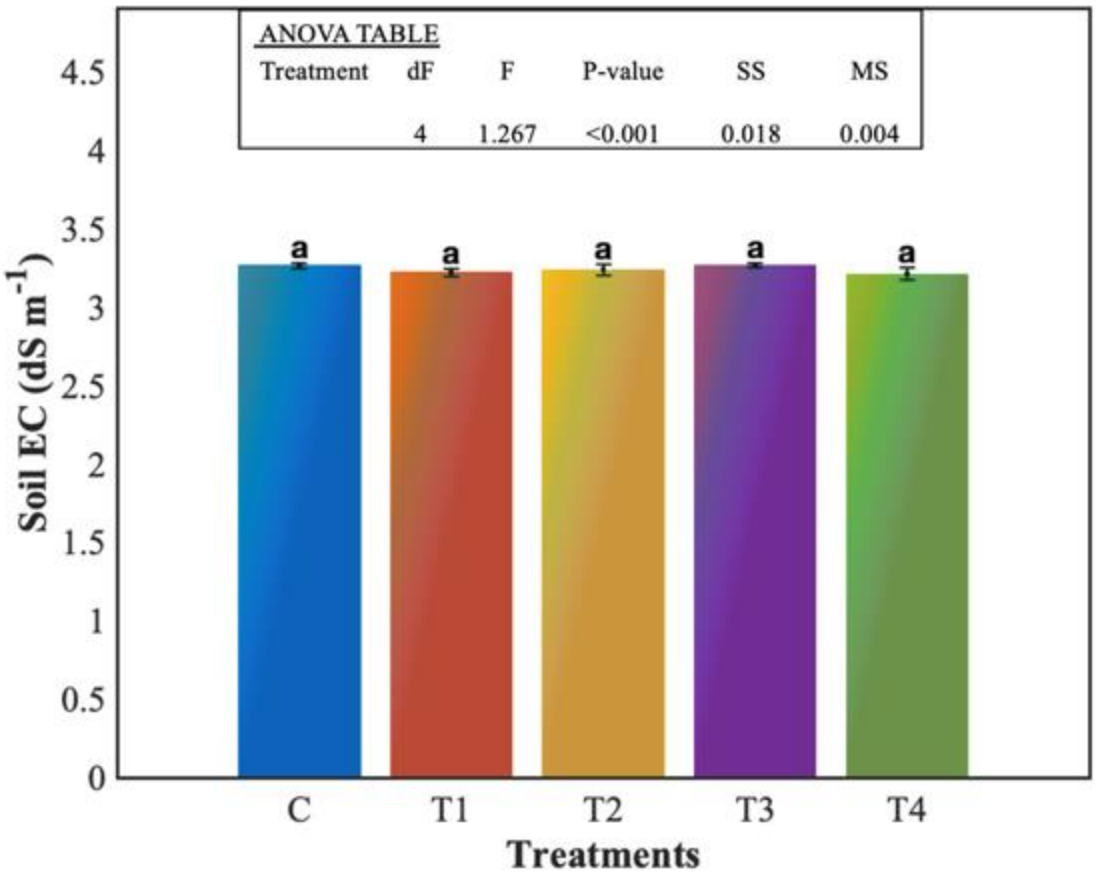

Figure 5.17: Effect of different treatments on Soil EC. C_Control, T1_uncoated DAP, T2_DAP coated with PSB, T3_DAP coated with PVA and T4_DAP coated with PSB and PVA. One-way ANOVA was performed for statistical analysis of data. Error bars represent the standard error of mean (n=6).

5.4.3 Soil Organic matter

Figure 5.18 shows the data recorded for Soil Organic Matter in different treatments. An increase in the quantity of organic matter has been observed in all treatments. The highest value of Soil Organic Matter has been recorded for T4 (4.82 ± 0.005) followed by T2 (4.61 ± 0.005) while the lowest change in the value of Soil organic matter was recorded for control (4.14± 0.001). The high value of organic matter indicated high nutrient amounts in soil which can be seen in the case of DAP coated with both PSB and PVA.

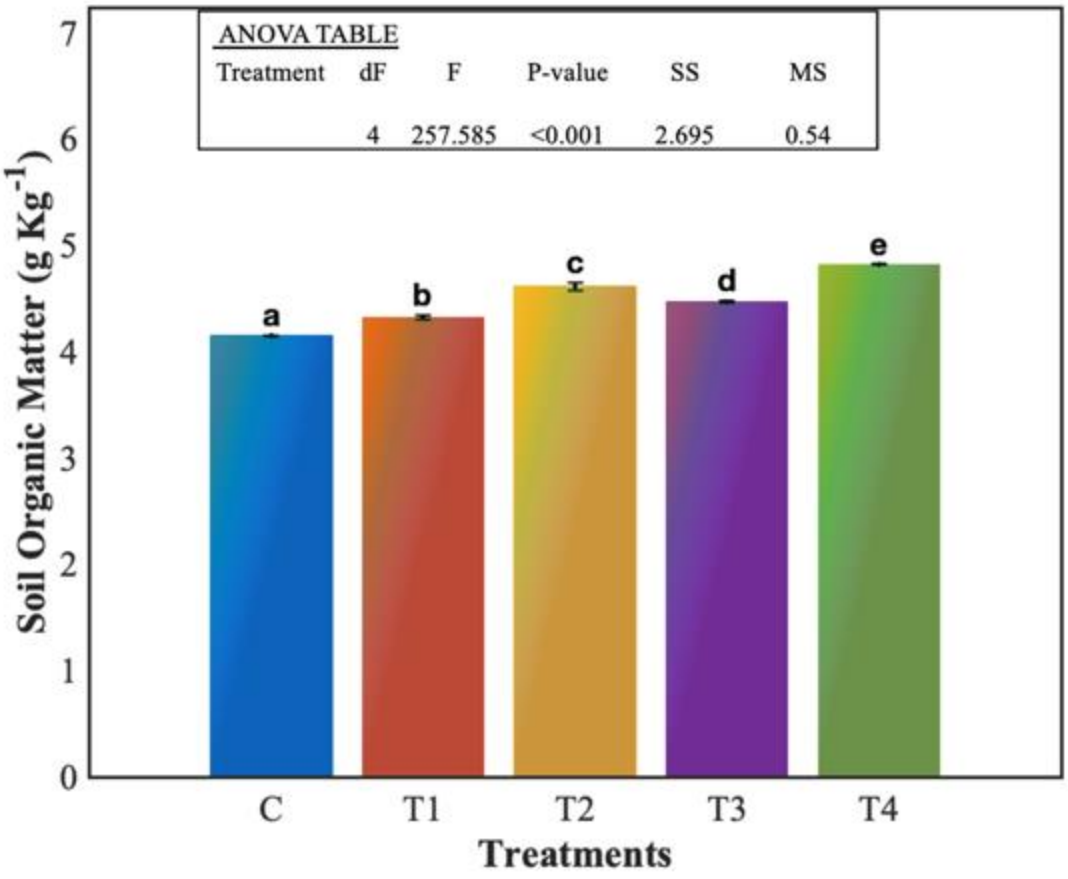

Figure 5.18: Effect of different treatments on Soil Organic matter. C_Control, T1_uncoated DAP, T2_DAP coated with PSB, T3_DAP coated with PVA and T4_DAP coated with PSB and PVA. One-way ANOVA was performed for statistical analysis of data. Error bars represent the standard error of mean (n=6).

5.4.4 Soil Mineral Nitrogen

Mineral nitrogen present in soil was determined before plantation and after harvesting as shown in Figure 5.19. The graph shows the change in the value of mineral nitrogen in all treatments compared to the initial value of mineral nitrogen. The highest amount of mineral nitrogen was observed in T4 (12.64 ± 0.11). This is due to the effective release of nutrients in soil from coated DAP. The control showed the lowest values of Soil Mineral Nitrogen (10.10± 0.17).

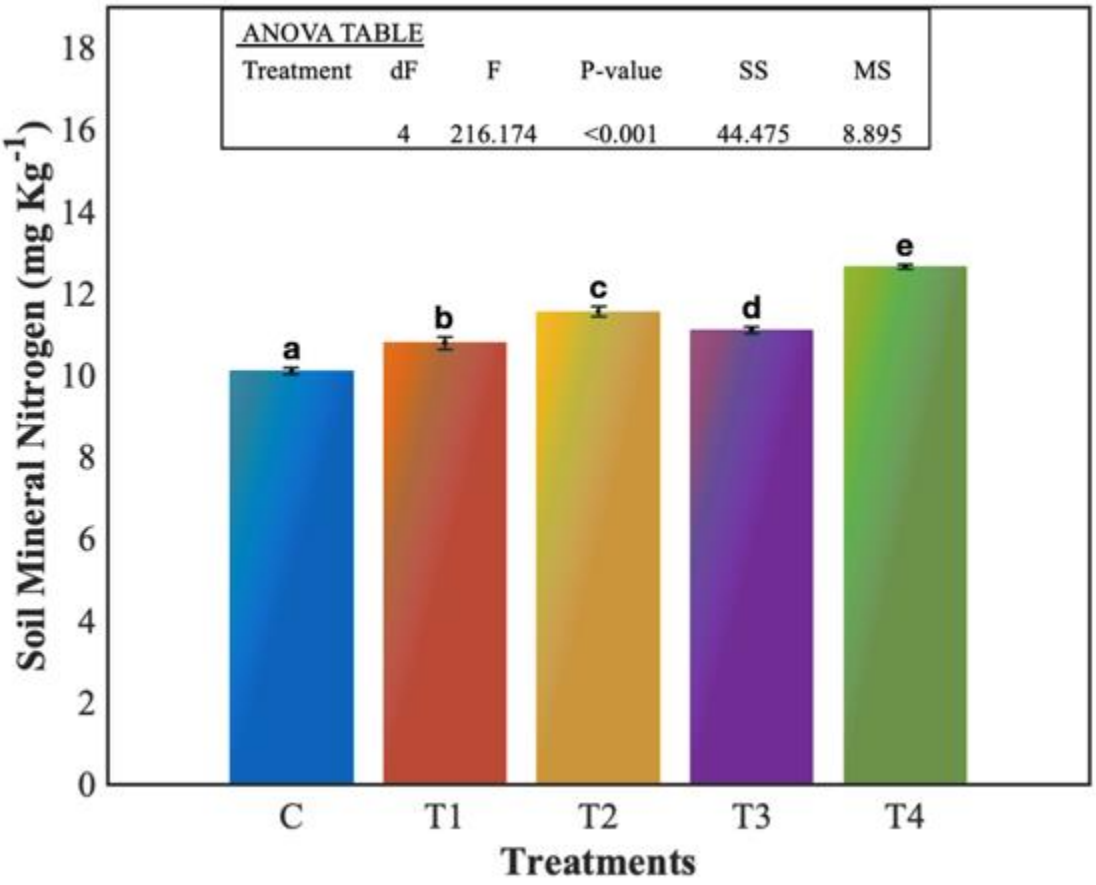

Figure 5.19: Effect of different treatments on Soil Mineral Nitrogen. C_Control, T1_uncoated DAP, T2_DAP coated with PSB, T3_DAP coated with PVA and T4_DAP coated with PSB and PVA. One-way ANOVA was performed for statistical analysis of data. Error bars represent the standard error of mean (n=6).

5.4.5 Soil available Phosphorous

The soil was tested to determine the amount of available phosphorous before the experiment and after that. The data obtained for an initial amount of soil available phosphorous, and the amount determined for other treatments have been shown in Figure 5.20. The highest amount of available phosphorous was observed in T4 (18.94 ± 0.10). This is due to the effective release of nutrients in the soil from coated DAP and the use of PSB has increased the amount of available phosphorous in the soil. The control showed the lowest values of Soil-available phosphorous (15.06± 0.01).

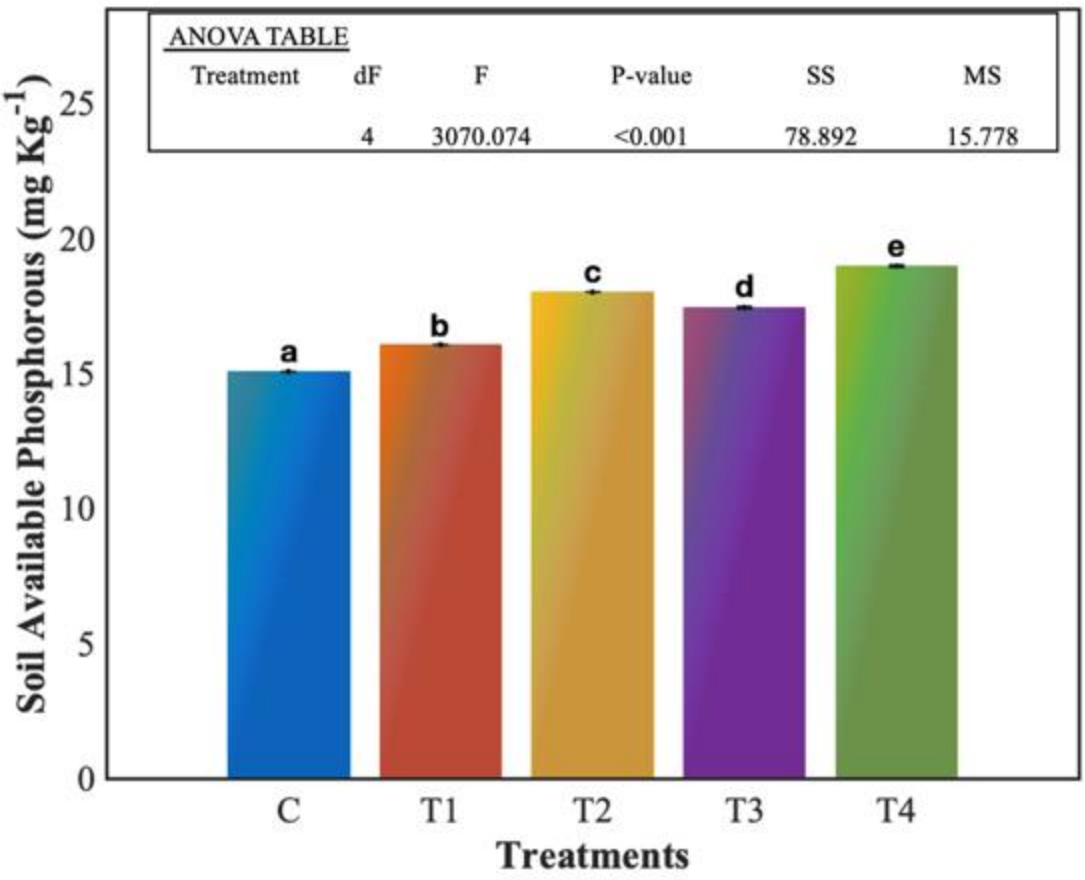

Figure 5.20: Effect of different treatments on Soil Available Phosphorous. C_Control, T1_uncoated DAP, T2_DAP coated with PSB, T3_DAP coated with PVA and T4_DAP coated with PSB and PVA. One-way ANOVA was performed for statistical analysis of data. Error bars represent the standard error of mean (n=6).

5.4.6 Soil Microbial Phosphorous

The soil was analyzed to determine the amount of microbial phosphorous before the experiment and after that. The data obtained for an initial amount of soil microbial phosphorous, and the amount determined for other treatments have been shown in Figure 5.21. The highest amount of microbial phosphorous was observed in T4 (18.94 ± 0.10) followed by T2. This is due to the effective release of nutrients in the soil from coated DAP and the use of PSB has increased the amount of microbial phosphorous in the soil. The control showed the lowest values of Soil-available phosphorous (15.06± 0.01).

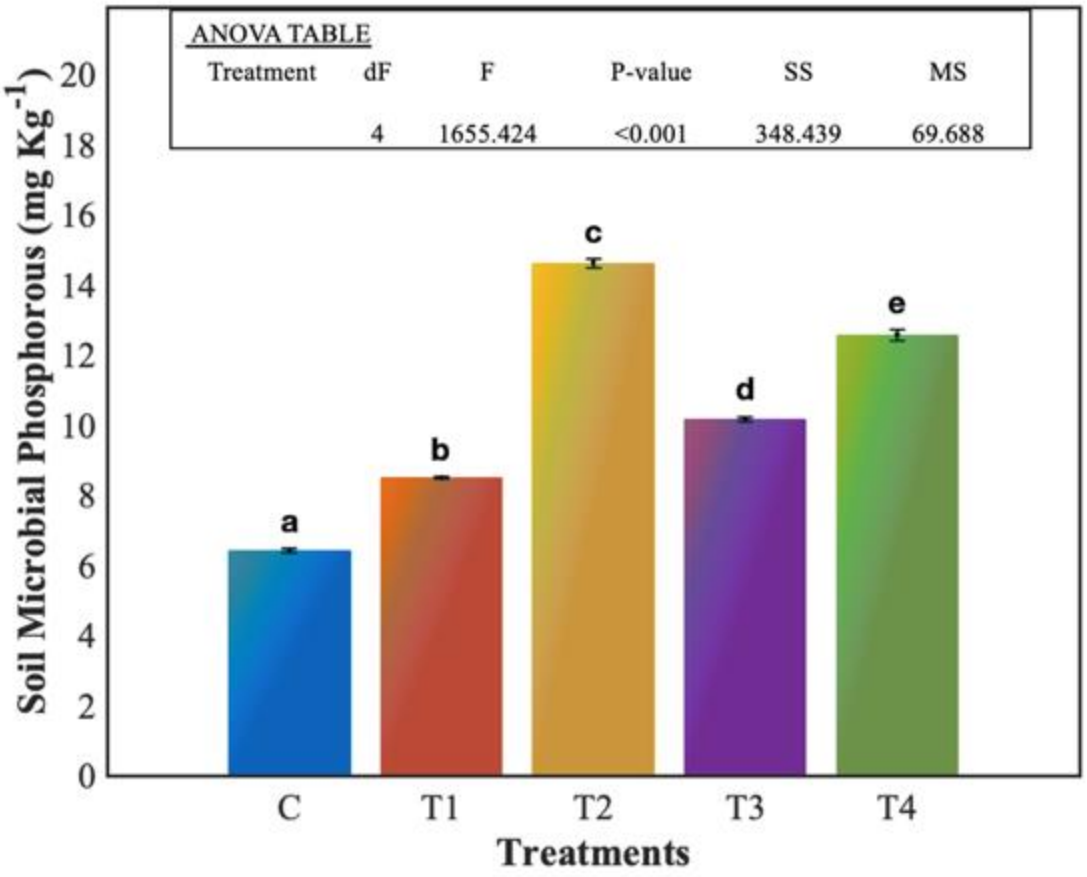

Figure 5.21: Effect of different treatments on Soil Microbial Phosphorous. C_Control, T1_uncoated DAP, T2_DAP coated with PSB, T3_DAP coated with PVA and T4_DAP coated with PSB and PVA. One-way ANOVA was performed for statistical analysis of data. Error bars represent the standard error of mean (n=6).

5.5 Machine Learning

5.5.1 Box and Violin Plot Presentation

The Box and Violin plot is a technique that can be utilized to display the distribution of a dataset. It displays the highest and lowest possible range, as well as the median, mode, tolerance, and lower and upper quartiles. The box plot is a useful tool for understanding data and the ranges it contains. The microbial strain, crop, fertilizer, soil pH, soil phosphorus, and change in phosphorus uptake are all plotted against their distribution in a box plot presentation shown in Figure 5.22.

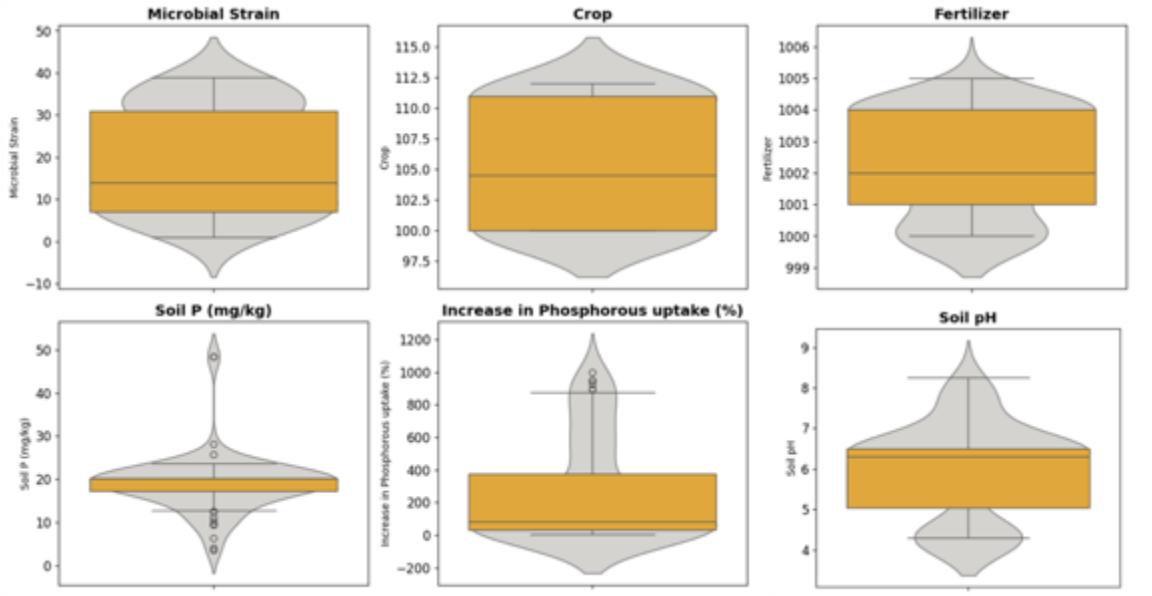

Figure 5.22: Box and Violin Plot presentation of data

5.5.2 Correlation Heat Map

A correlation heat map of the data set is displayed in Figure 5.23. A heat map is a useful tool for determining the degree to which one feature is dependent on another. This makes it easier to understand the data and the correlations that exist between its many features.

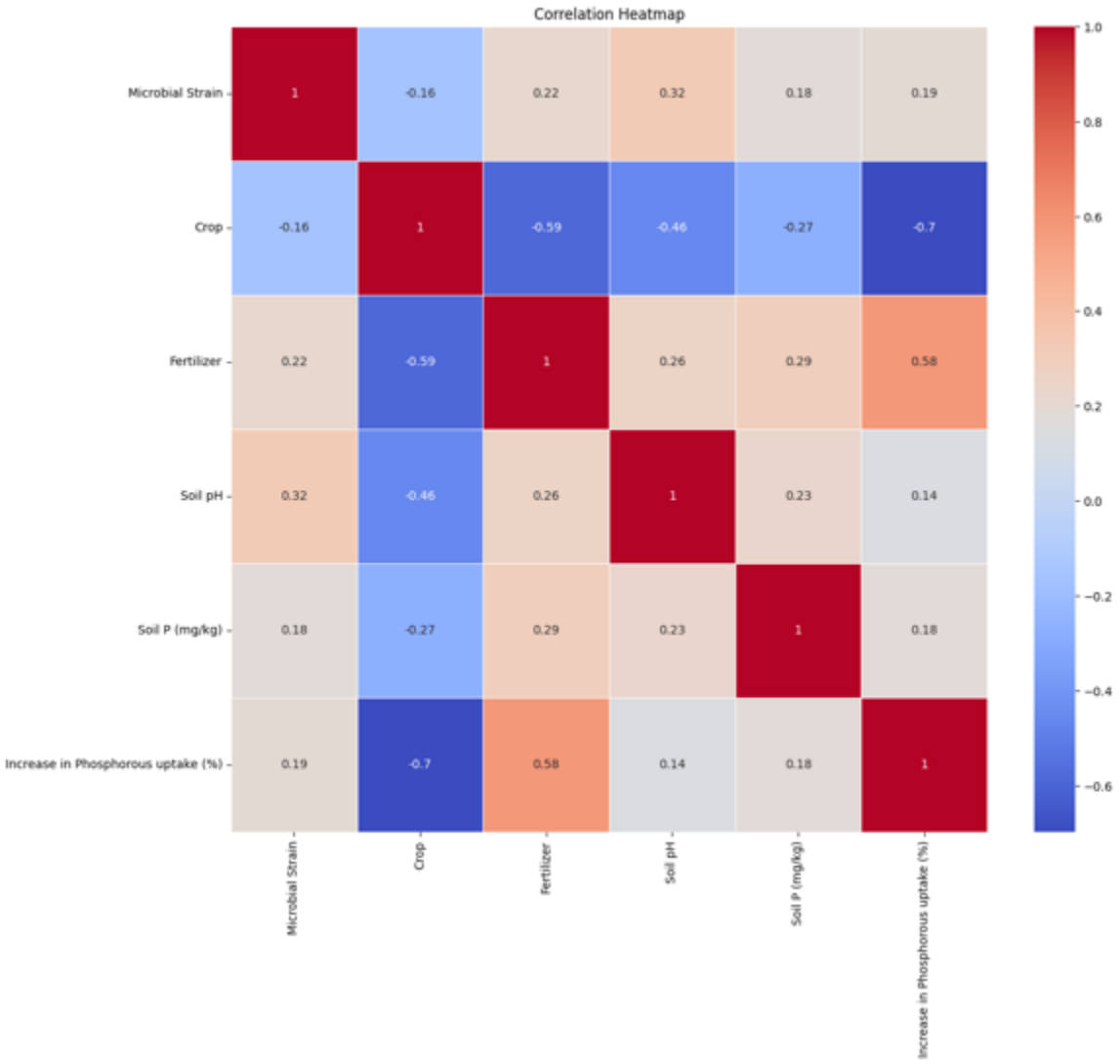

Figure 5.23: Heat map presentation of data

5.5.3 Performance Evaluation Criteria

The default hyperparameters were used to do preprocessing on the GPR, Ensembled tree, and DT that were obtained from the MATLAB library. Evaluation of preprocessing methods was carried out with the help of R-square, RMSE, and MAE. For pre-processing and deep modeling, the datasets were randomly split into two categories: training datasets (80%) and testing datasets (20%). Ranges for the tuning of the hyperparameters were established using the Regression model toolbox of each model, and then the models were optimized with the help of GA and PSO. Next, these hyperparameters were applied in the process of developing and testing models. To evaluate the performance of the validation

phase in comparison to the modeling technique, the average values of the statistical indices were applied. Table 5.1 shows the comparison of different ML models based on R^2, RMSE and MAE values.

Table 5.1: Comparison of different ML models

	Model	**Training R^2**	**Testing R^2**
GA	DT	0.5208	0.0000
	GPR	0.6169	0.8829
	ELT	0.7938	0.8887
PSO	DT	0.5208	6.6613
	GPR	0.6173	0.883
	ELT	0.6986	0.88

5.5.4 Hyperparameter Tuning

The regression toolbox was used to specify the parameters that were chosen for modifying amongst the several machine learning models. Table 5.2 shows the hyperparameters that were chosen and the values that were optimized for them. The Genetic Algorithm and Particle Swarm Optimization were utilized to tune and optimize these hyperparameters for the GPR, DT, and ELT models.

Table 5.2: Optimized values of selected parameters

	ML Method	**Parameter**	**Optimized value**
GA Model	**DT**	MinLeafsSize	21.0327780327756
		Surrogate	off

	GPR	Basic Function	constant, ...
		KernelFunction	ardexponential
		Sigma	1481.95794668497
		Standardize	false
	ELT	Method	LSBoost, ...
		NumLearningCycles	457.554169508120
		LearnRate	0.655442905969867
		Output	predict (Char_ensembled,X
PSO	**DT**	MinLeafsSize	21.0327780327756
		Surrogate	off
	GPR	Basic Function	constant, ...
		KernelFunction	ardexponential
		Sigma	1481.95794668497
		Standardize	false
	ELT	Method	Bag, …
		NumLearningCycles	239.811258540396,
		LearnRate	0. 0168725661655034
		Output	predict (Char_ensembled,X

5.5.5 Prediction Performance

A number of models, such as GPR, ELT, DT on GA, and PSO based algorithms, were used in order to make predictions regarding phosphorous uptake rates. Results demonstrate that the GA-based ELT model produced the best outcomes when compared to the R2 values of each model. With the help of the R-square function, GA-ELT was utilized to predict the value of phosphorous uptake. With the use of the GA-ELT model, Figure 5.24 illustrates the relationship between the actual value of phosphorus uptake and the predicted value.

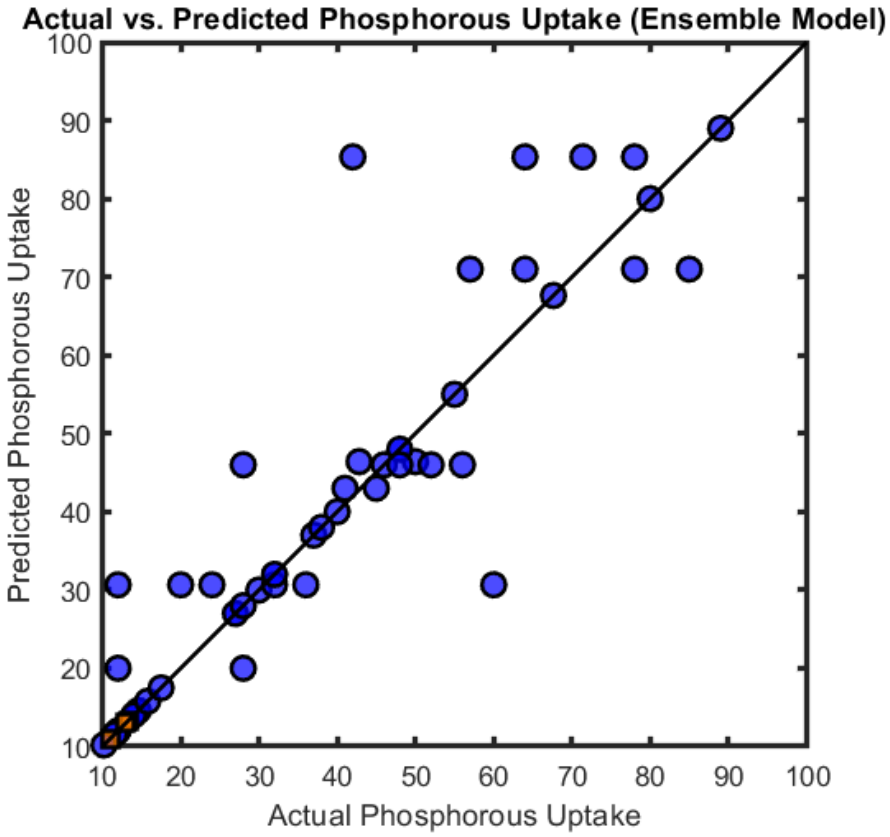

Figure 5.24: Validation of GA-ELT model

5.5.6 Shapley Plot

The GA-ELT model combined with the Shapley method can effectively illustrates the correlation between input parameters and phosphorus uptake. The Shapley approach works according to the significance of feature attribution. This was utilized to assess the relative importance of various input parameters on phosphorus uptake in plants. Figure 19 depicts the influence of crop type, fertilizer, microbial strain, soil pH, and soil phosphorus on phosphorus uptake. The specific microbial strain utilized in the study and tested crop significantly affects phosphorus uptake in plants.

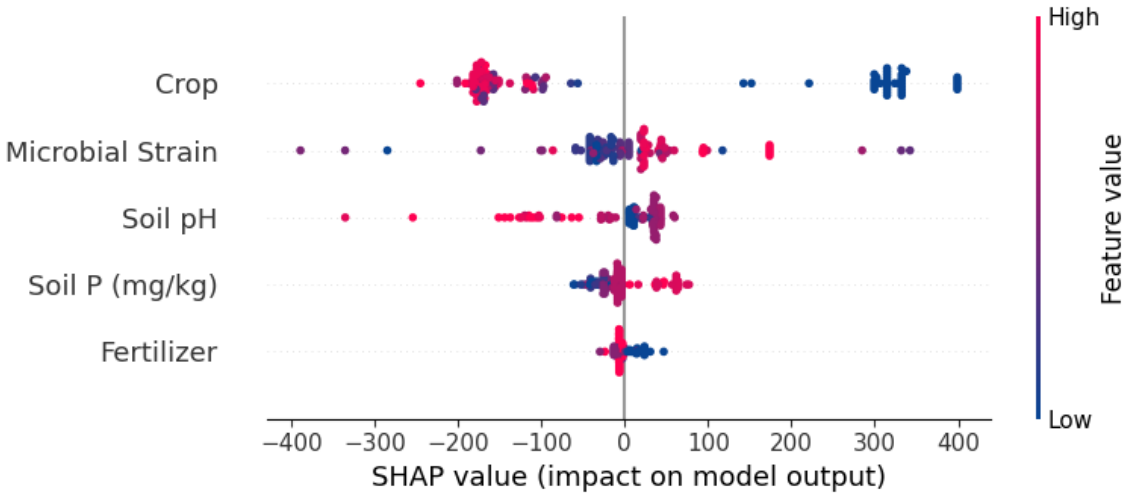

Figure 5.25: Shapley Plot

5.5.7 Partial Dependence Plots

Partial dependence plots illustrate the influence of input parameters on output. Phosphorous solubilization in soil is highly influenced by the type of microbial strain employed for solubilization and pH of the soil. Figure 5.26 illustrates partial dependence plots which demonstrate the effect of soil pH, Microbial strain and Soil phosphorous on an increase in phosphorous uptake in plants.

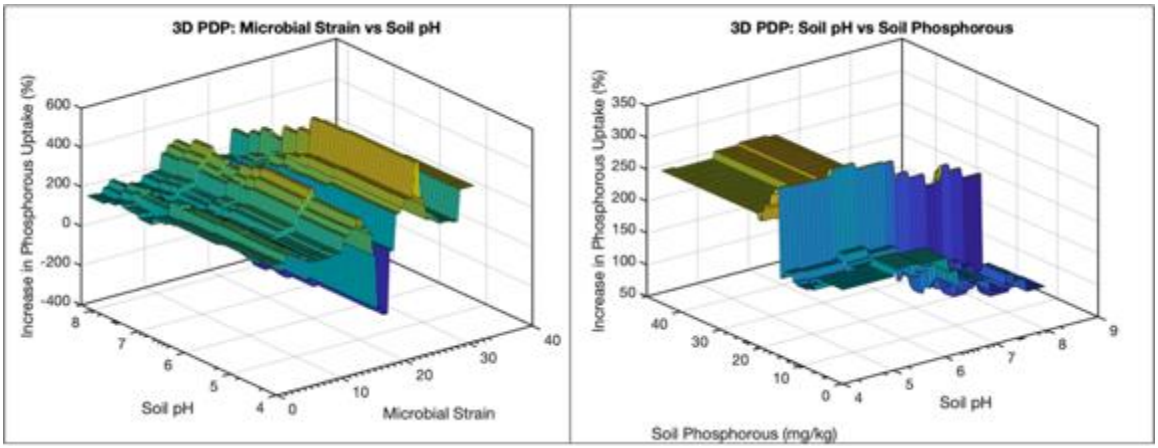

Figure 5.26: Partial Dependence Plots

Machine learning models indicate that increase in phosphorous uptake can be increased by lowering soil pH which will increase phosphorous solubilization and hence phosphorous uptake. Furthermore, the use of different microbial strain effects phosphorous uptake in plants.

5.5.8 Graphical User Interface

Graphical User Interface (GUI) enables users to deal with electronic devices through graphical icons, symbols, and intuitive software, as opposed to a command-driven interface. For this study, GUI was developed which makes use of sowing conditions including microbial strain, fertilizer, type of crop, soil phosphorous and soil pH and predicts an increase in phosphorous uptake. GUI was developed using the GA-ELT model to predict phosphorous uptake with the help of MATLAB 2024a. GUI illustrated in Figure 5.27 depicts the use of distinct values (Microbial Strain 10, Crop 104, Fertilizer 1000, P in soil 18.5mg/kg, Soil pH 8) as input. The GUI predicted an increase of 6.25% in phosphorous uptake as output.

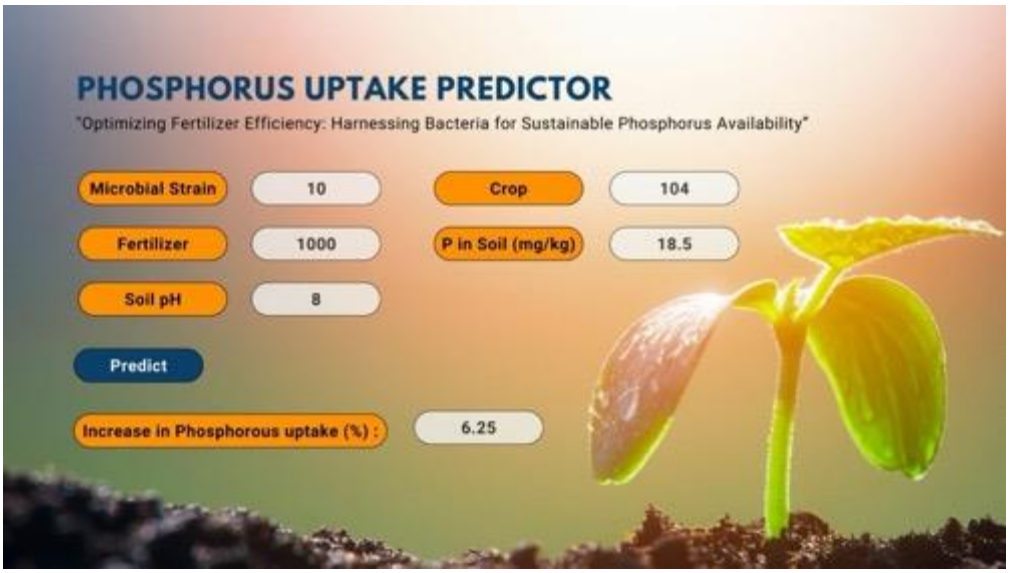

Figure 5.27: Graphical User Interface

CHAPTER 6 CONCLUSION AND RECOMMENDATIONS

The main finding of this study is that DAP coated with PSB and PVA proved to be the most efficient treatment in terms of plant height, plant diameter, leaf area, and nutrient availability. The slow-release characteristics, validated by UV-Vis spectroscopy, indicated that DAP coated with PSB and PVA exhibited a reduced rate of nutrient release. The controlled nutrient release increased the availability of nutrients for longer periods and thus making them available for plant uptake promoting consistent and enhanced plant growth. The improved fertilizer efficiency is evident for the viability of employing microbiological and polymer coatings to boost nutrient delivery in agriculture.

In addition to these, the integration of machine learning models provided a prediction of phosphorous uptake influenced by microbial strains. The cross-validation performance of the developed models indicated that the GA-based Ensembled Learning Tree (ELT) model achieved the highest R^2 of 0.7938. This modeling methodology highlights the potential of data-driven strategies to enhance empirical research by providing accurate prediction and optimal intervention strategies.

It is recommended to analyze the economic perspective of the use of PSB to enhance the efficiency of DAP fertilizer and make it market available. The machine learning model can be further improved to predict the effect of the use of PSB on the availability of other nutrients such as nitrogen and potassium.

REFERENCES

[1] L. Kumar *et al.*, 'Climate change and future of agri-food production', *Future Foods: Global Trends, Opportunities, and Sustainability Challenges*, pp. 49–79, Jan. 2022, doi: 10.1016/B978-0-323-91001-9.00009-8.

[2] A. Raza *et al.*, 'plants Impact of Climate Change on Crops Adaptation and Strategies to Tackle Its Outcome: A Review', doi: 10.3390/plants8020034.

[3] M. J. Luna Juncal, P. Masino, E. Bertone, and R. A. Stewart, 'Towards nutrient neutrality: A review of agricultural runoff mitigation strategies and the development of a decision-making framework', *Science of The Total Environment*, vol. 874, p. 162408, 2023, doi: https://doi.org/10.1016/j.scitotenv.2023.162408.

[4] M. V. S. R. Tavva S. S. Mohan Dev, Y. Venkateswara Rao, B. Venkateswara Rao, 'Plant Biology and Biotechnology - Apomixis in Crop Improvement', *Plant Biology and Biotechnology: Volume I: Diversity, Organisation, Function and Improvement.*, vol. I, pp. 281–306, 2015, Accessed: Sep. 01, 2024. [Online]. Available: http://link.springer.com/10.1007/978-81-322-2286-6

[5] E. A. Kirkby, 'Introduction, definition, and classification of nutrients', *Marschner's Mineral Nutrition of Plants*, pp. 3–9, Jan. 2023, doi: 10.1016/B978-0-12-819773-8.00016-2.

[6] P. J. White and P. H. Brown, 'Plant nutrition for sustainable development and global health', doi: 10.1093/aob/mcq085.

[7] R. Hänsch and R. R. Mendel, 'Physiological functions of mineral micronutrients (Cu, Zn, Mn, Fe, Ni, Mo, B, Cl)', *Curr Opin Plant Biol*, vol. 12, no. 3, pp. 259–266, Jun. 2009, doi: 10.1016/J.PBI.2009.05.006.

[8] S. Saleem, N. U. Mushtaq, A. Rasool, W. H. Shah, I. Tahir, and R. U. Rehman, 'Plant nutrition and soil fertility: physiological and molecular avenues for crop improvement', *Sustainable Plant Nutrition: Molecular Interventions and Advancements for Crop Improvement*, pp. 23–49, Jan. 2022, doi: 10.1016/B978-0-443-18675-2.00009-2.

[9] S. C. Hodges, 'SOIL FERTILITY BASICS NC Certified Crop Advisor Training Chapter 1 Basic Concepts'.

[10] H. T. Phuong, V. N. Ba, B. N. Thien, and L. Truong Thi Hong, ‘Accumulation and distribution of nutrients, radionuclides and metals by roots, stems and leaves of plants’, *Nuclear Engineering and Technology*, vol. 55, no. 7, pp. 2650–2655, Jul. 2023, doi: 10.1016/J.NET.2023.03.039.

[11] Z. Hossain, M. Bahar, B. Sarkar, S. Donne, Y. S. Ok, and N. Bolan, ‘Biochar and its importance on nutrient dynamics in soil and plant’, *Biochar*, vol. 2, Sep. 2020, doi: 10.1007/s42773-020-00065-z.

[12] P. Singh and B. Dadhe, ‘Essential Mineral Nutrients for Plant Growth: Nutrient Functions and Deficiency Symptoms’, 2022.

[13] H. Malhotra, Vandana, S. Sharma, and R. Pandey, ‘Phosphorus nutrition: plant growth in response to deficiency and excess’, *Plant nutrients and abiotic stress tolerance*, pp. 171–190, 2018.

[14] M. A. Khoso *et al.*, ‘Impact of plant growth-promoting rhizobacteria (PGPR) on plant nutrition and root characteristics: Current perspective’, *Plant Stress*, vol. 11, p. 100341, 2024, doi: https://doi.org/10.1016/j.stress.2023.100341.

[15] P. Sica, C. Kopp, D. S. Müller-Stöver, and J. Magid, ‘Acidification and alkalinization pretreatments of biowastes and their effect on P solubility and dynamics when placed in soil’, *J Environ Manage*, vol. 333, p. 117447, May 2023, doi: 10.1016/J.JENVMAN.2023.117447.

[16] E. Hanyabui *et al.*, ‘Phosphorus sorption in tropical soils’, *AIMS Agriculture and Food*, vol. 5, pp. 599–616, Sep. 2020, doi: 10.3934/agrfood.2020.4.599.

[17] P. D. Johan, O. H. Ahmed, L. Omar, and N. A. Hasbullah, ‘Phosphorus Transformation in Soils Following Co-Application of Charcoal and Wood Ash’, *Agronomy 2021, Vol. 11, Page 2010*, vol. 11, no. 10, p. 2010, Oct. 2021, doi: 10.3390/AGRONOMY11102010.

[18] A. M. M. Silva *et al.*, ‘Can arbuscular mycorrhizal fungi and rhizobacteria facilitate 33P uptake in maize plants under water stress?’, *Microbiol Res*, vol. 271, p. 127350, Jun. 2023, doi: 10.1016/J.MICRES.2023.127350.

[19] M. Ahmad *et al.*, ‘Perspectives of microbial inoculation for sustainable development and environmental management’, *Front Microbiol*, vol. 9, no. DEC, Dec. 2018, doi: 10.3389/FMICB.2018.02992.

[20] F. Battini, M. Grønlund, M. Agnolucci, M. Giovannetti, and I. Jakobsen, 'Facilitation of phosphorus uptake in maize plants by mycorrhizosphere bacteria article', *Sci Rep*, vol. 7, no. 1, Dec. 2017, doi: 10.1038/S41598-017-04959-0.

[21] R. Khan, N. Dhingra, and N. Bhati, 'Role of artificial intelligence in agriculture: A comparative study', in *Transforming Management with AI, Big-Data, and IoT*, Springer, 2022, pp. 73–83.

[22] D. J. Reddy and M. R. Kumar, 'Crop yield prediction using machine learning algorithm', in *2021 5th International Conference on Intelligent Computing and Control Systems (ICICCS)*, IEEE, 2021, pp. 1466–1470.

[23] V. Meshram, K. Patil, V. Meshram, D. Hanchate, and S. D. Ramkteke, 'Machine learning in agriculture domain: A state-of-art survey', *Artificial Intelligence in the Life Sciences*, vol. 1, p. 100010, 2021.

[24] A. Venugopal, S. Aparna, J. Mani, R. Mathew, and V. Williams, 'Crop yield prediction using machine learning algorithms', *International journal of engineering research & technology (IJERT) NCREIS*, vol. 9, no. 13, 2021.

[25] R. Sharma, S. S. Kamble, A. Gunasekaran, V. Kumar, and A. Kumar, 'A systematic literature review on machine learning applications for sustainable agriculture supply chain performance', *Comput Oper Res*, vol. 119, p. 104926, 2020.

[26] A. Nigam, S. Garg, A. Agrawal, and P. Agrawal, 'Crop Yield Prediction Using Machine Learning Algorithms', in *2019 Fifth International Conference on Image Information Processing (ICIIP)*, 2019, pp. 125–130. doi: 10.1109/ICIIP47207.2019.8985951.

[27] G. Ruß, 'Data mining of agricultural yield data: A comparison of regression models', in *Advances in Data Mining. Applications and Theoretical Aspects: 9th Industrial Conference, ICDM 2009, Leipzig, Germany, July 20-22, 2009. Proceedings 9*, Springer, 2009, pp. 24–37.

[28] A. Shah, A. Dubey, V. Hemnani, D. Gala, and D. R. Kalbande, 'Smart farming system: Crop yield prediction using regression techniques', in *Proceedings of International Conference on Wireless Communication: ICWiCom 2017*, Springer, 2018, pp. 49–56.

[29] C. J. Penn and J. J. Camberato, 'A critical review on soil chemical processes that control how soil ph affects phosphorus availability to plants', *Agriculture (Switzerland)*, vol. 9, no. 6, Jun. 2019, doi: 10.3390/AGRICULTURE9060120.

[30] J. M. Chaparro, A. M. Sheflin, D. K. Manter, and J. M. Vivanco, 'Manipulating the soil microbiome to increase soil health and plant fertility', *Biol Fertil Soils*, vol. 48, no. 5, pp. 489–499, Jul. 2012, doi: 10.1007/S00374-012-0691-4.

[31] A. R. Zaharah, H. Zulkifli, and H. A. H. Sharifuddin, 'Evaluating the efficacy of various phosphate fertiliser sources for oil palm seedlings', *Nutr Cycl Agroecosyst*, vol. 47, no. 2, pp. 93–98, Jun. 1996, doi: 10.1007/BF01991540.

[32] 'Phosphorus Behavior in Soil | Pioneer® Seeds'. Accessed: Sep. 06, 2024. [Online]. Available: https://www.pioneer.com/us/agronomy/phosphorus-soil.html

[33] A. Maru, A. O. Haruna, A. Asap, N. M. A. Majid, N. Maikol, and A. V. Jeffary, 'Reducing acidity of tropical acid soil to improve phosphorus availability and Zea mays L. Productivity through efficient use of chicken litter biochar and triple superphosphate', *Applied Sciences (Switzerland)*, vol. 10, no. 6, Mar. 2020, doi: 10.3390/APP10062127.

[34] P. D. Johan, O. H. Ahmed, L. Omar, and N. A. Hasbullah, 'Phosphorus Transformation in Soils Following Co-Application of Charcoal and Wood Ash', *Agronomy 2021, Vol. 11, Page 2010*, vol. 11, no. 10, p. 2010, Oct. 2021, doi: 10.3390/AGRONOMY11102010.

[35] J. Tian, F. Ge, D. Zhang, S. Deng, and X. Liu, 'Roles of phosphate solubilizing microorganisms from managing soil phosphorus deficiency to mediating biogeochemical p cycle', *Biology (Basel)*, vol. 10, no. 2, pp. 1–19, Feb. 2021, doi: 10.3390/BIOLOGY10020158.

[36] P. Hinsinger, 'Bioavailability of soil inorganic P in the rhizosphere as affected by root-induced chemical changes: A review', *Plant Soil*, vol. 237, no. 2, pp. 173–195, 2001, doi: 10.1023/A:1013351617532.

[37] H. Y. Ch'Ng, O. H. Ahmed, and N. M. A. Majid, 'Improving phosphorus availability in an acid soil using organic amendments produced from agroindustrial wastes', *Scientific World Journal*, vol. 2014, 2014, doi: 10.1155/2014/506356.

[38] P. D. Johan, O. Ahmed, L. Omar, and N. A. Hasbullah, 'Phosphorus Transformation in Soils Following Co-Application of Charcoal and Wood Ash', *Agronomy*, vol. 11, p. 2010, Oct. 2021, doi: 10.3390/agronomy11102010.

[39] H. Hong, C. Liu, and Z. Li, 'Chemistry of soil-type dependent soil matrices and its influence on behaviors of pharmaceutical compounds (PCs) in soils', *Heliyon*, vol. 9, no. 12, p. e22931, 2023, doi: https://doi.org/10.1016/j.heliyon.2023.e22931.

[40] Q.-X. Hua, J. Li, J.-M. ZHOU, H.-Y. Wang, C. Du, and X.-Q. CHEN, 'Enhancement of Phosphorus Solubility by Humic Substances in Ferrosols1', *Pedosphere*, vol. 18, pp. 533–538, Aug. 2008, doi: 10.1016/S1002-0160(08)60044-2.

[41] D. Chatterjee *et al.*, 'Transformation of crystalline and short-range order minerals in a long-term (47 years) rice-rice cropping system', *Catena (Amst)*, vol. 206, p. 105488, 2021, doi: https://doi.org/10.1016/j.catena.2021.105488.

[42] R. Adeleke, C. Nwangburuka, and B. Oboirien, 'Origins, roles and fate of organic acids in soils: A review', *South African Journal of Botany*, vol. 108, pp. 393–406, 2017, doi: https://doi.org/10.1016/j.sajb.2016.09.002.

[43] A. Seeda, E.-Z. Abou El-Nour, and S. Zaghloul, 'Improving of phosphorus use efficiency in Plant-Soil-System. A review', *Middle East Journal of Agriculture Research*, Sep. 2020, doi: 10.36632/mejar/2020.9.3.39.

[44] J. Rinklebe, 'Influence of common ions on sorption and mobility of soil phosphorus', 2015, pp. 319–341.

[45] E. Bortoluzzi, C. Samudio Pérez, J. Ardisson, T. Tiecher, and L. Caner, 'Occurrence of iron and aluminum sesquioxides and their implications for the P sorption in subtropical soils', *Appl Clay Sci*, vol. 104, pp. 196–204, Dec. 2015, doi: 10.1016/j.clay.2014.11.032.

[46] J. A. Carreira, B. Viñegla, and K. Lajtha, 'Secondary CaCO3 and precipitation of P–Ca compounds control the retention of soil P in arid ecosystems', *J Arid Environ*, vol. 64, no. 3, pp. 460–473, 2006, doi: https://doi.org/10.1016/j.jaridenv.2005.06.003.

[47] G. Feng, B. Zhou, R. Yuan, S. Luo, N. Gai, and H. Chen, 'Influence of soil composition and environmental factors on the adsorption of per- and polyfluoroalkyl substances: A review', *Science of The Total Environment*, vol. 925, p. 171785, 2024, doi: https://doi.org/10.1016/j.scitotenv.2024.171785.

[48] C. Xu, R. Liu, L. Chen, and Q. Wang, 'Efficient Adsorption Removal of Phosphate from Rural Domestic Sewage by Waste Eggshell-Modified Peanut Shell Biochar Adsorbent Materials', *Materials*, vol. 16, p. 5873, Aug. 2023, doi: 10.3390/ma16175873.

[49] S. Chaudhary, S. S. Sindhu, R. Dhanker, and A. Kumari, 'Microbes-mediated sulphur cycling in soil: Impact on soil fertility, crop production and environmental sustainability', *Microbiol Res*, vol. 271, p. 127340, 2023, doi: https://doi.org/10.1016/j.micres.2023.127340.

[50] V. Antoniadis and S. Koutroubas, ‘Phosphorus Availability in Low-P and Acidic Soils as Affected by Liming and P Addition’, *Commun Soil Sci Plant Anal*, vol. 46, pp. 1288–1298, Apr. 2015, doi: 10.1080/00103624.2015.1033539.

[51] L. Pan and B. Cai, ‘Phosphate-Solubilizing Bacteria: Advances in Their Physiology, Molecular Mechanisms and Microbial Community Effects’, *Microorganisms 2023, Vol. 11, Page 2904*, vol. 11, no. 12, p. 2904, Dec. 2023, doi: 10.3390/MICROORGANISMS11122904.

[52] A. Siedliska, P. Baranowski, J. Pastuszka-Woźniak, M. Zubik, and J. Krzyszczak, ‘Identification of plant leaf phosphorus content at different growth stages based on hyperspectral reflectance’, *BMC Plant Biol*, vol. 21, no. 1, Dec. 2021, doi: 10.1186/S12870-020-02807-4.

[53] W. Elhaissoufi, C. Ghoulam, A. Barakat, Y. Zeroual, and A. Bargaz, ‘Phosphate bacterial solubilization: A key rhizosphere driving force enabling higher P use efficiency and crop productivity’, *J Adv Res*, vol. 38, pp. 13–28, May 2022, doi: 10.1016/J.JARE.2021.08.014.

[54] F. E. Chouyia, V. Ventorino, and O. Pepe, ‘Diversity, mechanisms and beneficial features of phosphate-solubilizing Streptomyces in sustainable agriculture: A review’, *Front Plant Sci*, vol. 13, Dec. 2022, doi: 10.3389/FPLS.2022.1035358.

[55] H. L. Santos, G. F. da Silva, M. R. A. Carnietto, L. C. Oliveira, C. H. de C. Nogueira, and M. de A. Silva, ‘Bacillus velezensis Associated with Organomineral Fertilizer and Reduced Phosphate Doses Improves Soil Microbial—Chemical Properties and Biomass of Sugarcane’, *Agronomy*, vol. 12, no. 11, Nov. 2022, doi: 10.3390/AGRONOMY12112701.

[56] E. T. Alori, B. R. Glick, and O. O. Babalola, ‘Microbial phosphorus solubilization and its potential for use in sustainable agriculture’, *Front Microbiol*, vol. 8, no. JUN, Jun. 2017, doi: 10.3389/FMICB.2017.00971.

[57] A. D. Suleimanova *et al.*, ‘Novel glucose-1-phosphatase with high phytase activity and unusual metal ion activation from soil bacterium Pantoea sp. strain 3.5.1’, *Appl Environ Microbiol*, vol. 81, no. 19, pp. 6790–6799, 2015, doi: 10.1128/AEM.01384-15.

[58] J. Tian, F. Ge, D. Zhang, S. Deng, and X. Liu, ‘Roles of phosphate solubilizing microorganisms from managing soil phosphorus deficiency to mediating biogeochemical P cycle’, *Biology (Basel)*, vol. 10, no. 2, p. 158, 2021.

[59] J. Shen *et al.*, ‘Phosphorus dynamics: From soil to plant’, *Plant Physiol*, vol. 156, no. 3, pp. 997–1005, 2011, doi: 10.1104/PP.111.175232.

[60] A. K. Singh *et al.*, 'Understanding Soil Carbon and Phosphorus Dynamics under Grass-Legume Intercropping in a Semi-Arid Region', *Agronomy*, vol. 13, no. 7, Jul. 2023, doi: 10.3390/AGRONOMY13071692.

[61] A. Gross, Y. Lin, P. K. Weber, J. Pett-Ridge, and W. L. Silver, 'The role of soil redox conditions in microbial phosphorus cycling in humid tropical forests', *Ecology*, vol. 101, no. 2, Feb. 2020, doi: 10.1002/ECY.2928.

[62] J. L. Liang *et al.*, 'Novel phosphate-solubilizing bacteria enhance soil phosphorus cycling following ecological restoration of land degraded by mining', *ISME Journal*, vol. 14, no. 6, pp. 1600–1613, Jun. 2020, doi: 10.1038/S41396-020-0632-4.

[63] K. Kiprotich, J. Muoma, D. O. Omayio, T. S. Ndombi, and C. Wekesa, 'Molecular Characterization and Mineralizing Potential of Phosphorus Solubilizing Bacteria Colonizing Common Bean (Phaseolus vulgaris L.) Rhizosphere in Western Kenya', *Int J Microbiol*, vol. 2023, 2023, doi: 10.1155/2023/6668097.

[64] P. Vazquez, G. Holguin, M. E. Puente, A. Lopez-Cortes, and Y. Bashan, 'Phosphate-solubilizing microorganisms associated with the rhizosphere of mangroves in a semiarid coastal lagoon', *Biol Fertil Soils*, vol. 30, no. 5, pp. 460–468, 2000, doi: 10.1007/s003740050024.

[65] L. Chawngthu, R. Hnamte, and R. Lalfakzuala, 'Isolation and characterization of rhizospheric phosphate solubilizing bacteria from wetland paddy field of Mizoram, India', *Geomicrobiol J*, vol. 37, no. 4, pp. 366–375, 2020.

[66] H. Zhang, L. Han, B. Jiang, and C. Long, 'Identification of a phosphorus-solubilizing Tsukamurella tyrosinosolvens strain and its effect on the bacterial diversity of the rhizosphere soil of peanuts growth-promoting', *World J Microbiol Biotechnol*, vol. 37, no. 7, p. 109, 2021.

[67] Z. Udaondo *et al.*, 'Developing robust protein analysis profiles to identify bacterial acid phosphatases in genomes and metagenomic libraries', *Environ Microbiol*, vol. 22, no. 8, pp. 3561–3571, Aug. 2020, doi: 10.1111/1462-2920.15138.

[68] F. C. Gerretsen, 'The influence of microorganisms on the phosphate intake by the plant', *Plant Soil*, vol. 1, no. 1, pp. 51–81, Jan. 1948, doi: 10.1007/BF02080606.

[69] J. Liu *et al.*, 'Response of alfalfa growth to arbuscular mycorrhizal fungi and phosphate-solubilizing bacteria under different phosphorus application levels', *AMB Express*, vol. 10, no. 1, Dec. 2020, doi: 10.1186/S13568-020-01137-W.

[70] P. Xing *et al.*, 'Effects of Bradyrhizobium Co-Inoculated with Bacillus and Paenibacillus on the Structure and Functional Genes of Soybean Rhizobacteria Community', *Genes (Basel)*, vol. 13, no. 11, Nov. 2022, doi: 10.3390/GENES13111922.

[71] Y. Cao, D. Fu, T. Liu, G. Guo, and Z. Hu, 'Phosphorus solubilizing and releasing bacteria screening from the rhizosphere in a Natural Wetland', *Water (Switzerland)*, vol. 10, no. 2, Feb. 2018, doi: 10.3390/W10020195.

[72] L. R. Massucato *et al.*, 'Efficiency of Combining Strains Ag87 (Bacillus megaterium) and Ag94 (Lysinibacillus sp.) as Phosphate Solubilizers and Growth Promoters in Maize', *Microorganisms*, vol. 10, no. 7, Jul. 2022, doi: 10.3390/MICROORGANISMS10071401.

[73] C. Liu *et al.*, 'Integration and Potential Application Ability of Culturable Functional Microorganism in Oil Tea Camellia', *Indian J Microbiol*, vol. 61, no. 1, Mar. 2021, doi: 10.1007/S12088-020-00904-4.

[74] A. D. Suleimanova *et al.*, 'Novel glucose-1-phosphatase with high phytase activity and unusual metal ion activation from soil bacterium Pantoea sp. strain 3.5. 1', *Appl Environ Microbiol*, vol. 81, no. 19, pp. 6790–6799, 2015.

[75] W. Shi, Y. Xing, Y. Zhu, N. Gao, and Y. Ying, 'Diverse responses of pqqC-and phoD-harbouring bacterial communities to variation in soil properties of Moso bamboo forests', *Microb Biotechnol*, vol. 15, no. 7, pp. 2097–2111, 2022.

[76] Z. K. Bagewadi, D. A. Yaraguppi, S. I. Mulla, and S. H. Deshpande, 'Response surface methodology based optimization, partial purification and characterization of alkaline phosphatase isolated from Pseudomonas asiatica strain ZKB1 and its application in plant growth promotion', *Mol Biotechnol*, vol. 64, no. 9, pp. 984–1002, 2022.

[77] T. H. Rombola, E. A. N. Pedrinho, E. G. de Macedo Lemos, A. M. Gonçalves, L. F. J. dos Santos, and J. M. Pizauro, 'Identification and enzymatic characterization of acid phosphatase from Burkholderia gladioli', *BMC Res Notes*, vol. 7, pp. 1–7, 2014.

[78] I. A. F. Djuuna, S. Prabawardani, and M. Massora, 'Population Distribution of Phosphate-solubilizing Microorganisms in Agricultural Soil', *Microbes Environ*, vol. 37, no. 1, 2022, doi: 10.1264/JSME2.ME21041.

[79] K. S. Li, V. Zeghbroeck J, Q. Liu, and S. Zhang, 'Isolating and Characterizing Phosphorus Solubilizing Bacteria From Rhizospheres of Native Plants Grown in

Calcareous Soils', *Front Environ Sci*, vol. 9, Dec. 2021, doi: 10.3389/FENVS.2021.802563.

[80] I. Bahadur, B. R. Maurya, V. S. Meena, M. Saha, A. Kumar, and A. Aeron, 'Mineral Release Dynamics of Tricalcium Phosphate and Waste Muscovite by Mineral-Solubilizing Rhizobacteria Isolated from Indo-Gangetic Plain of India', *Geomicrobiol J*, vol. 34, no. 5, pp. 454–466, May 2017, doi: 10.1080/01490451.2016.1219431.

[81] S. Sahu *et al.*, 'Bacterial strains found in the soils of a municipal solid waste dumping site facilitated phosphate solubilization along with cadmium remediation', *Chemosphere*, vol. 287, Jan. 2022, doi: 10.1016/J.CHEMOSPHERE.2021.132320.

[82] R. Ghosh, S. Barman, R. Mukherjee, and N. C. Mandal, 'Role of phosphate solubilizing Burkholderia spp. for successful colonization and growth promotion of Lycopodium cernuum L. (Lycopodiaceae) in lateritic belt of Birbhum district of West Bengal, India', *Microbiol Res*, vol. 183, pp. 80–91, Feb. 2016, doi: 10.1016/J.MICRES.2015.11.011.

[83] A. S. Kashyap *et al.*, 'Screening and biocontrol potential of rhizobacteria native to gangetic plains and hilly regions to induce systemic resistance and promote plant growth in chilli against bacterial wilt disease', *Plants*, vol. 10, no. 10, Oct. 2021, doi: 10.3390/PLANTS10102125.

[84] Z. Dai *et al.*, 'Long-term nutrient inputs shift soil microbial functional profiles of phosphorus cycling in diverse agroecosystems', *ISME Journal*, vol. 14, no. 3, pp. 757–770, Mar. 2020, doi: 10.1038/S41396-019-0567-9.

[85] A. Hegyi, T. B. K. Nguyen, and K. Posta, 'Metagenomic analysis of bacterial communities in agricultural soils from vietnam with special attention to phosphate solubilizing bacteria', *Microorganisms*, vol. 9, no. 9, Sep. 2021, doi: 10.3390/MICROORGANISMS9091796.

[86] I. Mahdi, N. Fahsi, M. Hafidi, A. Allaoui, and L. Biskri, 'Plant growth enhancement using rhizospheric halotolerant phosphate solubilizing bacterium bacillus licheniformis qa1 and enterobacter asburiae qf11 isolated from chenopodium quinoa willd', *Microorganisms*, vol. 8, no. 6, pp. 1–21, Jun. 2020, doi: 10.3390/MICROORGANISMS8060948.

[87] M. Rasul *et al.*, 'Glucose dehydrogenase gene containing phosphobacteria for biofortification of Phosphorus with growth promotion of rice', *Microbiol Res*, vol. 223–225, pp. 1–12, Jun. 2019, doi: 10.1016/J.MICRES.2019.03.004.

[88] Y. Zhang *et al.*, ‘Long-term partial substitution of chemical fertilizer by organic amendments influences soil microbial functional diversity of phosphorus cycling and improves phosphorus availability in greenhouse vegetable production’, *Agric Ecosyst Environ*, vol. 341, Jan. 2023, doi: 10.1016/J.AGEE.2022.108193.

[89] G. Luo *et al.*, ‘Understanding how long-term organic amendments increase soil phosphatase activities: Insight into phoD- and phoC-harboring functional microbial populations’, *Soil Biol Biochem*, vol. 139, Dec. 2019, doi: 10.1016/J.SOILBIO.2019.107632.

[90] S. Chen *et al.*, ‘The role of long-term mineral and manure fertilization on P species accumulation and phosphate-solubilizing microorganisms in paddy red soils’, *SOIL*, vol. 9, no. 1, pp. 101–116, Feb. 2023, doi: 10.5194/SOIL-9-101-2023.

[91] J. Tian *et al.*, ‘Biochar application under low phosphorus input promotes soil organic phosphorus mineralization by shifting bacterial phoD gene community composition’, *Science of the Total Environment*, vol. 779, Jul. 2021, doi: 10.1016/J.SCITOTENV.2021.146556.

[92] S. Joshi, S. Gangola, V. Jaggi, and M. Sahgal, ‘Functional characterization and molecular fingerprinting of potential phosphate solubilizing bacterial candidates from Shisham rhizosphere’, *Sci Rep*, vol. 13, no. 1, Dec. 2023, doi: 10.1038/S41598-023-33217-9.

[93] E. D. Sonnenburg and J. L. Sonnenburg, ‘The ancestral and industrialized gut microbiota and implications for human health’, *Nat Rev Microbiol*, vol. 17, no. 6, pp. 383–390, Jun. 2019, doi: 10.1038/S41579-019-0191-8.

[94] D. KOUR *et al.*, ‘Biodiversity, current developments and potential biotechnological applications of phosphorus-solubilizing and -mobilizing microbes: A review’, *Pedosphere*, vol. 31, no. 1, pp. 43–75, Feb. 2021, doi: 10.1016/S1002-0160(20)60057-1.

[95] M. Garcia-Sanchez, I. Bertrand, A. Barakat, Y. Zeroual, A. Oukarroum, and C. Plassard, ‘Improved rock phosphate dissolution from organic acids is driven by nitrate assimilation of bacteria isolated from nitrate and CaCO3- rich soil’, *PLoS One*, vol. 18, no. 3 March, Mar. 2023, doi: 10.1371/JOURNAL.PONE.0283437.

[96] M. Suleman, S. Yasmin, M. Rasul, M. Yahya, B. M. Atta, and M. S. Mirza, ‘Phosphate solubilizing bacteria with glucose dehydrogenase gene for phosphorus uptake and beneficial effects on wheat’, *PLoS One*, vol. 13, no. 9, Sep. 2018, doi: 10.1371/JOURNAL.PONE.0204408.

[97] A. G. Gad, ‘Particle Swarm Optimization Algorithm and Its Applications: A Systematic Review’, vol. 29, pp. 2531–2561, 2022, doi: 10.1007/s11831-021-09694-4.

[98] R. Thangaraj, M. Pant, A. Abraham, and V. Snasel, ‘Modified particle swarm optimization with time varying velocity vector’, *International Journal of Innovative Computing, Information and Control*, vol. 8, no. 1, pp. 201–218, 2012.

[99] N. Bhargava, G. Sharma, R. Bhargava, and M. Mathuria, ‘Decision Tree Analysis on J48 Algorithm for Data Mining’, 2013. [Online]. Available: https://api.semanticscholar.org/CorpusID:63487772

[100] J. Kocijan, K. Ažman, and A. Grancharova, ‘The concept for Gaussian process model based system identification toolbox’, in *Proceedings of the 2007 International Conference on Computer Systems and Technologies*, in CompSysTech ’07. New York, NY, USA: Association for Computing Machinery, 2007. doi: 10.1145/1330598.1330647.

[101] C. E. Rasmussen, ‘Gaussian Processes in Machine Learning’, in *Advanced Lectures on Machine Learning: ML Summer Schools 2003, Canberra, Australia, February 2 - 14, 2003, Tübingen, Germany, August 4 - 16, 2003, Revised Lectures*, O. Bousquet, U. von Luxburg, and G. Rätsch, Eds., Berlin, Heidelberg: Springer Berlin Heidelberg, 2004, pp. 63–71. doi: 10.1007/978-3-540-28650-9_4.

[102] B. Beig *et al.*, ‘Facile coating of micronutrient zinc for slow release urea and its agronomic effects on field grown wheat (Triticum aestivum L.)’, *Science of The Total Environment*, vol. 838, p. 155965, 2022, doi: https://doi.org/10.1016/j.scitotenv.2022.155965.

[103] B. Abdullah *et al.*, ‘Zinc-Coated Urea with Gelatin-Enhanced Zinc Biofortification, Apparent Nitrogen Recovery, and Ryegrass Production’, *J Soil Sci Plant Nutr*, vol. 24, no. 1, pp. 1460–1473, 2024, doi: 10.1007/s42729-024-01649-5.

[104] B. Beig, M. B. K. Niazi, Z. Jahan, A. Hussain, M. H. Zia, and M. T. Mehran, ‘Coating materials for slow release of nitrogen from urea fertilizer: A review’, *J Plant Nutr*, vol. 43, no. 10, pp. 1510–1533, 2020.

[105] B. Beig *et al.*, ‘Slow-Release Urea Prills Developed Using Organic and Inorganic Blends in Fluidized Bed Coater and Their Effect on Spinach Productivity’, *Sustainability*, vol. 12, no. 15, 2020, doi: 10.3390/su12155944.

[106] M. Akhter, G. A. Shah, M. B. K. Niazi, S. Mir, Z. Jahan, and M. I. Rashid, ‘Novel water-soluble polymer coatings control NPK release rate, improve soil quality and

maize productivity', *J Appl Polym Sci*, vol. 138, no. 42, Sep. 2021, doi: 10.1002/app.51239.

[107] N. Zafar *et al.*, 'Starch and polyvinyl alcohol encapsulated biodegradable nanocomposites for environment friendly slow release of urea fertilizer', *Chemical Engineering Journal Advances*, vol. 7, p. 100123, 2021.

[108] G. Estefan, R. Sommer, and J. Ryan, 'Methods of Soil, Plant, and Water Analysis: A manual for the West Asia and North Africa region', 2013. [Online]. Available: www.icarda.org

[109] K. R. Reddy and R. D. DeLaune, 'Biogeochemistry of Wetlands : Science and Applications', *Biogeochemistry of Wetlands*, Jul. 2008, doi: 10.1201/9780203491454.

[110] H. Sun, Y. Wu, D. Yu, and J. Zhou, 'Altitudinal Gradient of Microbial Biomass Phosphorus and Its Relationship with Microbial Biomass Carbon, Nitrogen, and Rhizosphere Soil Phosphorus on the Eastern Slope of Gongga Mountain, SW China', *PLoS One*, vol. 8, no. 9, p. e72952, Sep. 2013, doi: 10.1371/JOURNAL.PONE.0072952.